THE USE OF REAL GASES IN A SHOCK TUBE

by

Russell Earl Duff

A dissertation submitted in partial fulfillment
of the requirements for the degree of
Doctor of Philosophy in the
University of Michigan
1951

Committee in charge:

Professor Otto Laporte, Chairman
Assistant Professor Ernst Katz
Professor Wilbur C. Nelson
Professor Gordon B. B. M. Sutherland
Professor George E. Uhlenbeck

ensn
UMR0891

ACKNOWLEDGEMENTS

TABLE OF CONTENTS

LIST OF TABLES

LIST OF FIGURES

THE USE OF REAL GASES IN A SHOCK TUBE

I. INTRODUCTION

1. Historical Sketch

In spite of the fact that the shock tube was first used over

fifty years ago, its full potentialities are only now being recognized.

In 1899, Vieille[1] proved the fundamental fact that a compression wave pro-

duced by breaking a diaphragm separating regions of different pressure

travels faster than sound.

The theory of the ideal shock tube was developed as early as 1910

by Kobes[2] in a paper discussing the hydrodynamic theory of vacuum and pres-

sure-air brakes for railroad rolling stock.

In 1932, Schardin[3] referred to the work of Kobes in a discussion

of the noise generated when a diaphragm separating regions of different

pressure in a pipe is ruptured.

These early papers were unknown to the several scientists who

derived the shock tube theory independently within the last decade.

---

[1] Vieille, Paul, "Sur les Discontinuities produites par la detent brusque de gas compremés", Comptes Rendus, 129, 1228-1230 (1899).

[2] Kobes, K., "Die Durchschlagsgeschwindigkeit bei den Luftsauge- und Druckluftbremsen", Zeitschrift des Osterreichischen Ingenieur- und Architekten-Vereines, 62, 558 (1910).

[3] Schardin, H., "Bemerkungen zum Druckausgleichvorgang in einer Rohr- leitung", Physikalische Zeitschrift, 33, 60 (1932).

Apparently no experimental investigation was made of shock waves produced in the shock tube until Payman and Shepherd[4] performed a series of experiments in which the processes occurring in the tube were investigated in some detail by means of a wave-speed camera.

Then, at Princeton University in 1943, Reynolds[5] devised a shock tube for the calibration of pressure gauges suitable for blast measurements. Several other laboratories now have shock tubes designed solely for this purpose. The fundamental equation relating initial pressure ratio across the diaphragm to the shock strength produced was derived by Taub for this report. For convenience, this relation shall be referred to as the Taub equation throughout this report.

The first quantitative use of the shock tube in a hydrodynamic investigation was made by Smith[6] at Princeton University in 1945. Shock reflections, both regular and Mach, were examined by observing the primary tube shock after reflection from a wall whose inclination could be varied.

This investigation of Mach reflection has been continued by Bleakney[7,8] and his co-workers at Princeton University using a much better shock tube and a Mach-Zehnder interferometer.

[4] Payman, W., and Shepherd, W. F. C., "Explosion Waves and Shock Waves: VI, The Disturbance Produced by Bursting Diaphragms with Compressed Air", Proceedings of the Royal Society, A-186, 293-321 (1946).

[5] Reynolds, George T., A Preliminary Study of Plane Shock Waves Formed by Bursting Diaphragms in a Tube, OSRD Report No. 1519, June, 1943.

[6] Smith, Lincoln G., Photographic Investigation of the Reflection of Plane Shocks in Air, OSRD Report No. 6271, November, 1945.

[7] Bleakney, W., Fletcher, C. H., and Weimer, D. K., "The Density Field in Mach Reflection of Shock Waves", Physical Review, 76, 323 (1949).

[8] Bleakney, W., and Taub, A. H., "Interaction of Shock Waves", Reviews of Modern Physics, 21, 584 (1949).

The possibility of using a shock tube as an intermittent wind tunnel was first proposed by Mautz, Geiger, and Epstein[9] at the University of Michigan in 1948. This suggestion was investigated and found promising by Mautz and and Geiger.[10,11,12] At the present time the investigation of the applicability of the shock tube as an instrument for aerodynamic research is being continued.

During the past year the shock-tube laboratories at Princeton and Michigan have prepared numerous reports on the diffraction of shock waves around various obstacles.[13-18] Shadowgraph, schlieren, and interferometric photography were used in these investigations.

This paper will discuss the advantages of using gases other than air in the shock tube to extend its range and increase its usefulness.

[9] Mautz, C. W., Geiger, F. W., and Epstein, H. T., "On the Investigation of Supersonic Flow Patterns by Means of a Shock Tube", Physical Review, 74, 1872 (1948).

[10] Mautz, C. W., The Use of the Shock Tube in the Production of Uniform Fields of Transonic and Supersonic Flow, Dissertation, University of Michigan, 1949.

[11] Geiger, F. W., On the Shock Tube as a Tool for the Investigation of Flow Phenomena, Dissertation, University of Michigan, 1949.

[12] Geiger, F. W., and Mautz, C. W., The Shock Tube as an Instrument for the Investigation of Transonic and Supersonic Flow Patterns, Report on ONR Contract N6-ONR-232, TO IV, Engineering Research Institute, University of Michigan, 1949.

[13] Bleakney, Walker, The Diffraction of Shock Waves Around Obstacles and the Transient Loading of Structures, Princeton University, Technical Report II-3, Contract N6-ONR-105, TO II, March 16, 1950.

[14] White, D. R., Weimer, D. K., and Bleakney, Walker, The Diffraction of Shock Waves Around Obstacles and the Resulting Transient Loading of Structures, Princeton University, Technical Report II-6, Contract N6-ONR-105, TO II, August 1, 1950.

[15] Uhlenbeck, G. (submitting work done by R. E. Duff and R. N. Hollyer, Jr.), Diffraction of Shock Waves Around Various Obstacles, Engineering Research Institute, University of Michigan, Report No. 50-1, Contract N6-ONR-232, TO IV, March 21, 1950.

2. Brief Description of the Apparatus

The procedures and techniques of shock tube research are well described in the papers of Mautz and Geiger.[10,11,12] However, the shock tube and auxiliary equipment originally installed by Mautz have been extensively modified for this investigation.

The shock tube itself now consists of a rectangular tube 26-1/2 feet long of 2-in. x 7-in. rectangular cross section. The compression chamber is 8-1/2 feet long, and the distance from the diaphragm to the test-section window is 15 feet. The lengths of the compression and expansion chambers were chosen so that the contact surface would limit the duration of uniform flow at all supersonic Mach numbers. One outstanding feature of this tube is its 7-in. x 11-1/2-in. test-section window. This very large window makes it possible to examine the flow in the shock tube from the top to the bottom of the tube and along a considerable length of the expansion chamber. The study of shock wave diffraction about obstacles on the floor of the tube is thus facilitated. Furthermore, the investigation of flow phenomena several chord lengths in front of and behind airfoil sections is also simplified.

---

[16] Hollyer, R. N., Jr., and Duff, R. E., The Effect of Wall Boundary Layer on the Diffraction of Shock Waves Around Cylindrical and Rectangular Obstacles, Engineering Research Institute, University of Michigan, Report No. 50-2, Contract N6-ONR-232, TO IV, June 21, 1950.

[17] Duff, R. E., and Hollyer, R. N., Jr., The Diffraction of Shock Waves Through Obstacles with Various Openings in Their Front and Back Surfaces, Engineering Research Institute, University of Michigan, Report No. 50-3, Contract N6-ONR-232, TO IV, November 7, 1950.

[18] Hollyer, R. N., Jr., and Duff, R. E., Growth of the Turbulent Region at the Leading Edge of Rectangular Obstacles in Shock Wave Diffraction, Engineering Research Institute, University of Michigan, Report No. 51-2, Contract N6-ONR-232, TO IV, January 18, 1951.

Flow pictures may be taken by shadowgraph or schlieren photography. The basic photographic optical system now consists of a high-intensity, short-duration spark light source which illuminates an f/8.0, 6-in. parabolic mirror which produces a beam of parallel light. A similar mirror is used as the focussing element when schlieren photographs are desired. The reduction of aperture of the photographic optical system from f/2.5 to f/8.0, which resulted when the original lens was replaced by the new mirror, necessitated a ten-fold increase in spark intensity. This increase was obtained by doubling the spark voltage and capacity and enclosing the spark gap in an atmosphere of argon at a pressure of 200 lbs per sq in. Sufficient freedom was provided in the mountings for the spark, for the shadowgraph and schlieren mirrors, and for the plate holders so that any portion of the test section could be photographed easily.

The strength of the primary tube shock is determined by measuring the transit time of the shock between two light stations. The equipment used is, however, very different from that used by Mautz. The stations now consist essentially of single-lens schlieren systems* mounted on ground optical benches which, in turn, are fastened to an adjustable bench completely isolated from the tube.

The greatest improvement in the shock tube instrumentation has been made in the electronic control equipment. Two new binary counters and associated gates, oscillator, and delay circuit have been designed and

---

* It was found that light scattered from the surfaces of the lens which had focussed parallel light onto the schlieren knife edge, in a double-lens schlieren system, caused a large fraction of the background noise of the photomultiplier tube. Elimination of the lens improved the signal-to-noise ratio and therefore lowered by approximately 35 per cent the minimum expansion-chamber pressure at which shock velocities could be determined.

constructed by Mr. R. N. Hollyer, Jr. This new equipment allows both the shock velocity and the time at which the photograph was taken to be determined every time the shock tube is fired. Of course, this has reduced the uncertainty in shock velocity inherent in all earlier shock tube photographs made at this laboratory. At the same time the techniques of shock tube research have been greatly simplified. A complete description of the shock tube and its associated electronic equipment will be given by Mr. R. N. Hollyer and the author in an Engineering Research Institute Report now in preparation.

As the Michigan shock tube now exists, it is far from a perfect instrument; but it is definitely superior to the original tube, and it is quite adequate for the investigation of many classes of hydrodynamic phenomena.

3. Preliminary Statement of the Problem of Employing Gases Other Than Air in a Shock Tube

In all the early shock tube work, air was used in both chambers of the tube. However, both Smith and Mautz have pointed out that by using helium in the compression chamber, a much stronger shock wave can be produced by a given initial pressure ratio across the diaphragm; or, conversely, when helium is in the compression chamber, a higher pressure can be used in the expansion chamber to produce a given strength shock wave. This has the great advantage of increasing the contrast and definition of the resulting photographs of the flow. Furthermore, the use of helium in the compression chamber makes it possible to obtain shock strengths that cannot be obtained in the shock tube with air.

One of the limitations of the shock tube as an instrument for aerodynamic research is the fact that the flow Mach number is limited to

a relatively low value. This limit is inherent in the method for producing flow used in the shock tube and it is a function of the specific heat ratio of the gas used in the expansion chamber. Mautz first noted that the limit of 1.89 for air could easily be surpassed by using a complex gas with a low specific heat ratio in the expansion chamber.

This investigation is concerned with a detailed consideration of the advantages and disadvantages of using gases other than air in the compression and expansion chambers of a shock tube.

Examination of the generalized Taub equation (cf. page 2) shows that, in order to produce strong shock waves, a light gas with a high velocity of sound should be used in the compression chamber; and fundamental shock theory (cf. page 29) reveals that high Mach number flows can be obtained by using a complex gas, with low specific heat ratio, in the expansion chamber. Therefore, when considering a wide variety of real gases for use in a shock tube, one must be prepared for possible deviations from ideal shock theory caused by (1) temperature dependence of the specific heat, (2) deviations from the ideal gas equation of state, and (3) relaxation phenomena.

Only the first two perturbations need be considered as possibly important for the flow produced by the rarefaction wave in the compression chamber. In Chapter II expressions for the flow velocity produced by a rarefaction wave in an ideal gas with temperature-dependent specific heat and in a van der Waals' gas with constant specific heat are calculated. By insertion of numerical values it is shown that the velocity perturbations are negligible for hydrogen. The calculations were performed for this gas because the Taub equation indicates that the strongest shock waves for a given initial pressure ratio across the diaphragm can

be produced by using hydrogen in the compression chamber. Special pre-
cautions must be taken, however, to eliminate oxygen from the expansion
chamber in order to prevent a hydrogen-oxygen explosion which could be
initiated by the high temperatures behind the shock wave reflected from
the end of the expansion chamber.

In Chapter III shock theory analogous to the Rankine-Hugoniot
theory is developed for a gas with temperature-dependent specific heat
(deviations from the ideal gas equation of state are not important here).
Flow parameters calculated from these equations show that the temperature
ratio across a shock wave (for all shock velocities) is lower than pre-
dicted by the Rankine-Hugoniot theory. Also, the pressure and density be-
hind a shock wave, as well as the flow Mach number, are higher than pre-
dicted by the simple theory. Numerical calculations are made for the
hydrodynamic variables behind shock waves in carbon dioxide, nitrogen,
and sulfur hexafluoride. Finally, the results of a flow calibration in
carbon dioxide, in the supersonic region, are shown to be in good agree-
ment with the more general shock theory.

Relaxation phenomena are investigated in Chapter IV insofar as
they influence the flow through a shock wave. In general, relaxation
phenomena are caused by the destruction of thermal equilibrium between
various degrees of molecular freedom by rapid temperature variations.
This is one refinement of shock wave theory which as yet has not been
viewed from the shock tube point of view.

It is usually assumed that a shock wave is, to all intents and
purposes, a surface of discontinuity separating two regions of uniform
state. This tacit assumption is made in the calculations of Chapter III.
However, under certain conditions this is not true; specifically, it has
been found that even though the rotational degrees of freedom are usually

in equilibrium with the translational degrees, the energy associated with the vibrational modes is often not able to follow abrupt temperature changes. Under these conditions, one may say that the shock wave is followed by an extended transition region in which the vibrational energy is approaching its equilibrium value. The relative rate of change of vibrational energy may be associated with a relaxation time.

A large amount of theoretical and experimental work has been done in order to determine the relations between vibrational relaxation and periodic disturbances. In particular, the effects of vibrational relaxation on sound velocity and absorption in the ultrasonic region have been investigated in great detail since 1925.[19] However, the effects of vibrational relaxation on an aperiodic disturbance like a shock wave have not been thoroughly investigated as yet.

In Chapter IV an approximate calculation of the flow variables in the transition region behind a shock wave is carried out. The results of earlier work by Bethe and Teller are used.

Experiments are described whereby the velocity of a shock wave reflected normally from a surface is determined as a function of time. For shock waves in carbon dioxide, this velocity is found to be variable, while it is constant in nitrogen and sulfur hexafluoride. The result is that, in a shock tube, vibrational relaxation influences slightly the flow of carbon dioxide, but does not affect the flows of the other gases. The conclusion is reached that, insofar as practical hydrodynamic research in a shock tube is concerned, vibrational relaxation can be ignored.

The discussion of the use of various gases in a shock tube would not be complete without an analysis of their effects on the relative

---

[19] Richards, W. T., "Supersonic Phenomena", Reviews of Modern Physics, 11, 36-64 (1939).

duration of uniform flow. This problem is treated in Chapter V. If it is assumed that the rate of development of a flow field is inversely proportional to the sound speed behind a shock wave, a duration index can be defined which is proportional to the relative duration of uniform flow. This duration index is a function of the shock strength and specific heat ratio. It is shown that for a given Mach number, the duration index is practically independent of the gas used in the expansion chamber. Furthermore, experiments are described which demonstrate the validity of the assumptions made in deriving the duration index.

The additional effects of a large number of chemical and physical properties of gases are discussed in the final chapter (VI). In particular, the conclusion is reached that the best combination of gases for routine aerodynamic investigation is hydrogen in the compression chamber and nitrogen in the expansion chamber. However, for investigations of the fundamental hydrodynamic principles that govern the transonic and supersonic flow of gases, sulfur hexafluoride has a unique combination of properties that makes it one of the best gases for use in the expansion chamber.

II. GAS FLOW IN THE COMPRESSION CHAMBER

1. Taub Equation for a Gas with Constant Specific Heat

As derived by Taub and generalized by Mautz, the basic shock tube equation which relates the pressure ratio across the diaphragm to the shock strength produced is

$$\frac{p_0}{p_3} = \xi \left[1 - \frac{a_{OE}\,(\mu_E - 1)}{a_{OC}\,(\mu_C - 1)} \frac{(1 - \xi)}{\sqrt{(\mu_E + 1)\,\xi\,(\mu_E + \xi)}} \right]^{\mu_C + 1}, \qquad (1)$$

where ξ is the ratio, p_0/p_1, of the pressure in front of the shock to that behind it, p_3 is the initial pressure in the compression chamber, a_{OE} and a_{OC} are the sound speeds in the expansion and compression chambers, respectively, and μ_E and μ_C are the functions $(\gamma + 1)/(\gamma - 1)$ of the specific heat ratios in the expansion and compression chambers. It is assumed that ideal gases with constant specific heats are used in both chambers of the shock tube. If the same diatomic gas is used in both chambers, this becomes simply

$$\frac{p_0}{p_3} = \xi \left[1 - \frac{1 - \xi}{\sqrt{7\xi\,(6 + \xi)}} \right]^{7}, \qquad (2)$$

where γ is assumed to be 1.40.

However, if $a_{OE}(\mu_E - 1)/a_{OC}(\mu_C - 1)$ or $\mu_C + 1$ could be reduced, the pressure ratio corresponding to a given ξ would be increased. In this way the initial expansion chamber pressure can also be increased

because the pressure in the compression chamber is usually adjusted to
that of the atmosphere. As a result, the quality of flow photographs
is improved because the optical effect associated with a given density
ratio in the flow about a model is proportional to the absolute density
of the gas in the expansion chamber. Furthermore, very strong and useful
shock waves can be produced in a shock tube only by a manipulation of
these constants.

The most effective way to increase the initial pressure ratio
across the diaphragm at constant ξ is to increase the velocity of sound
of the gas in the compression chamber. In other words, hydrogen or helium
are to be used as this gas. The velocity of sound ratio appearing in
Eq 1 can easily be increased by a factor of 3 in this way. Variations
in the specific heat function, μ , are usually less effective because
this function may only be reduced from 6 to 4 by substituting a mon-
atomic gas for a diatomic one in the compression chamber.

As mentioned in the introduction, both Smith and Mautz sugges-
ted that helium be used; but hydrogen, which would be even more effec-
tive, was not considered for fear that an explosion of hydrogen and at-
mospheric oxygen might be initiated by the extremely high temperatures
behind the shock wave reflected from the end of the expansion chamber.
This fear was justified because an explosion does result when hydrogen
and air are used in the chambers of a shock tube to produce strong shocks.
However, this difficulty can be avoided by substituting nitrogen for
air in the expansion chamber. The use of nitrogen does not complicate
the firing procedure, because, in order to introduce hydrogen or helium
into the compression chamber without breaking the diaphragm prematurely,
both chambers of the tube must be evacuated. In fact, there are several

additional reasons why it is desirable to use nitrogen instead of air in the expansion chamber of a shock tube. These reasons will be discussed in detail in subsequent chapters.

When nitrogen and helium are used in the chambers of a shock tube, Eq 1 becomes:

$$\frac{p_0}{p_3} = \xi \left[1 - .5796 \frac{(1-\xi)}{\sqrt{7\xi(6+\xi)}} \right]^5, \qquad (3)$$

and for nitrogen and hydrogen one obtains:

$$\frac{p_0}{p_3} = \xi \left[1 - .2727 \frac{(1-\xi)}{\sqrt{7\xi(6+\xi)}} \right]^{6.878}, \qquad (4)$$

where γ for hydrogen is assumed to be 1.410.

Eqs 2, 3, and 4 are plotted in Fig. 1.

It can be easily seen that hydrogen produces the strongest shock wave for a given pressure ratio across the diaphragm. In particular, the advantage of using hydrogen to produce strong shocks, small values of ξ, is obvious. It can also be seen that hydrogen has a lower limit shock strength for an infinite initial pressure ratio than either helium or nitrogen.

2. Compression Chamber Temperature

The temperature produced by the adiabatic expansion wave in the compression chamber can be easily calculated from the p_0/p_2 versus ξ relationship. For an adiabatic process

$$\frac{p_1}{p_3} = \left(\frac{T_1}{T_3} \right)^{\frac{\gamma}{\gamma-1}}$$

FIG I

P_0/P_3 VERSUS ξ
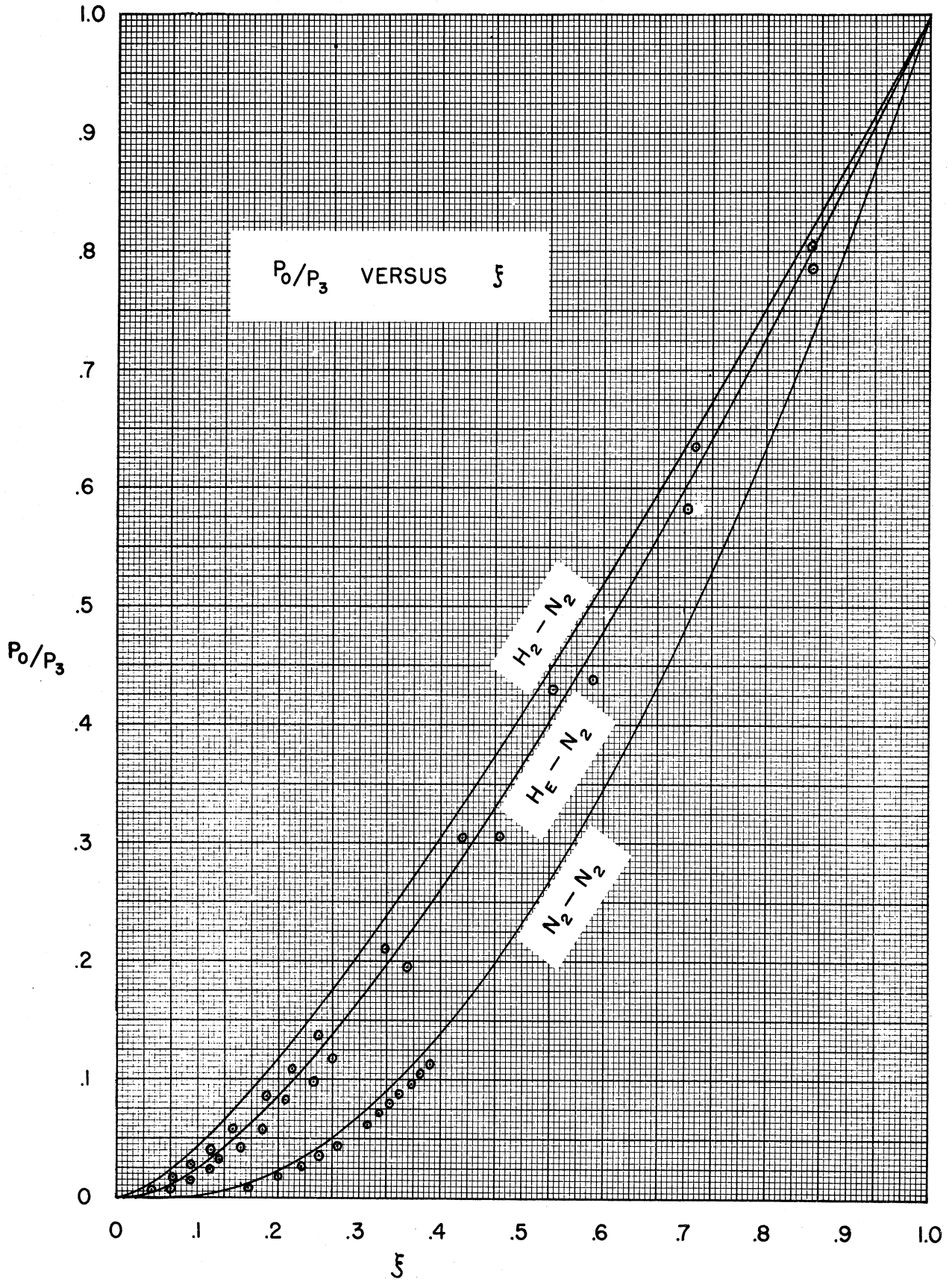
and

$$\frac{P_1}{P_3} = \frac{P_0}{P_3} \cdot \frac{P_1}{P_0} = \frac{1}{\xi} \cdot \frac{P_0}{P_3}$$

Thus,

$$\frac{T_1}{T_3} = \left[1 - \frac{a_{0E}(\mu_E - 1)}{a_{0C}(\mu_C - 1)} \cdot \frac{(1 - \xi)}{\sqrt{(\mu_E + 1)\xi(\mu_E + \xi)}} \right]^2 . \tag{5}$$

This relation is plotted in Fig. 2 for the three gas combinations discussed above. It is interesting to note that with nitrogen in the compression chamber, the temperature there falls well below the freezing point of the gas (63°K) for very strong shocks.*

It should be noted, however, that the optical system used to detect the passage of the shock wave has only a limited sensitivity. Therefore, when nitrogen is used in the compression chamber, it is not possible to operate the tube for shocks of strength much less than ξ = .2. The corresponding limits for helium and hydrogen are approximately ξ = .05 and ξ = .03, respectively. The lowest temperatures actually obtained in the compression chamber are, therefore, much higher than Fig. 2 indicates at first glance.

3. Flow Velocity Produced by a Rarefaction Wave in an Ideal Gas with Temperature-Dependent Specific Heat

Eq 1 has been derived under the assumption that the specific heat of the gases used in both chambers of the tube is constant. Unfortunately, this is not strictly correct for either chamber. The

---

* It has actually been suggested by Antonio Ferri that the cold flow in a shock tube be used to investigate the problem of condensation of air which is very important in the nozzles of hypersonic wind tunnels.

FIG 2

COMPRESSION CHAMBER
TEMPERATURE

$H_2 - N_2$

$He - N_2$

$N_2 - N_2$
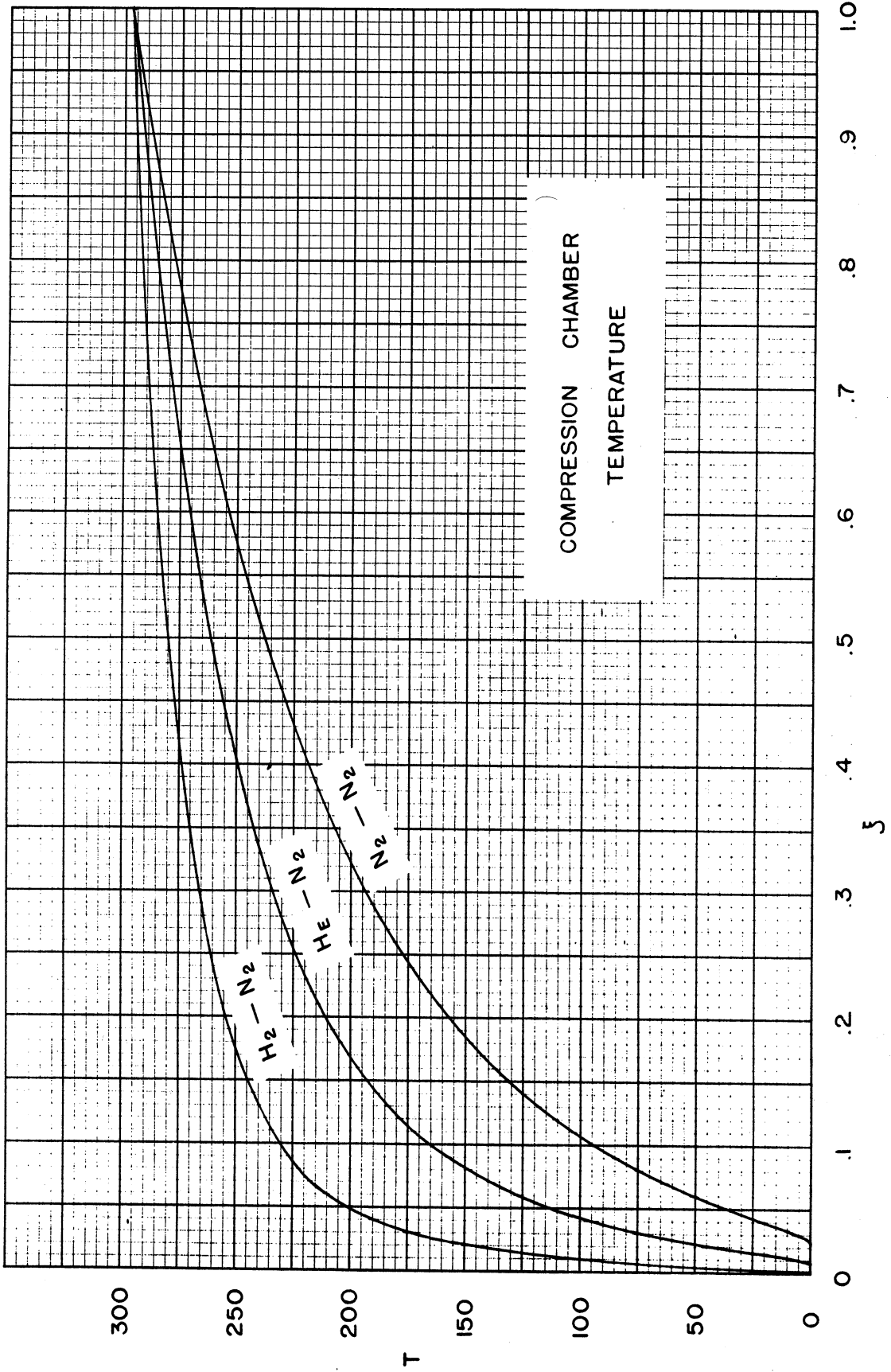
modifications of the fundamental shock equations brought about by the temperature dependence of the specific heat of the gas in the expansion chamber will be considered in Chapter III.

The temperature changes in the compression chamber discussed in the last section are sufficient to cause an 8 per cent decrease in the specific heat of hydrogen and a 2 per cent decrease in the specific heat of nitrogen. Since helium is a monatomic gas, its specific heat is not a function of temperature.

The velocity imported to a gas initially at rest, by a rarefaction wave is

$$u = \int_{\rho}^{\rho_0} \sqrt{\frac{dp}{d\rho}} \; \frac{d\rho}{\rho} \; , \tag{6}$$

where $dp/d\rho$ is usually calculated along an adiabatic path.

A comparison of the flow velocity produced, for a given pressure ratio across the rarefaction wave, by real and ideal gases will suffice to determine the effect of specific-heat variations on the flow from the compression chamber. This velocity integral can be reduced to a quadrature in the general case of an ideal gas whose specific heat is a given function of temperature. Assume an ideal gas with the equation of state $p = \rho RT$. The specific heat may be written as

$$C_v = f(T).$$

For an adiabatic process, the first law of thermodynamics becomes

$$dE = \frac{p}{\rho^2} d\rho. \tag{7}$$

The change in internal energy can be written as $dE = C_V dT$. However, by changing the independent variables to p and ρ, it can be shown immediately that

$$\frac{dp}{d\rho} = \frac{f(T)+R}{f(T)} \cdot \frac{p}{\rho} \; . \tag{8}$$

Since $C_p - C_V = R$ for an ideal gas, it has been shown that the adiabatic compressibility is the isothermal compressibility multiplied by the ratio of specific heats at constant pressure and constant volume.

In addition, by eliminating p from Eq 6, one obtains

$$\frac{dp}{\rho} = \frac{f(T) \, dT}{RT} \; . \tag{9}$$

By substituting Eqs 8 and 9 into the velocity equation, 6, the following general expression is obtained.

$$u = \int_T^{T_0} \sqrt{\frac{[f(T)+R]\,f(T)}{RT}} \; dT \; . \tag{10}$$

Between 190° and 300°K, the specific heat of hydrogen may be represented by

$$f(T) = C_V' \left[1 - \alpha \left(T_0 - T \right)^2 \right] \; , \tag{11}$$

where $C_V' = 10.1$ ergs/g; $\alpha = 9.31 \times 10^{-6}$ degree^{-2}; and $T_0 = 300°K$. The integrand of Eq 10 can be expanded by the binomial theorem. Only first-order terms need be retained.

$$u = \sqrt{\frac{C_p' C_v'}{R}} \int_T^{T_0} \left[1 - \frac{\alpha\, C_p' C_v'}{2\, C_p'} (T_0 - T)^2 \right] \frac{dT}{\sqrt{T}} . \quad (12)$$

After integration and simplification, the following expression for flow velocity is obtained.

$$u = \frac{2 a_0}{\gamma - 1} \left(1 - \sqrt{\frac{T}{T_0}} \right) - \frac{\alpha (\gamma+1)}{a_0 C_v'} T_0^3 \left\{ \frac{8}{15} - \sqrt{\frac{T}{T_0}} \left(1 - \frac{2}{3}\frac{T}{T_0} + \frac{1}{5}\frac{T^2}{T_0^2} \right) \right\} \quad (13)$$

where $\gamma = C_p'/C_v'$ and $a_0 = \sqrt{\gamma R T_0}$. The first term of Eq 13 can be recognized as the flow velocity produced by a rarefaction wave in an ideal gas with constant specific heat.

The flow velocity is given as a function of temperature by Eq 13. However, for shock tube applications, it would be preferable if the velocity were expressed as a function of pressure. In order to transform variables, it is necessary to obtain an equation for the adiabatic curve. If one changes the independent variables of Eq 7 to T and p, the following differential equation is obtained:

$$\frac{C_p\, dT}{RT} = \frac{dp}{p} .$$

This equation can be integrated if Eq 11 is substituted for C_p. The resulting equation for the adiabatic curve is

$$\frac{p}{p_3} = \frac{T}{T_0}^{\left(\frac{C_p' - \alpha C_v' T_0^2}{R} \right)} e^{-\frac{\alpha C_v'}{2R} T_0^2 \left(3 - \frac{T}{T_0} \right)\left(1 - \frac{T}{T_0} \right)} . \quad (14)$$

Eqs 13 and 14 constitute a system of parametric equations which determine the flow velocity as a function of pressure.

The values of flow velocity, temperature, and pressure ratio for a rarefaction wave in hydrogen are shown in Table I. The values included were calculated for both constant and variable specific heats.

TABLE I

HYDRODYNAMIC VARIABLES FOR A RAREFACTION WAVE IN HYDROGEN

CONSTANT AND VARIABLE SPECIFIC HEAT

$T^{\circ}K$	* mm/μ sec	p/p_0 constant specific heat	p/p_0 variable specific heat
300	0	1.0	1.0
290	.1082	.8900	.8900
280	.2183	.7886	.7888
270	.3304	.6960	.6965
260	.4450	.6113	.6125
250	.5609	.5340	.5360
240	.6801	.4641	.4671
230	.8011	.4010	.4052
220	.9248	.3440	.3496
210	1.052	.2932	.3001
200	1.182	.2479	.2565
190	1.315	.2077	.2177

* The change in flow velocity at a given temperature, produced by assuming variable specific heat is negligible.

The pressure ratio across a rarefaction wave in hydrogen is plotted as a function of flow velocity in Fig. 3 for constant and for temperature-dependent specific heat. It will be seen that there is little difference between the two curves. In fact, the specific heat variations will be sufficient to cause an increase in flow Mach number of

FIG 3

FLOW VELOCITY PRODUCED
BY A
RAREFACTION WAVE

P/P_3 VARIABLE C_v

P/P_3 TAUB

μ (MM / μ SEC)
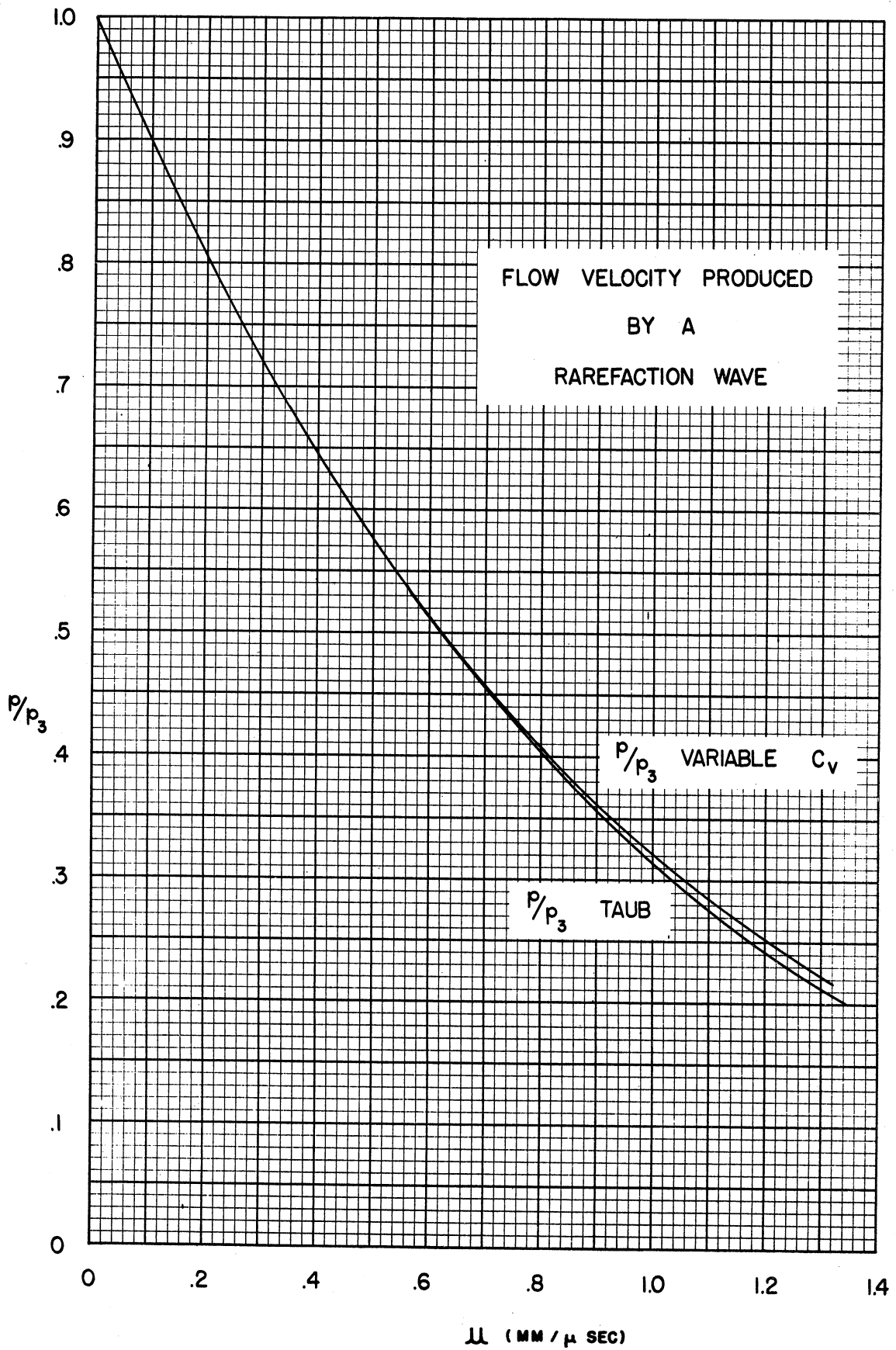
only approximately 1 per cent in the shock tube. It is interesting to
note that the flow velocity, for a particular pressure ratio, is higher
for a gas with temperature-dependent specific heat than for a gas with
constant specific heat. This is the direct result of the transfer of
energy from the rotational to the translational degrees of freedom, which
causes the specific heat variations.

It has thus been shown that the small change of specific heat
with temperature in hydrogen does not appreciably perturb the flow vari-
ables of a rarefaction wave from their values as predicted by constant
specific heat theory. Furthermore, this statement is true for all rare-
faction waves produced in routine shock tube research because the speci-
fic heat variations in helium and nitrogen are even smaller than those of
hydrogen; and they will be correspondingly less important. However, it
would not be true for almost complete expansions where the temperature
in the wave may approach absolute zero.

4. Flow Velocity Produced by a Rarefaction Wave in a Van der Waals' Gas
with Constant Specific Heat

It is possible that deviations from the ideal gas equation of
state would become important at the low temperatures found in the com-
pression chamber. This may be investigated by determining the flow vel-
ocity produced by a rarefaction wave in a van der Waals' gas. The
van der Waals' equation is superior to a virial approximation because
the constants, a and b, can be associated with molecular dimensions and
intermolecular forces. For convenience, the C_V will now be considered
constant.

The van der Waals' equation of state can be written

$$p = \frac{\rho R T}{1 - b\rho} - a\rho^2. \qquad (15)$$

For an adiabatic process the first law of thermodynamics becomes

$$dE = \frac{p}{\rho^2} d\rho.$$

It will be convenient to make temperature and density the independent variables in this equation. It then follows as a consequence of the first and second laws of thermodynamics that

$$C_V \, dT = (p + a\rho^2)\frac{d\rho}{\rho^2}. \qquad (16)$$

An equation for the adiabatic curve can be obtained by integrating this expression.

$$T\left(\frac{\rho}{1-b\rho}\right)^{-\frac{R}{C_V}} = A$$

or

$$(p + a\rho^2)\left(\frac{1-b\rho}{\rho}\right)^{\frac{C_V + R}{C_V}} = B. \qquad (17)$$

Eq 17 is exact. For convenience, it can be expanded. Only first-order corrections will be retained and $\frac{C_V + R}{C_V} = \gamma'$.

$$\frac{p}{p_3} = \left(\frac{\rho}{\rho_3}\right)^{\gamma'}\left\{ 1 + \frac{a\rho_3^2}{p_3}\left[1 - \left(\frac{\rho}{\rho_3}\right)^{2-\gamma'}\right] - b\gamma'\rho_3\left(1 - \frac{\rho}{\rho_3}\right)\right\} \qquad (18)$$

An approximate expression for $dp/d\rho$ can be obtained from Eq 18, but it is more convenient to derive an exact expression by

changing variables in Eq 16. After simplification and elimination of p by using Eq 17, one obtains

$$\frac{dp}{d\rho} = B\gamma' \frac{\rho^{\gamma'-1}}{(1-b\rho)^{\gamma'+1}} - 2a\rho .$$

(19)

The flow velocity produced by a rarefaction wave can now be obtained from Eqs 6 and 19.

$$u = \int_{\rho}^{\rho_3} \sqrt{B\gamma' \frac{\rho^{\gamma'-1}}{(1-b\rho)^{\gamma'+1}} - 2a\rho} \; \frac{d\rho}{\rho} .$$

(20)

Because a and b are small, the integrand can be expanded to give

$$u = \sqrt{B\gamma'} \int_{\rho}^{\rho_3} \rho^{\frac{\gamma'-3}{2}} \left[1 + (\gamma'+1)\frac{b\rho}{2} - \frac{a}{B\gamma'}\rho^{2-\gamma'} \right] d\rho .$$

After integration one obtains

$$u = \frac{2}{\gamma'-1}\sqrt{\frac{\gamma' P_3}{\rho_3}} \left[1 - \left(\frac{\rho}{\rho_3}\right)^{\frac{\gamma'-1}{2}} \right]$$

(21)

$$+ \frac{a\rho_3^2}{P_3}\sqrt{\frac{\gamma' P_3}{\rho_3}} \left\{ \frac{1}{\gamma'-1}\left[1 - \left(\frac{\rho}{\rho_3}\right)^{\frac{\gamma'-1}{2}} \right] - \frac{2}{\gamma'(3-\gamma')}\left[1 - \left(\frac{\rho}{\rho_3}\right)^{\frac{3-\gamma'}{2}} \right] \right\}$$

$$- b\rho_3\sqrt{\frac{\gamma' P_3}{\rho_3}} \left\{ \frac{\gamma'}{\gamma'-1}\left[1 - \left(\frac{\rho}{\rho_3}\right)^{\frac{\gamma'-1}{2}} \right] - \left[1 - \left(\frac{\rho}{\rho_3}\right)^{\frac{\gamma'+1}{2}} \right] \right\}$$

The initial conditions for the rarefaction wave in a shock tube are usually atmospheric pressure, density, and temperature. There-fore $\sqrt{\frac{\gamma' P_3}{\rho_3}} = a_0$ and $\gamma' = \gamma$.

Eq 21 reduces to the ideal gas equation immediately when a and b are zero.

The flow velocity produced by a rarefaction wave in a van der Waals' gas can now be determined as a function of pressure from Eqs 18 and 21. The values of flow velocity, density ratio, and pressure ratio for rarefaction waves in hydrogen, considered as an ideal gas and as a van der Waals' gas, are presented in Table II. The following constants were used in the calculation:

$$a = .2444 \ (liter)^2 \ (atm)/(mole)^2$$

$$b = .02661 \ liters/mole$$

$$\gamma = 1.41$$

$$a_0 = 1.321 \times 10^5 \ cm/sec$$

TABLE II

HYDRODYNAMIC VARIABLES FOR A RAREFACTION WAVE IN HYDROGEN
IDEAL AND VAN DER WAALS' GAS

ρ/ρ_0	u, mm/μsec ideal gas	u, mm/μsec van der Waals' gas	p/p_0 ideal gas	p/p_0 van der Waals' gas
.9	.1377	.1378	.8619	.8618
.8	.2882	.2883	.7301	.7299
.7	.4543	.4544	.6048	.6045
.6	.6406	.6408	.4866	.4864
.5	.8536	.8537	.3763	.3761
.4	1.104	1.104	.2747	.2745
.3	1.409	1.409	.1831	.1830

If these results were plotted as in Fig. 3, the two curves would be indistinguishable. It has thus been shown that equation-of-state variations influence the flow of hydrogen from the compression chamber even less than specific heat variations.

It is true that the deviations from ideal gas behavior might be more important if a heavy gas were being used in the compression chamber in order to increase the pressure difference across the diaphragm when very weak shocks are desired. However, the effects would probably be small even here.

Experimentally, the fact that the specific-heat and equation-of-state variations are not important is shown by the experimental points in Fig. 1. Since nitrogen is used in the expansion chamber in each case, the p_0/p_3 versus ξ results are indicative of the behavior of the gas in the compression chamber. If specific-heat or equation-of-state perturbations were important, one would expect the results for nitrogen and hydrogen to be noticeably different from those for helium, because helium is a monatomic gas with very small van der Waals' constants. However, it is apparent that all the experimental results exhibit the same trend.[*]

From a practical point of view the most important result of this phase of the investigation is the demonstration of the fact that hydrogen can be used in the compression chamber of a shock tube if oxygen is excluded from the expansion chamber. Hydrogen will produce a stronger shock wave than any other gas for a given initial pressure ratio across the diaphragm.

---

[*] See Chapter III, Section 4, for a discussion of two mechanical factors which cause the shock wave produced by a given initial pressure ratio to be weaker than predicted.

III. SHOCK WAVE EQUATIONS

1. Rankine-Hugoniot Shock Equations

The determination of the hydrodynamic variables behind the shock wave in the expansion chamber is the fundamental problem of shock tube theory. This problem is quite easily solved by consideration of the conservation laws for mass, momentum, and energy across a discontinuity surface. Elementary algebraic manipulation leads to the desired results.

In case the specific heat of a gas may be assumed to be constant, the conservation laws for the one-dimensional steady flow through a stationary discontinuity surface become:

$$V_0 , \rho_0 \qquad\qquad V_1 , \rho_1$$
$$P_0 , T_0 \longrightarrow \Big| \longrightarrow \qquad p_1 , T_1$$
$$a_0 \qquad\qquad\qquad a_1$$

Conservation of mass,

$$\rho_0 V_0 = \rho_1 V_1 . \tag{22}$$

Conservation of momentum,

$$p_0 + \rho_0 V_0^2 = p_1 + \rho_1 V_1^2 . \tag{23}$$

Conservation of energy,

$$\frac{1}{2}V_0^2 + \frac{\gamma}{\gamma-1}\frac{p_0}{\rho_0} = \frac{1}{2}V_1^2 + \frac{\gamma}{\gamma-1}\frac{p_1}{\rho_1} \; . \tag{24}$$

V_0 and V_1 can be eliminated from these equations; the resultant relation between p and ρ is the well-known Rankine-Hugoniot equation

$$\frac{\rho_0}{\rho_1} = \frac{1+\mu\xi}{\mu+\xi} = \frac{V_1}{V_0} \; . \tag{25}$$

This equation shows that a discontinuity surface can exist in an ideal compressible fluid if a particular relation between the hydrodynamic variables is satisfied.

In a shock tube the gas in front of the shock wave is stationary with respect to the laboratory frame of reference; but the shock wave is not. Therefore, the velocities V_0 and V_1 can be transformed to more significant variables by translating the frame of reference so that the gas in front of the shock wave is at rest. Thus

$$\frac{U-u}{U} = \frac{1+\mu\xi}{\mu+\xi}$$

where U is the shock velocity and u is the flow speed behind the shock wave.

An expression for the shock velocity itself can be obtained from the Rankine-Hugoniot relation, the energy equation, and Prandtl's relation.

$$U = a_0 \sqrt{\frac{\mu+\xi}{(\mu+1)\xi}} \; . \tag{26}$$

Substituting this into Eq 14 gives

$$u = a_0 \frac{(\mu-1)(1-\xi)}{\sqrt{(\mu+1)\,\xi\,(\mu+\xi)}} \qquad . \qquad (27)$$

Finally, the Mach number of the flow behind the shock wave relative to the laboratory system is

$$M = \frac{u}{a_1} = \frac{u}{a_0}\frac{a_0}{a_1} = \frac{u}{a_0}\sqrt{\frac{p_0 p_1}{p_1 p_0}} = \frac{u}{a_0}\sqrt{\frac{\xi(\mu+\xi)}{1+\mu\xi}} \qquad .$$

$$M = \frac{(\mu-1)(1-\xi)}{\sqrt{(\mu+1)(1+\mu\xi)}} \qquad . \qquad (28)$$

The last equation illustrates one of the more serious limitations of the shock tube as an intermittent supersonic wind tunnel. The Mach number of the flow, even for infinitely strong shocks, is limited to a comparatively low value.

$$\lim_{\xi \to 0} M = \frac{\mu-1}{\sqrt{\mu+1}} \qquad . \qquad (29)$$

For a diatomic gas with $\gamma = 1.40$ this limit is $5/\sqrt{7}$ or 1.89.

The obvious way to raise the Mach number limit in the hot flow of the shock tube is to use a gas with a lower specific heat ratio, that is, higher μ, in the expansion chamber. This was suggested by Mautz and Geiger[10,11,12] but no investigation of the consequences of such a substitution was made by them.

2. Shock Equations for a Gas with Temperature-Dependent Specific Heat

If a polyatomic gas is used in the expansion chamber of a shock tube, the assumption that the specific heat does not depend on temperature is not valid. Therefore, the basic conservation equations must be revised. Eqs 22 and 23, expressing the conservation of mass and momentum, are equations involving only the mechanical variables of the problem; and they are independent of any variation in the thermo-dynamic properties of the gas. The energy equation, on the other hand, must be rewritten, because the assumption of constant specific heat was fundamental to its derivation.

The energy balance for adiabatic flow can be stated as follows: The increase in kinetic plus internal energy of the gas must be equal to the work done on the gas by pressure forces.

$$d T + d E = d W .$$

The increase in kinetic energy per unit mass is udu, and the increase in internal energy for an ideal gas* is $C_v dT$.

In a one-dimensional flow the work done on the gas is

$$\frac{p}{\rho} - (p + dp)\left(\frac{1}{\rho} + d\left(\frac{1}{\rho}\right)\right) = - d\left(\frac{p}{\rho}\right) ;$$

---

* The ideal gas equation of state $P = RT\rho$ will be used throughout this discussion. This is valid to a very good approximation because the pressures found in the expansion chamber of the shock tube are always less than atmospheric. In the case of strong shocks, where the relative change in the state variables is large, the expansion chamber pressure is usually less than 1/50 of an atmosphere. Furthermore, molecular dissociation is also neglected because the maximum temperatures attained in the shock tube are below those at which dissociation becomes important for most gases.

where infinitesimals of higher order have been neglected. Thus

$$v \, dv + c_v \, dT + R \, dT = 0 .$$

This equation can be integrated from one side of a shock wave to the other.

$$\frac{1}{2}\left(V_0^2 - V_2^2\right) + \int_{T_2}^{T_0} c_p \, dT = 0 .$$

For convenience this can be written in a form similar to Eq 24.[20]

$$\frac{V_0^2}{2} + \int^{T_0} c_p \, dT = \frac{V_2^2}{2} + \int^{T_2} c_p \, dT .$$

The $\int^{T} c_p \, dT$ is a function of temperature which can be represented by

$$\int^{T} c_p \, dT = \beta(T) \, RT .$$

The lower limit of the specific-heat integral is arbitrary.

In general, the specific heat integrals or $\beta(T)$ must be determined experimentally. The usual procedure is to use infra-red spectroscopic data to assign frequencies to the various possible modes of molecular oscillation. The thermodynamic functions for the gas can then be calculated from the "zustandsumme" constructed from these frequencies. When necessary, corrections for anharmonicity can also be included. In most cases the specific heats calculated in this way are more accurate than direct thermal measurements.

---

[20] The following solution of the conservation equations is similar to that given by Bethe, H. E., and Teller, E., Deviations from Thermal Equilibrium in Shock Waves, Aberdeen Proving Grounds, Ballistic Research Laboratory, Report No. X-117.

32

For a diatomic gas like nitrogen, $\beta(T)$ may be represented by

$$\beta(T) = \frac{C_{pa}}{R} + \frac{\theta}{T}\frac{1}{e^{\frac{\theta}{T}}-1} \, ,$$

where C_{pa} is the specific heat at constant pressure associated with the translational and rotational degrees of freedom, and θ is a characteristic temperature of the gas. For polyatomic molecules more than one Einstein function will usually be needed to allow for the several modes of oscillation.

The three conservation equations take the form:

(30)

$$\frac{V_0^2}{2} + \beta_0 R T_0 = \frac{V_2^2}{2} + \beta_2 R T_2$$

$$\rho_0 V_0 = \rho_2 V_2$$

$$p_0 + \rho_0 V_0^2 = p_2 + \rho_2 V_2^2 .$$

The mass and momentum equations can be combined to give a relation involving only T and V.

$$V_0 \left(V_2^2 + R T_2 \right) = V_2 \left(V_0^2 + R T_0 \right) . \qquad (31)$$

Since β is usually a transcendental function of T, it is advisable to consider this system of equations as two equations in the four unknowns V_0, V_1, T_0, and T_1. An expression analogous to the Rankine-Hugoniot equation can then be derived, and the velocities on

each side of a shock wave can be determined from the temperatures assumed to exist in the two uniform regions.

Eqs 22 and 23 now constitute two equations in two unknowns which can be solved for the velocities. Let

$$V_0 = \frac{V_0}{V_2} V_2 = f V_2 .$$

Now solve for f by eliminating V_2 from the two equations.

$$V_2^2 = \frac{R(T_0 - f T_2)}{f(1-f)} . \tag{32}$$

As a result

$$f = \frac{V_0}{V_2} = b + \sqrt{b^2 + \frac{T_0}{T_2}} \tag{33}$$

where

$$b = \left(\beta_2 - \frac{1}{2}\right) - \frac{T_0}{T_2}\left(\beta_0 - \frac{1}{2}\right) .$$

The positive square root was chosen in Eq 33 to insure that the velocity ratio be greater than zero. Substituting Eq 33 in Eq 32 gives

$$V_2^2 = R T_2 \frac{2b + 1 - \frac{T_0}{T_2}}{\left(\frac{V_0}{V_2}\right)^2 - 1} . \tag{34}$$

When the temperatures on each side of the shock wave are given, Eqs 33 and 34 are in convenient form for calculation of the flow velocitites. The density and pressure ratios can then be found immediately by using the continuity equation and the equation of state.

As expected, Eq 33 reduces to the Rankine-Hugoniot equation when

$\beta_0 = \beta_2$, as shown in Appendix to Chapter III, page 54.

In order to calculate the Mach number of the flow behind the shock wave, it is necessary to change the frame of reference to one in which the gas in front of the shock is at rest. The flow velocity behind the shock becomes

$$u_2 = V_0 - V_2 ,$$

and the local Mach number is

$$M_2 = \frac{V_0 - V_2}{\sqrt{\gamma_2 R T_2}} , \tag{35}$$

where γ_2 is the value of γ corresponding to T_2.

A relation between p_0/p_3 and the shock Mach number, U/a_0, can also be derived easily. The assumption is made that the flow velocity and pressure are continuous across the contact surface which separates the gases initially in the expansion chamber from those from the compression chamber. Therefore, the velocity produced by the rarefaction wave must be equal to the flow velocity behind the shock wave. It is then possible to determine the pressure ratio across the rarefaction wave from the first part of Eq 13.

$$u_2 = \frac{2a_0}{\gamma - 1} \left[1 - \left(\frac{p_2}{p_3} \right)^{\frac{\gamma - 1}{2\gamma}} \right] .$$

Then

$$\frac{p_0}{p_3} = \frac{\frac{p_2}{p_3}}{\frac{p_2}{p_0}} . \tag{36}$$

3. Numerical Calculation of Shock Parameters for Various Real Gases

The methods outlined in the last section were used to calculate the characteristics of shock waves in carbon dioxide. The necessary values of β were obtained from enthalpy data given by Kassel.[21]

Table III contains values of β as a function of temperature for carbon dioxide, nitrogen, and sulfur hexafluoride. The values of flow velocity, temperature, pressure, density, Mach number, and required diaphragm pressure ratio for shock waves in carbon dioxide are tabulated in Table IV. The corresponding values calculated from the simple constant specific-heat equations are also included. The p_0/p_3 calculations were made assuming helium in the compression chamber in order to remove completely the complication of specific-heat or equation-of-state variations there. Figs. 4 - 8 show these shock wave characteristics as functions of the shock Mach number. The considerations which dictated this method of presentation of the data and the curves T_1/T_0, ρ_1/ρ_0, and p_1/p_0, also included in the figures, will be discussed in Chapter IV, Section 2.

Table V and Figs. 9 and 10 present similar information for shock waves in nitrogen. The values of $\beta(T)$ used in this calculation were taken from the Bethe and Teller report.

Table VI and Figs. 11 and 12 show shock characteristics in sulfur hexafluoride. The calculations were based on C_p values calculated by Meyer and Buell.[22]

---

[21] Kassel, Louis S., "Thermodynamic Functions of Nitrous Oxide and Carbon Dioxide", Journal of the American Chemical Society, 56, 1838 (1934).

[22] Meyer, Gerald E., and Buell, C. E., "Note on the Specific Heat of Sulfur Hexafluoride", Journal of Chemical Physics, 16, 744 (1948).

TABLE III

VALUES OF β FOR CARBON DIOXIDE, NITROGEN, AND SULFUR HEXAFLUORIDE

T_3	$\beta - CO_2$	$\beta - N_2$	$\beta - SF_6$
300	4.411	3.493	11.47
350			11.57
400	4.450	3.499	11.79
450			12.06
500	4.579	3.508	12.35
550			12.64
600	4.732	3.521	12.92
650			13.19
700	4.886	3.541	13.44
800	5.034	3.564	13.89
900	5.173	3.594	14.28
1000	5.302	3.625	
1100	5.421		
1200	5.531		
1250		3.702	
1300	5.632		
1400	5.725		
1500	5.811	3.780	
1750	5.999		

TABLE IV

SHOCK WAVE CHARACTERISTICS IN CO_2

$T_0 = 297°K$

	Variable Specific Heat							Constant Specific Heat				
T_3	$\dfrac{V_0}{a_0}$	$\dfrac{\rho_2}{\rho_0}$	$\dfrac{p_2}{p_0}$	M_2	$\dfrac{p_0}{p_3}$		T_2	$\dfrac{V_0}{a_0}$	$\dfrac{\rho_1}{\rho_0}$	$\dfrac{p_1}{p_0}$	M_1	$\dfrac{p_0}{p_3}$
300	1.013	1.035	1.045	0.037	.941		300	1.013	1.035	1.045	0.037	.941
400	1.710	2.399	3.229	0.859	.195		400	1.684	2.329	3.135	0.828	.204
500	2.337	3.674	6.185	1.319	.0712		500	2.252	3.351	5.641	1.217	.0828
600	2.876	4.699	9.493	1.615	.0340		600	2.712	4.041	8.163	1.435	.0451
700	3.364	5.533	13.050	1.824	.0188		700	3.102	4.596	10.84	1.581	.0272
800	3.798	6.226	16.78	1.982	.0113		800	3.454	4.992	13.46	1.680	.0180
900	4.204	6.814	20.68	2.109	.0070		900	3.770	5.302	16.07	1.754	.0126
1000	4.583	7.321	24.65	2.211	.0047		1000	4.064	5.552	18.69	1.813	.0091
1100	4.946	7.765	28.76	2.308	.0031		1100	4.339	5.755	21.32	1.862	.0069

limit Mach number $\dfrac{\mu-1}{\sqrt{\mu+1}}\,1 = 2.25$

FIG 4

SHOCK WAVE TEMPERATURE RATIO IN CO_2

FIG 5

P/P₀ RANKINE — HUGONIOT

P/ρ_0 RANKINE — HUGONIOT

ρ_1/ρ_0

ρ_2/ρ_0

SHOCK WAVE DENSITY RATIO

IN CO_2

U/a_0

DENSITY RATIO

FIG 6

SHOCK WAVE PRESSURE RATIO IN CO_2

P_2/P_0

P/P_0 RANKINE — HUGONIOT

P_1/P_0

PRESSURE RATIO

u/a_0

SHOCK WAVE FLOW MACH NUMBER IN CO_2

FIG 8

INITIAL PRESSURE RATIO

$H_E - CO_2$

P_0/P_3 TAUB

P_0/P_3

u/a_0

INITIAL PRESSURE RATIO
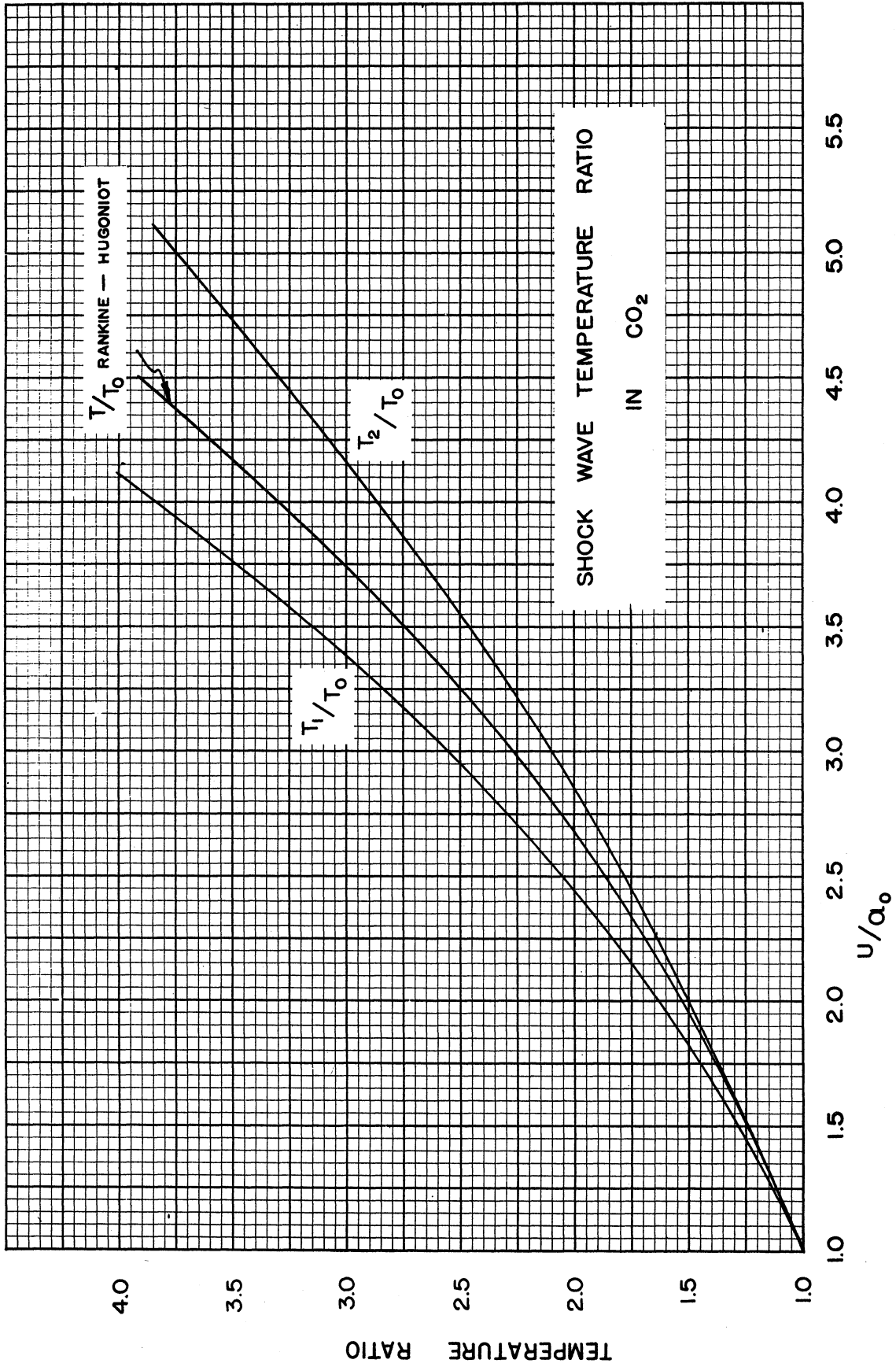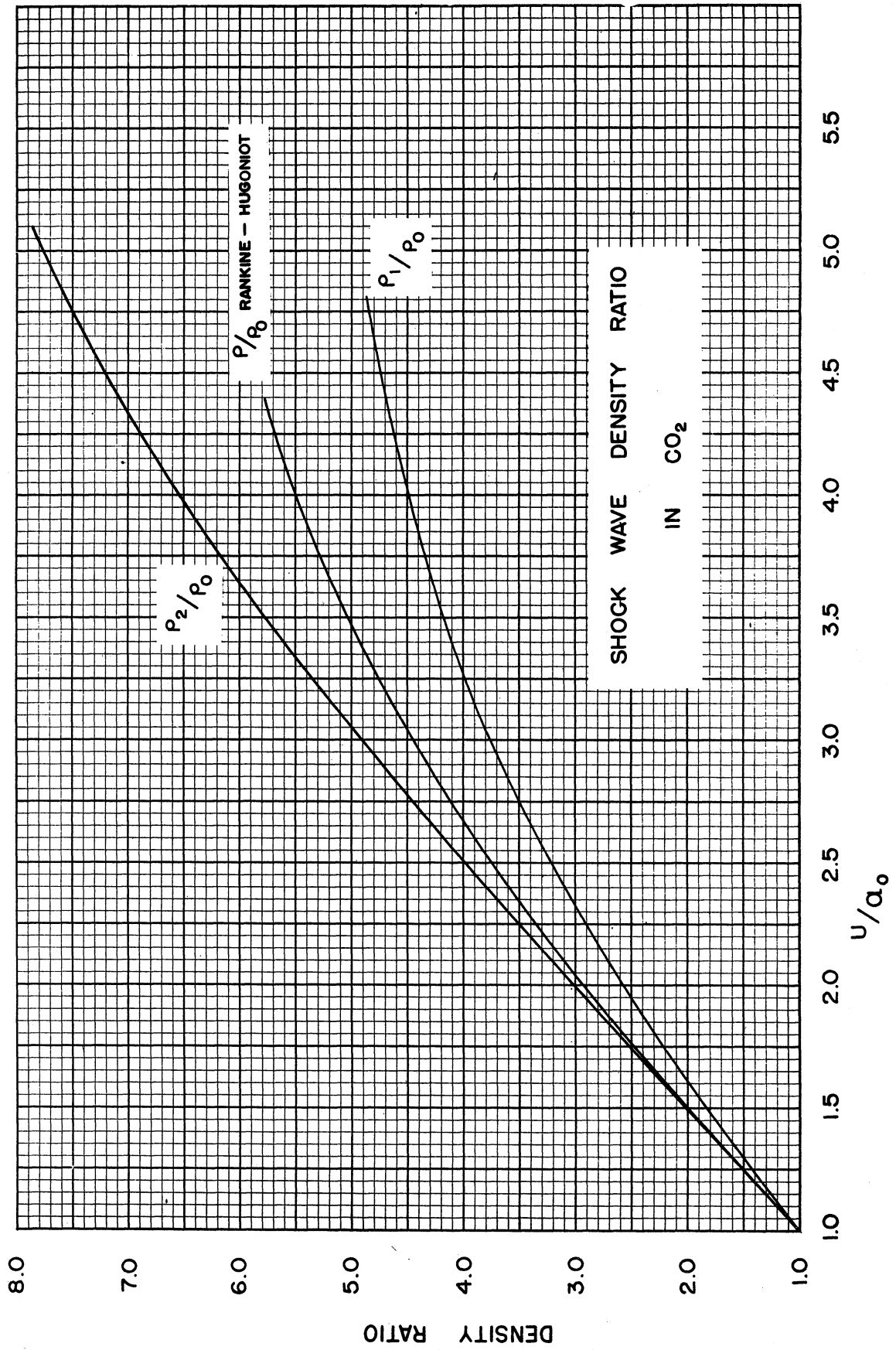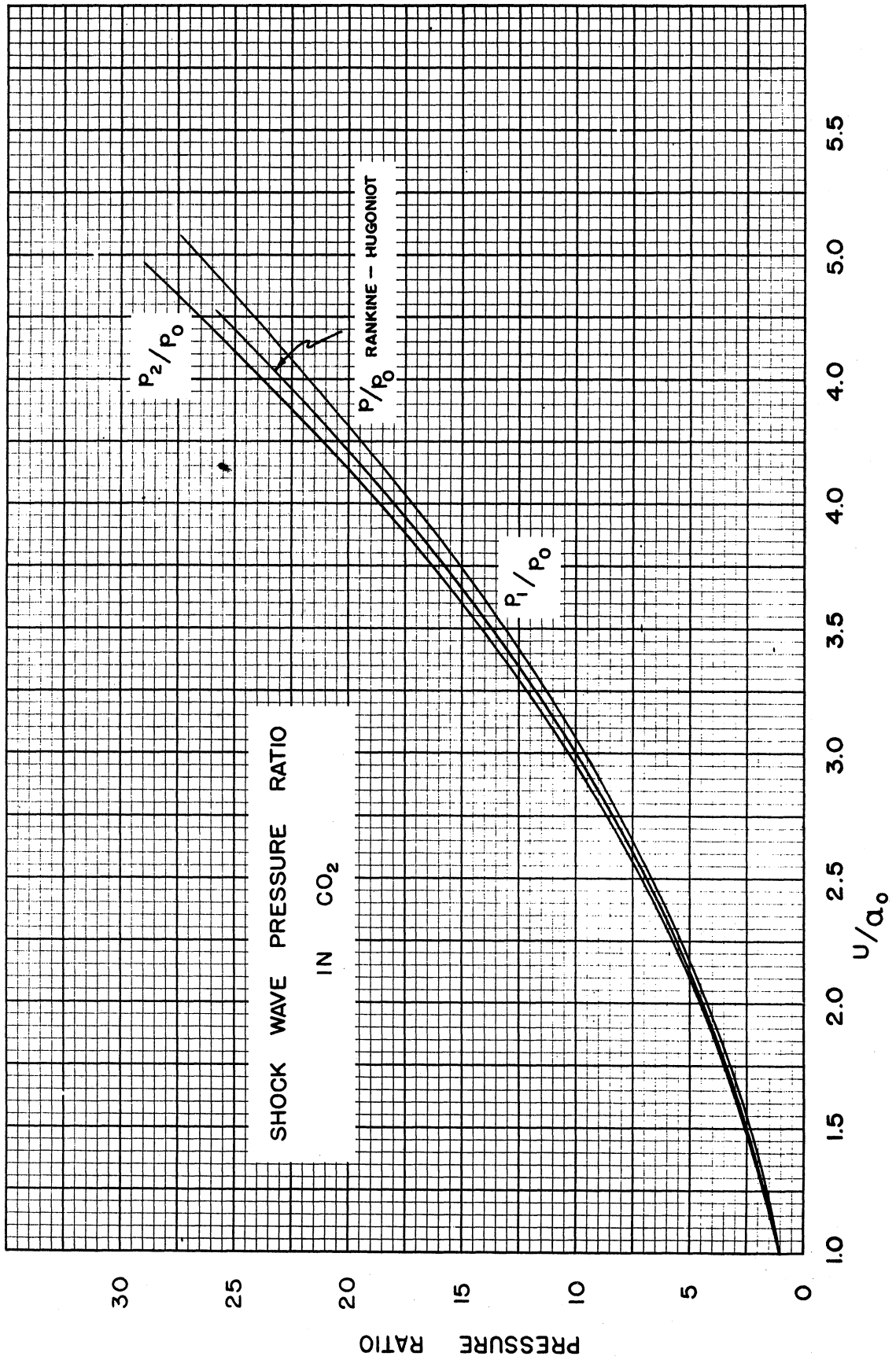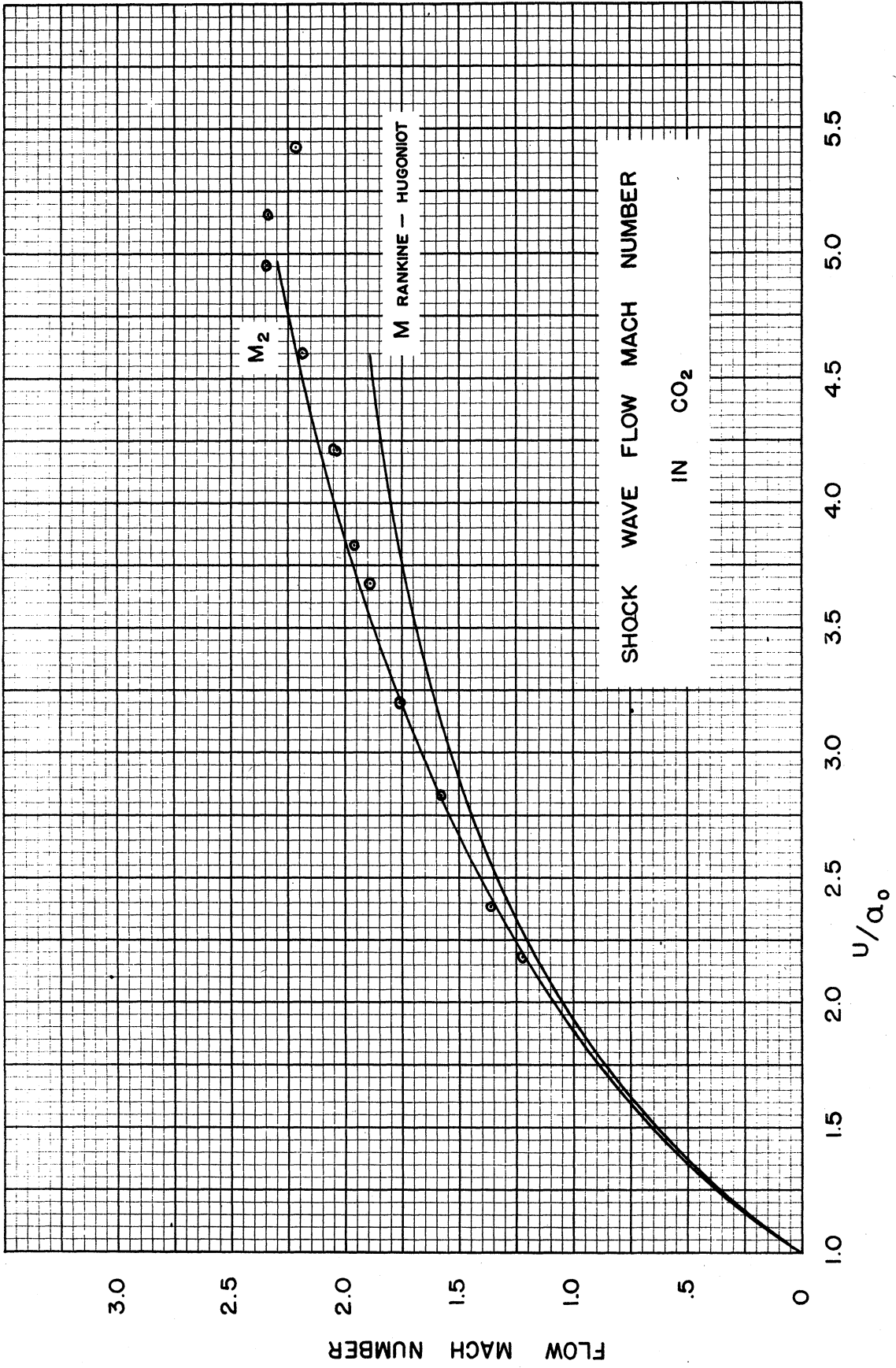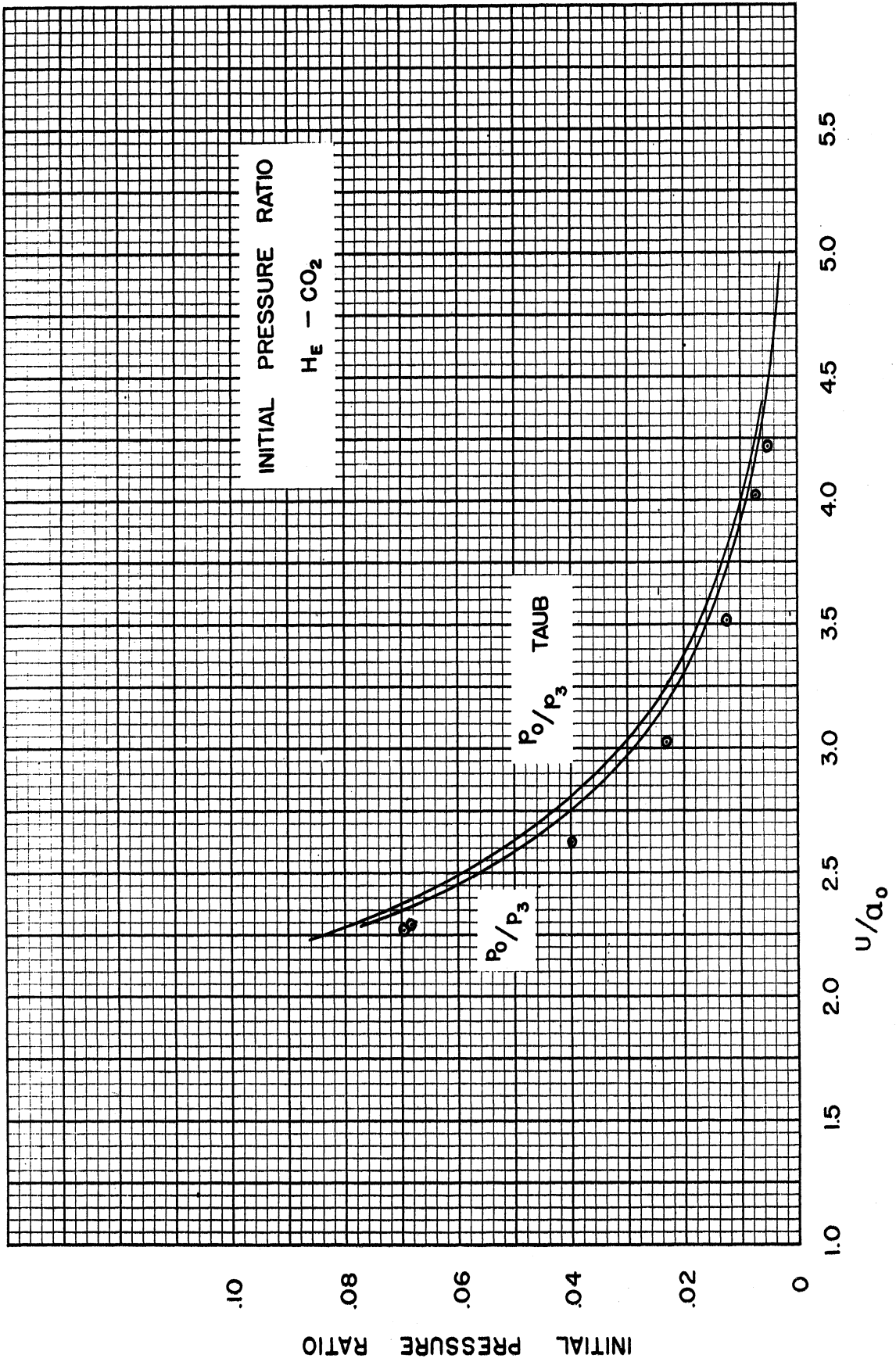
TABLE V

SHOCK WAVE CHARACTERISTICS IN N_2

$T_0 = 297°K$

T_2	Variable Specific Heat				Constant Specific Heat				
	$\frac{V_0}{a_0}$	$\frac{\rho_2}{\rho_0}$	$\frac{P_2}{P_0}$	M_2	$\frac{T_1}{T_0}$	$\frac{V_0}{a_0}$	$\frac{\rho_1}{\rho_0}$	$\frac{P_1}{P_0}$	M_1
400	1.540	1.937	2.608	0.6421	1.328	1.512	1.882	2.50	0.6189
500	2.000	2.682	4.515	0.9684	1.774	2.104	2.818	5.00	1.019
600	2.390	3.232	6.530	1.165	2.140	2.503	3.337	7.143	1.198
700	2.736	3.658	8.622	1.300	2.623	2.952	3.813	10.00	1.345
800	3.049	3.998	10.768	1.401	3.043	3.295	4.108	12.50	1.429
900	3.341	4.290	12.998	1.482	3.740	3.799	4.456	16.67	1.523
1000	3.616	4.538	15.278	1.549	5.132	4.645	4.871	25.0	1.629
1250	4.239	5.0291	21.166	1.676					
1500	4.798	5.4114	27.330	1.773					

FIG 9

SHOCK WAVE TEMPERATURE RATIO IN N_2

T/T_0 RANKINE — HUGONIOT

T_2/T_0

SHOCK WAVE DENSITY RATIO IN N_2

ρ_2/ρ_0

ρ/ρ_0 RANKINE — HUGONIOT

SHOCK WAVE PRESSURE RATIO IN N_2

P_2/P_0

P/P_0 RANKINE — HUGONIOT

PRESSURE RATIO

U/a_0

M_2

M RANKINE — HUGONIOT

SHOCK WAVE FLOW MACH NUMBER IN N_2

FLOW MACH NUMBER

U/a_0
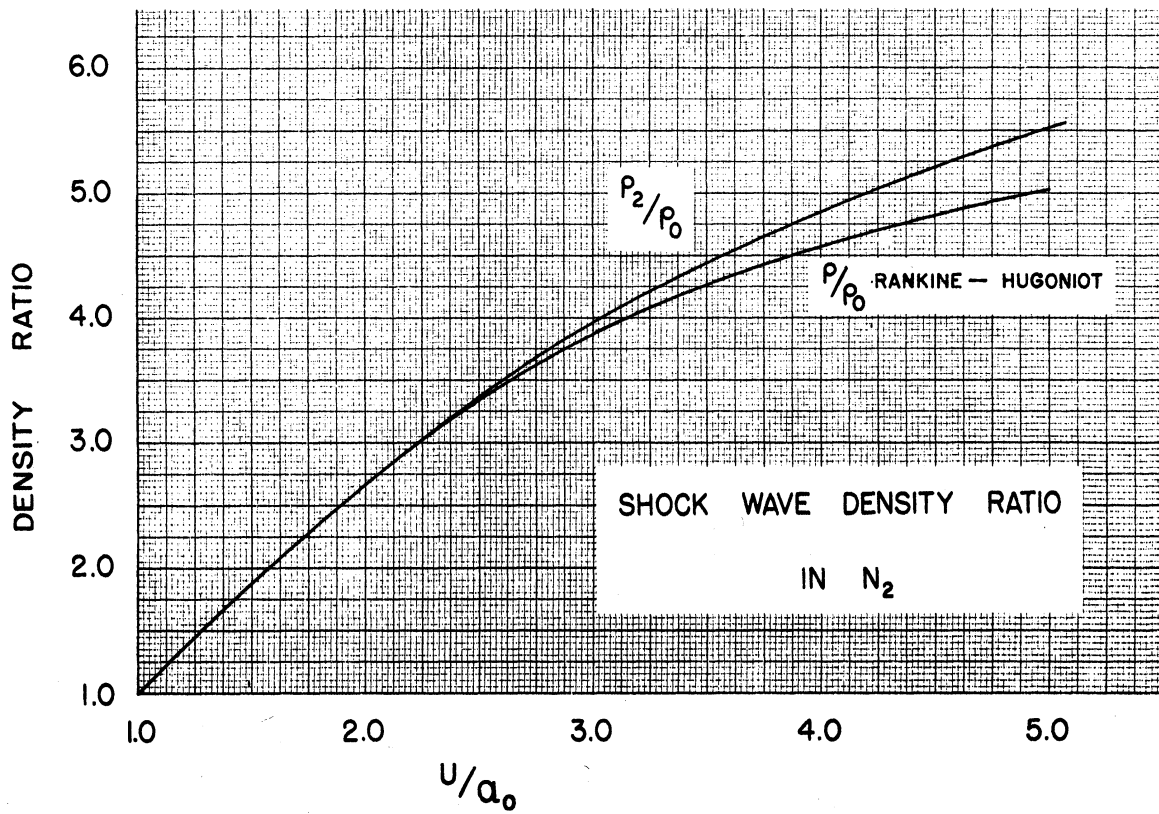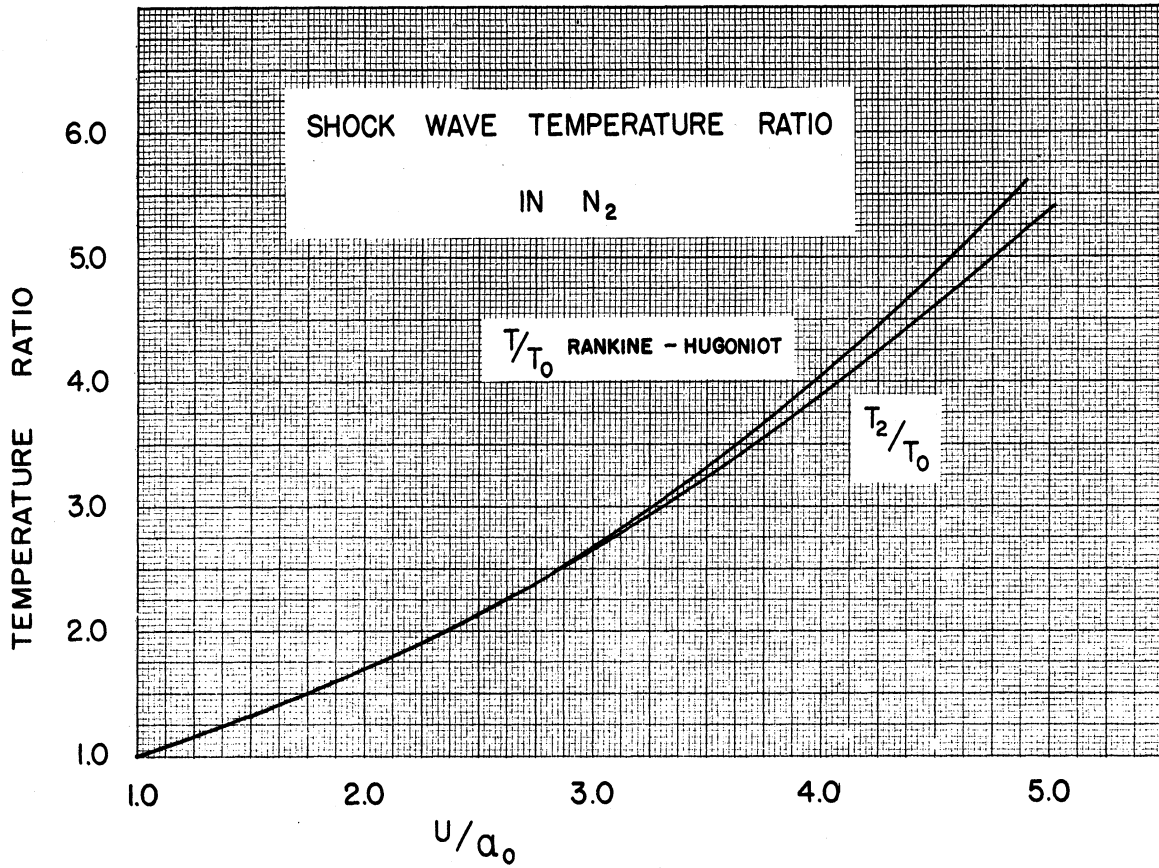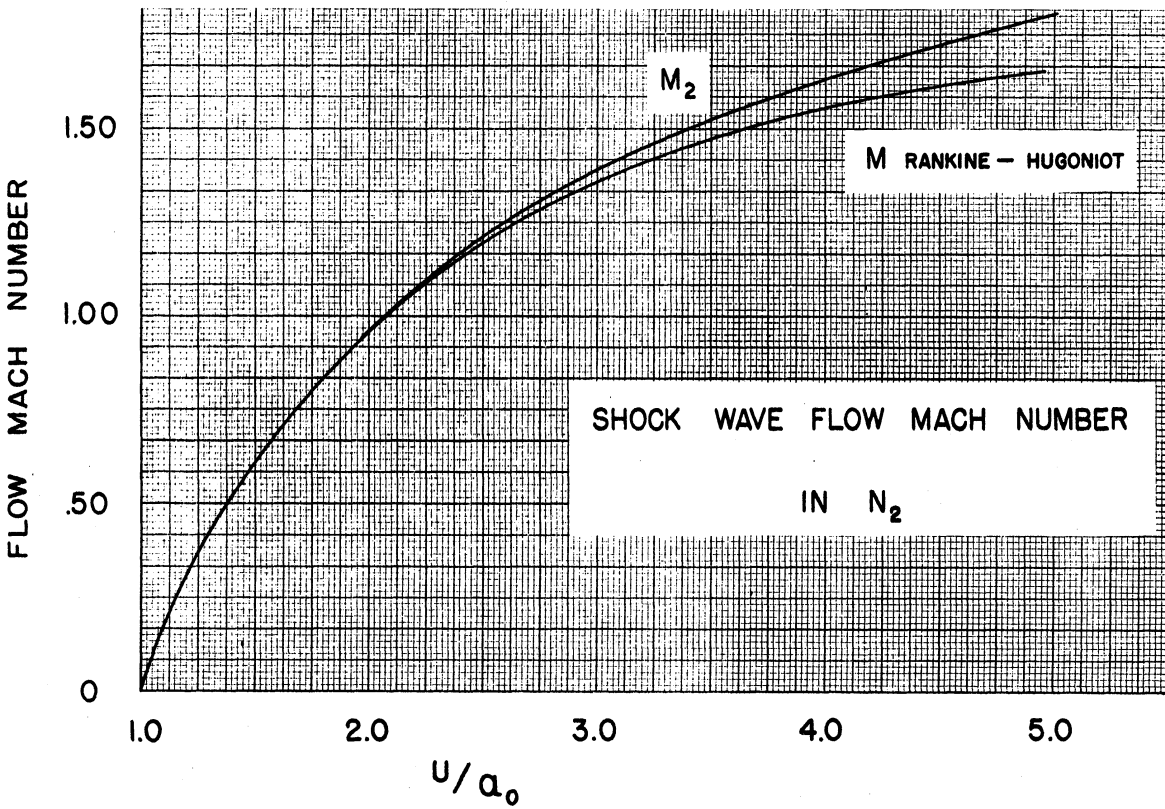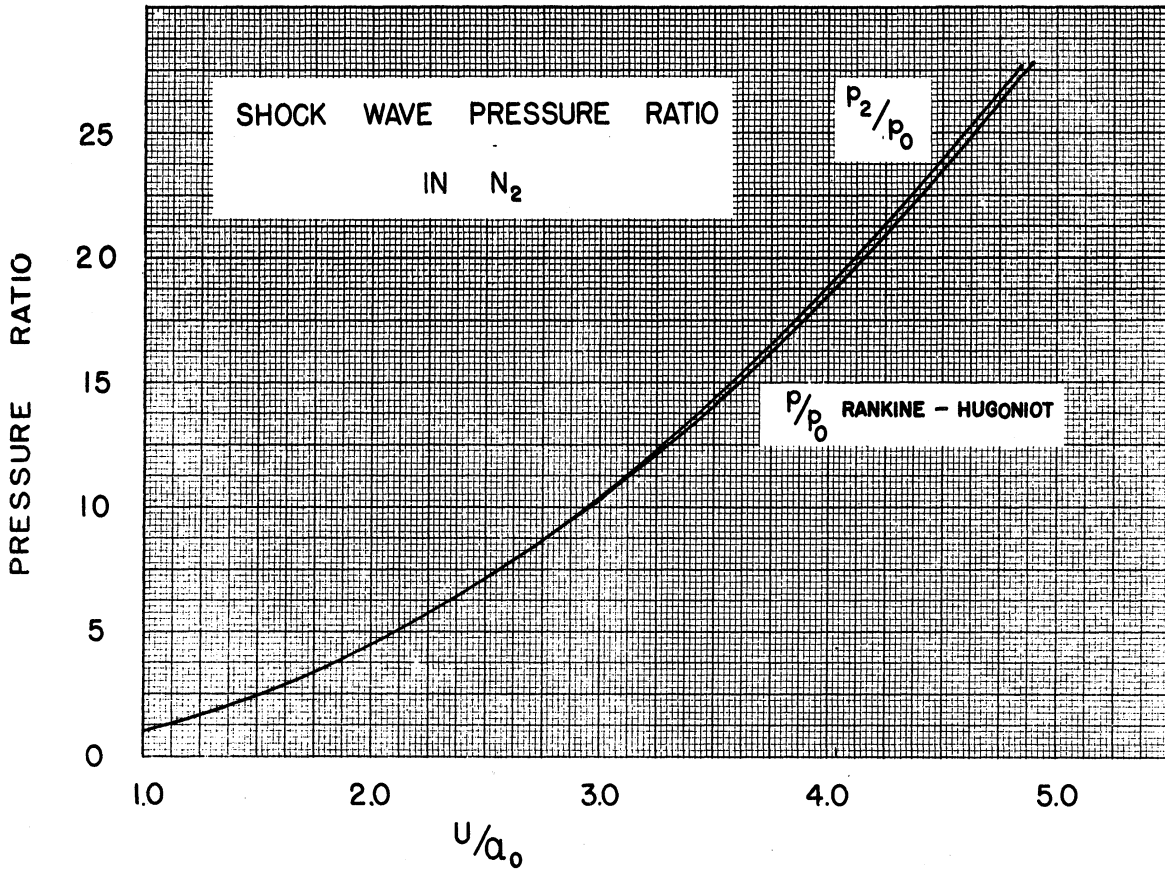
TABLE VI

SHOCK WAVE CHARACTERISTICS IN SF_6

$T_0 = 298°K$

	Variable Specific Heat					Constant Specific Heat			
T_3	$\frac{V_0}{a_0}$	$\frac{\rho_2}{\rho_0}$	$\frac{p_2}{p_0}$	M_2	T_2	$\frac{V_0}{a_0}$	$\frac{\rho_1}{\rho_0}$	$\frac{p_1}{p_0}$	M_1
325	1.556	2.285	2.492	.8386	325	1.538	2.244	2.447	.8146
350	2.043	3.691	4.335	1.378	350	1.994	3.503	4.114	1.311
375	2.471	5.063	6.372	1.778	375	2.381	4.674	5.882	1.663
400	2.854	6.351	8.525	2.087	400	2.719	5.724	7.682	1.932
425	3.205	7.551	10.77	2.343	425	3.022	6.663	9.504	2.144
450	3.531	8.76	13.09	2.561	450	3.297	7.500	11.33	2.319
475	3.837	9.703	15.47	2.748	475	3.553	8.252	13.16	2.466
500	4.126	10.68	17.92	2.913	500	3.790	8.931	14.99	2.591
525	4.404	11.60	20.43	3.061	525	4.015	9.544	16.82	2.707
550	4.667	12.44	22.96	3.191	550	4.228	10.11	18.65	2.796
575	4.927	13.27	25.61	3.315	575	4.431	10.62	20.49	2.882
600	5.165	13.98	28.15	3.410	600	4.626	10.89	21.93	2.953

SHOCK WAVE TEMPERATURE RATIO IN SF₆

T/T_0 RANKINE – HUGONIOT

T_2/T_0

TEMPERATURE RATIO

U/a_0

SHOCK WAVE DENSITY RATIO IN SF₆

ρ_2/ρ_0

ρ/ρ_0 RANKINE – HUGONIOT

DENSITY RATIO

U/a_0

FIG 12

SHOCK WAVE PRESSURE RATIO IN SF_6

SHOCK WAVE FLOW MACH NUMBER IN SF_6
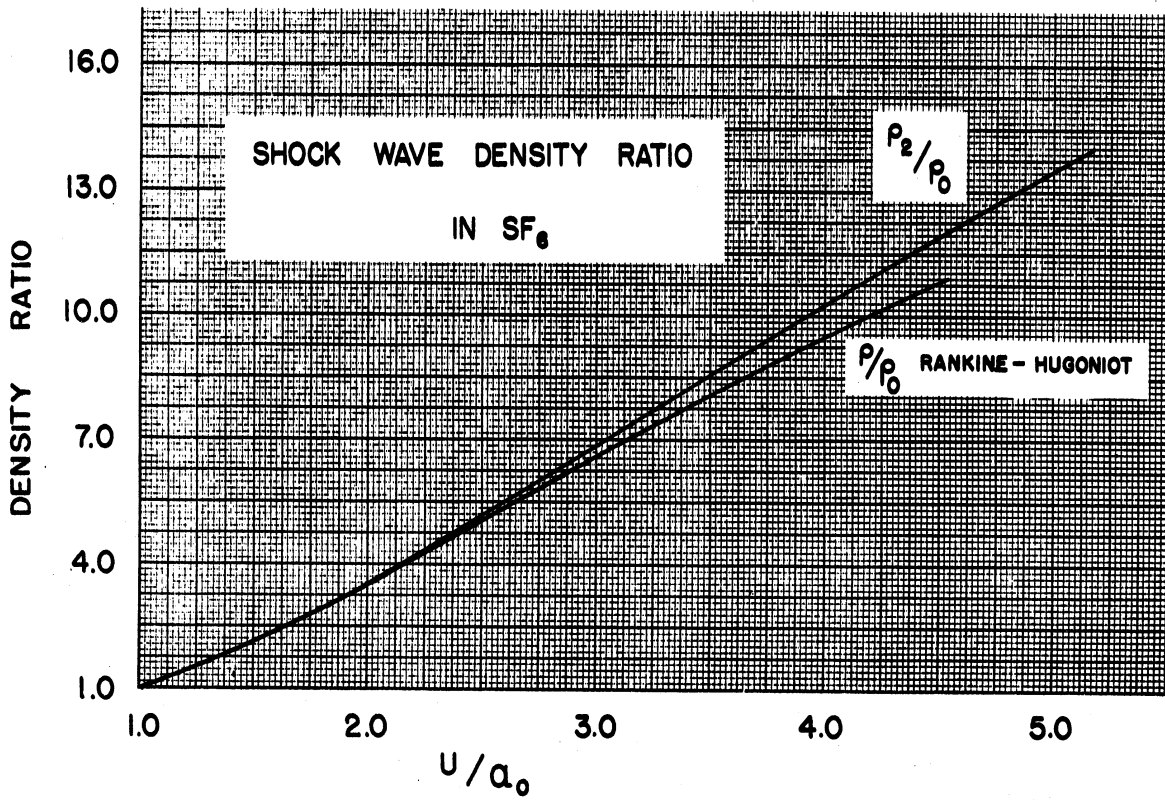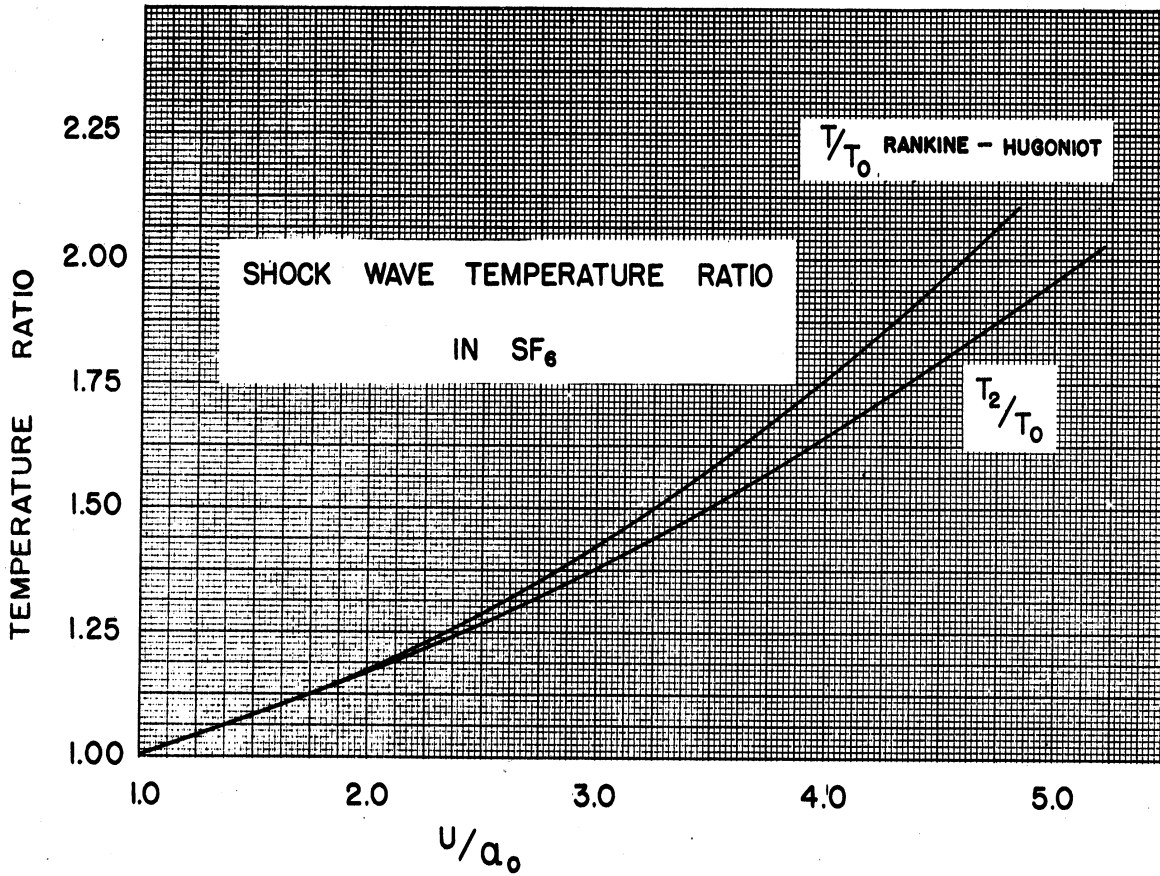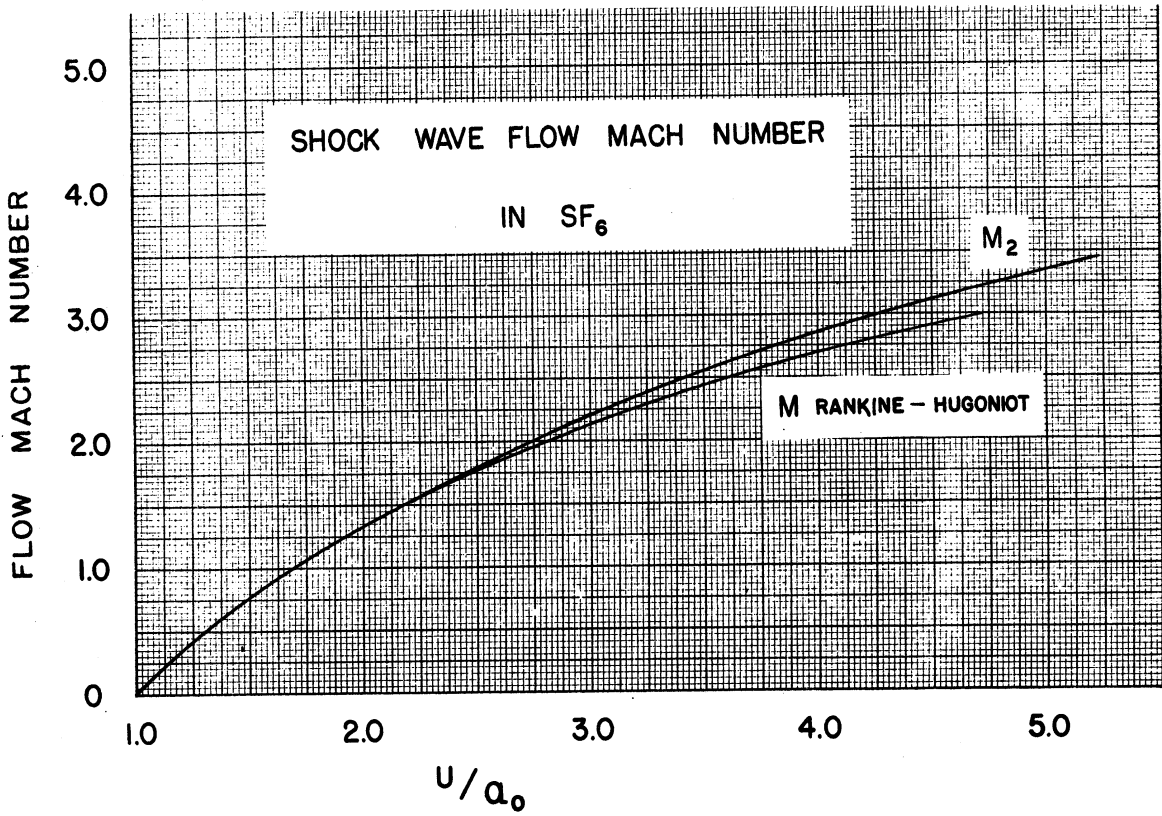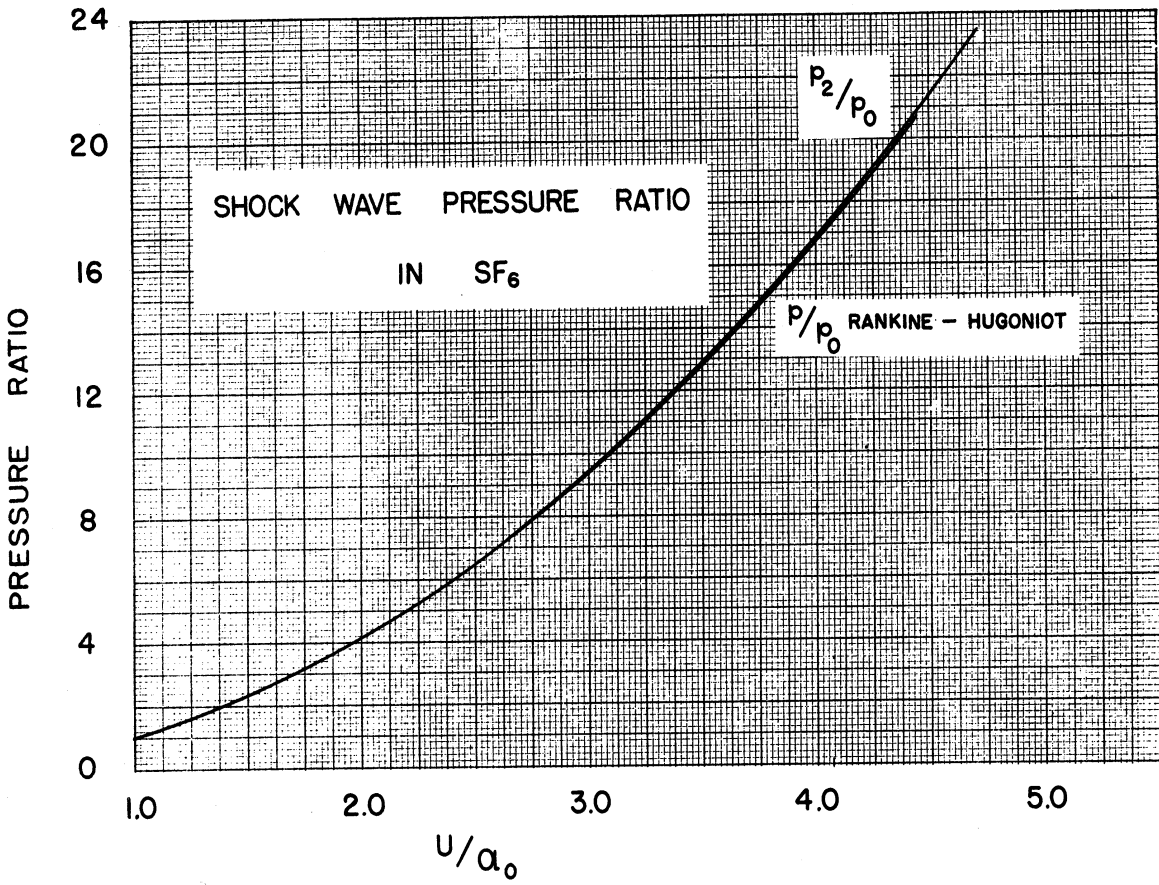
All the figures show that when weak shocks are considered there
is very little difference between the shock wave parameters calculated
from the usual Rankine-Hugoniot relations and those determined by con-
sidering temperature-dependent specific heat. However, the difference
becomes very pronounced for strong shock waves. The change in specific
heat that does occur is brought about by a temperature increase behind
the shock wave. From a generalization of Le Chatelier's principle, one
should expect the adjustment to cause the temperature behind the shock to
be lower than predicted by simple theory. This expectation is verified
by Fig. 4. Figs. 5 and 6 show that the pressure is slightly higher and
the density is much higher for a particular shock velocity than that
given by the Rankine-Hugoniot equations. The continuity equation pre-
dicts that if the density ratio across a shock increases, the velocity
ratio must decrease. Thus, the flow velocity behind a stationary shock
wave goes down; but, through the transformation to the laboratory frame
of reference, the flow velocity behind a shock is increased. Further-
more, the decrease in temperature coupled with the decrease of γ insures
the decrease in the speed of sound behind the shock wave. Thus, both
the increase in flow speed and the decrease in sound speed tend to cause
the Mach number to rise above that predicted by Eq 28. Finally, since in
the laboratory frame of reference the flow velocity behind the shock wave
increases as specific heat variations are considered, the pressure ratio
across the rarefaction wave must also increase to match this increased
flow speed. Therefore, p_0/p_3 must decrease as shown in Fig. 8.

These results can be summarized as follows: For a given shock
Mach number,

1. the temperature behind a shock wave is reduced considerably,

2. the pressure ratio across a shock wave increases slightly,

3. the density ratio across a shock wave increases,

4. the flow Mach number behind a shock wave is increased, and

5. the initial pressure across the diaphragm is decreased if the temperature dependence of specific heat is considered.

The changes in the flow parameters discussed above are not necessarily related in any way to changes produced by vibrational relaxation that actually do occur in the flow field behind a shock wave. This section has only compared two methods for calculating shock characteristics. See Chapter IV, Section 2.

Perhaps a word of explanation is in order at this point. It was shown in Chapter II that specific heat variations did not produce important perturbations on rarefaction waves. However, it has just been shown that shock wave parameters are definitely dependent on the specific heat behavior of the gas. This seemingly contradictory situation comes about because the temperature change across a shock wave is always much greater than the change across a rarefaction wave. Furthermore, the specific-heat changes produced by the shock wave result from the excitation of vibrational degrees of freedom, whereas the rarefaction wave can only partially "freeze out" the rotational contribution to the specific heat. In many cases, there are several vibrational modes to be excited, each contributing two degrees of freedom to the specific heat. In view of these facts, the importance of specific heat variations in the calculation of shock characteristics is intuitively obvious.

4. Experimental Verification of Variable Specific Heat Predictions

Because the duration of flow in the shock tube is so short, it
is impossible to measure the temperature or pressure behind the shock
wave precisely. The density could be determined if a Mach-Zehnder
interferometer were available. However, it is possible to determine the
flow Mach number with fair accuracy. This was done with carbon dioxide
in the expansion chamber in order to see if the results obtained agree
with the predictions of constant or variable specific heat theory.

The calibration was made by measuring the angle of a bow wave
attached to a 5° wedge parallel with the flow. This method was used in
spite of the fact that boundary layer on the wedge itself perturbs the
bow wave to such an extent that a calibration accurate to three or four
significant figures is impossible. In this instance, however, two sig-
nificant figures are sufficient to select between the constant and vari-
able specific heat predictions.

The semi-wedge angle, bow-wave angle, ratio of specific heats,
and stream Mach number are related by the following expression:[23]

$$M_2^2 = \frac{2(\cot\theta + \tan\delta)}{\sin 2\theta - \tan\delta(\gamma + \cos 2\theta)} \tag{37}$$

where the angles are as indicated in Fig. 13, page 52. Note that M_2 is
almost independent of γ for small δ .

The results of this calibration experiment are given in Table
VII and the points are plotted in Fig. 7.

[23] Notes and Tables for Use in the Analysis of Supersonic Flow, by the
Staff of the Ames 1 x 3 ft Supersonic Wind-Tunnel Section, NACA, TN
1428 (1947).
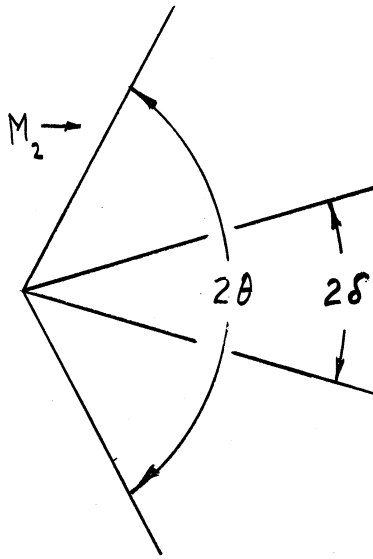
Fig. 13
Bow Wave Attached to a Wedge

As expected, these results agree quite well with the Mach number predicted by considering the specific heat to be a function of temperature. The fact that two of the experimental points lie above the maximum Mach number predicted by the Rankine-Hugoniot theory is particularly significant.

TABLE VII

FLOW MACH NUMBER BEHIND SHOCK WAVES IN CO_2

U/a_0	θ	δ	M_0
2.18	58.75°	2.50°	1.23
2.38	50.25	2.50	1.37
2.83	41.75	2.50	1.58
3.20	36.50	2.50	1.77
3.83	32.50	2.50	1.96
4.22	31.25	2.50	2.04
4.22	31.0	2.50	2.05
4.61	29.0	2.50	2.19
4.96	27.25	2.50	2.32
5.16	27.0	2.50	2.34
5.43	28.5	2.50	2.22

It was also possible to check the p_0/p_2 versus shock Mach number curves. The results of this series of experiments are plotted in

Fig. 8. Unfortunately, there are two factors other than specific-heat variations which influence this experiment. First, in the derivation of the Taub equation, an ideal diaphragm is assumed to be removed instantaneously at the start of the flow in the tube. This situation is never found in practice, of course. The energy required to shatter the diaphragm and accelerate the resultant fragments must be subtracted from the flow. In addition, the interface between expansion and compression chamber gases is highly turbulent. Therefore, it is not unreasonable to expect that the strength of a shock wave produced by a given initial pressure ratio will be less than predicted. This argument has been used by all shock tube investigators to explain the discrepancy between theoretical and experimental shock strength determinations. Second, the compression chamber of the shock tube at the University of Michigan is about two per cent narrower than the expansion chamber. The strength of the shock wave produced by a given initial pressure ratio is further reduced as a result.

These last two factors affecting the shock strength are apparently more important than specific heat variations. Therefore, all that can safely be said about these experiments is that the results fall on the right side of the theoretical curve.

APPENDIX TO CHAPTER III

PROOF OF THE EQUIVALENCE OF THE RANKINE-HUGONIOT EQUATION

AND THE SHOCK EQUATION

FOR A GAS WITH VARIABLE SPECIFIC HEAT IN THE LIMIT $\beta_2 = \beta_0$

The Rankine-Hugoniot equation can be written in terms of velocity and temperature ratios as follows:

$$\frac{V_0}{V_1} = \frac{\rho_1}{\rho_0} = \frac{\mu + \frac{\rho_0 T_0}{\rho_1 T_1}}{1 + \mu \frac{\rho_0 T_0}{\rho_1 T_1}}$$

This equation can be solved for the velocity ratio.

$$\frac{V_0}{V_1} = \frac{1}{2} \left[\mu \left(1 - \frac{T_0}{T_1} \right) + \sqrt{\mu^2 \left(1 - \frac{T_0}{T_1} \right)^2 + 4 \frac{T_0}{T_1}} \right]$$

If $\beta_2 = \beta_0$, Eq 33 becomes

$$\frac{V_0}{V_2} = b + \sqrt{b^2 + \frac{T_0}{T_1}}$$

where

$$b = \frac{1}{2} \mu \left(1 - \frac{T_0}{T_1} \right)$$

Thus

$$\frac{V_0}{V_2} = \frac{1}{2} \left[\mu \left(1 - \frac{T_0}{T_1} \right) + \sqrt{\mu^2 \left(1 - \frac{T_0}{T_1} \right)^2 + 4 \frac{T_0}{T_1}} \right]$$

Q.E.D.

IV. VIBRATIONAL RELAXATION

1. General Discussion of Vibrational Relaxation

The specific heat variations discussed in the last chapter result

from the excitation of vibrational degrees of freedom within the molecule.

This variation is described by Einstein's specific heat theory in which

the vibrational degrees of freedom are treated as quantized harmonic os-

cillators. However, this is an equilibrium theory; i.e., a theory which

predicts the energy contained in the harmonic oscillators in equilibrium

with a particular temperature, defined in terms of the average kinetic

energy of translation of the molecules. When abrupt temperature changes

occur, this equilibrium distribution will be temporarily disturbed. The

remainder of this section will discuss the mechanism whereby equilibrium is

re-established and define a relaxation time related to the rate of read-

justment.

If the temperature of a volume of gas is suddenly increased,

the tacit assumption is that energy has been supplied to the translational

degrees of freedom of the molecules. The fundamental problem is now to

determine the probability for the transfer of some of this energy to the

rotational and vibrational degrees of freedom of the molecule.

Landau and Teller[24] postulated that the efficiency of a colli-

sion in exciting a degree of freedom is indicated by the ratio

$$\chi = \frac{\tau_c}{\tau_o} \qquad (38)$$

---

[24] Landau, L., and Teller, E., "Zur Theorie der Schalldispersion",
Physikalische Zeitschrift der Sowjetunion, 10, 34 (1936).

where τ_c is the effective duration of the collision and τ_o is the natural period for the degree of freedom. It is intuitively obvious that this ratio should be closely related to the transition probability because it represents in a simple way the departure from adiabatic conditions during the collision. If χ is of the order of unity or smaller, only a few collisions will be required to excite the degree of freedom; but if χ is much greater than unity, many hundreds of thousands of collisions will be required to effect the transfer of a quantum from the translational to some other degree of freedom. In general τ_c will be approximately a/V, where a is the radius of interaction and V the relative molecular velocity.

When molecular rotation is considered, τ_o is the time for one revolution. This time will be of the order of the distance of an atom from the center of mass divided by the velocity of the atom about the center of mass. It follows from the equipartition principle that the velocity of the atom about its center of mass must be of the order of its translational velocity. Furthermore, the radius of the molecule will be approximately equal to or greater than its range of interaction. It follows, therefore, that $\chi \lesssim 1$ for molecular rotation. As a result, molecular collisions will fully excite a rotational degree of freedom within several mean free paths.

For a vibrational degree of freedom, τ_o is the inverse of the frequency of oscillation, ν; and in this case χ becomes

$$\chi \approx \frac{\nu a}{V}$$

Nitrogen may be considered as an example. If the relative kinetic energy of the colliding particles is kT, then V = 7 x 10^4 cm/sec at room temperature; the vibrational frequency is ν = 7 x 10^{13} sec^{-1}; and the molecular radius is approximately a $\approx$ 1.6 x 10^{-8} cm. Thus for nitrogen

$$\chi \approx \frac{7 \times 10^{13} \times 16 \times 10^{-8}}{7 \times 10^4} = 16.$$

Since χ is an order of magnitude larger than 1, many thousands of collisions will be required to excite the molecular vibration; or, in other words, the probability for the transfer of energy from translation to vibration is very small. An analogous situation would arise in an attempt to excite a tuning fork by striking it with a very soft rubber mallet.

The translational and rotational degrees of freedom can be considered as active degrees because, to a first approximation, they are always in equilibrium with the temperature. All other degrees of freedom, vibration, dissociation, and electronic excitation will not always be in equilibrium with rapid temperature changes. These shall be called inert degrees of freedom.

When $\chi \gg$ 1, Landau and Teller have shown that the probability of de-exciting a vibrational state in a collision is

$$p_{10} = C \, e^{-\frac{a\nu}{V}}, \tag{39}$$

where C is a geometric factor assumed arbitrarily to be 1/10.[19] If this probability is averaged over a Maxwellian velocity distribution, the average de-excitation probability per collision is

$$p_{10} = \frac{4}{3^{\frac{3}{2}}} \sigma \, e^{-\sigma}, \tag{40}$$

where
$$\sigma = \frac{3}{2} (a\nu)^{\frac{2}{3}} \left(\frac{m}{kT}\right)^{\frac{1}{3}}$$

and m is the molecular mass.

The de-excitation probability per second is more useful than the probability per collision. If N is the number of collisions per second,

$$K_{10} = p_{10} N .$$

The probability of excitation per second can be obtained immediately by using the statistical principle of detailed balancing which states that, in equilibrium, the number of molecules that return to the ground state from the first excited state per second is equal to the number raised to the first excited state in the same time. Thus,

$$K_{10} e^{-\frac{h\nu}{kT}} = K_{01} . \tag{41}$$

If the vibrational degree of freedom is considered as a linear harmonic oscillator, the transition probability from a higher excited state can be shown to be

$$K_{n,n-1} = n K_{10} . \tag{42}$$

Again, using the principle of detailed balancing

$$K_{n,n-1} e^{-\frac{h\nu}{kT}} = K_{n-1,n} .$$

Only transitions between neighboring levels are allowed.

As a consequence, the time rate of change of the number of molecules, y_0, in the ground state is

$$\frac{dy_0}{dt} = k_{10} y_1 - k_{01} y_0 \, ,$$

and the time rate of change of the number of molecules, y_n, in the nth excited state is

$$\frac{dy_m}{dt} = k_{m+1,m} y_{m+1} + k_{m-1,m} y_{m-1} - \left(k_{n,m+1} + k_{m,m-1} \right) y_m. \quad (43)$$

Except for an unimportant zero-point contribution, the vibrational energy in the nth excited state is

$$E_v^m = h\nu \, n \, y_m$$

and the total vibrational energy of the system is

$$E_v = h\nu \sum_{m=1}^{\infty} n \, y_m. \quad (44)$$

The rate of change of vibrational energy,

$$\frac{dE_v}{dt} = h\nu \sum_{m=1}^{\infty} n \, \frac{dy_m}{dt} \, ,$$

can be determined by summing Eq 43 over all possible states. The result of this summation is,

$$\frac{dE_v}{dt} = k_{10} \left(1 - e^{-\frac{h\nu}{kT}} \right) \left(E_v' - E_v \right) \quad (45)$$

where E_v' is the vibrational energy in equilibrium with the local temperature as determined from the Einstein formula.

$$E_v' = \frac{n \, h\nu}{e^{\frac{h\nu}{kT}} - 1}$$

where n is the number of molecules in the gas; $n = \sum_n y_n$.

The relaxation time for the excitation of a vibrational degree of freedom can be defined from Eq 45 by letting

$$\frac{1}{\tau} = K_{10}\left(1 - e^{-\frac{h\nu}{kT}}\right). \tag{46}$$

Therefore, the fundamental equation describing the time rate of change of vibrational energy is

$$\frac{dE_V}{dt} = \frac{E_V' - E_V}{\tau} , \tag{47}$$

where

$$\tau = \frac{1}{\frac{2}{\sqrt{3}}N(a\nu)^{\frac{2}{3}}\left(\frac{m}{kT}\right)^{\frac{1}{3}} e^{-\frac{2}{3}(a\nu)^{\frac{2}{3}}\left(\frac{m}{kT}\right)^{\frac{1}{3}}}\left(1 - e^{-\frac{h\nu}{kT}}\right)}$$

The temperature dependence of τ is determined mainly by the factor $e^{T^{-\frac{1}{3}}}$.

2. The Effect of Vibrational Relaxation on Shock Waves

A shock wave is considered to be a surface of discontinuity in the usual mathematical treatments based on a continuum theory of an ideal fluid. For a molecular point of view, however, the thickness of a shock wave must be of the order of several mean free paths because at least one or two collisions are required to establish a new Boltzmann distribution of translational energy behind the shock wave. In the last section it was shown that the rotational degrees of freedom of a molecule can usually be excited by several collisions; or in this case, within the thickness of the shock wave or at least within a distance very small compared to the dimensions of a shock tube experiment.

A much different situation can exist, however, for the vibrational degrees of freedom. Many thousands of collisions may be required

to excite the vibrational states of some molecules. In this case, no change in the vibrational energy can occur within the thickness of the shock wave.

However, if a stationary shock wave is considered, the equations for the conservation of mass, momentum, and energy must be satisfied throughout the entire flow.
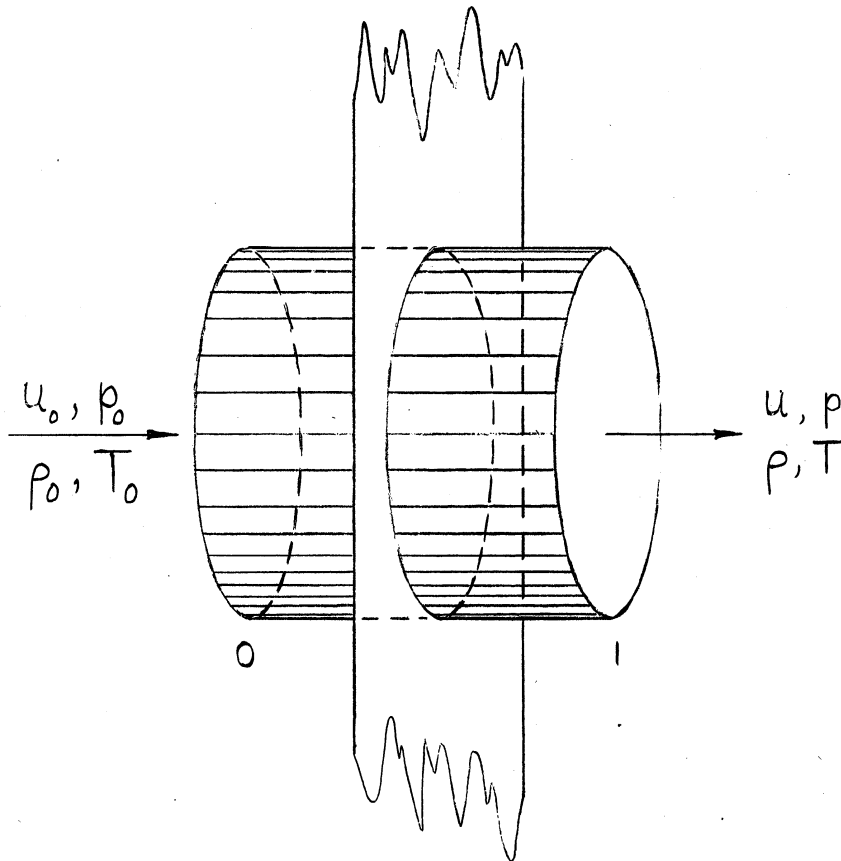
Fig. 14

"Pillbox" through a Shock Wave

In other words, the conservation laws may be applied to the ends of a "pillbox" of arbitrary length. Thus, in Fig. 14, as the surface, 1, is moved away from the shock wave downstream, the vibrational degrees of freedom gradually come into equilibrium. As they absorb energy from the active degree of freedom, the temperature of the flow will decrease, and the other shock wave characteristics will also be changed. Far downstream,

where equilibrium has been established between vibration, rotation, and translation, the specific heat of the gas will assume the equilibrium value associated with the flow temperature. The shock wave characteristics will then be the limit values as calculated from Eqs 33 and 34 of Chapter III.

Immediately behind the shock wave, for a gas with a long relaxation time, the conservation of energy equation can be written as

$$\frac{V_0^2}{2} + C_{pa} T_0 + E_V = \frac{V_1^2}{2} + C_{pa} T_1 + E_V \qquad (48)$$

where $C_{pa}T$ is the kinetic energy of the active degrees of freedom and E_V is the vibrational energy which is assumed not to vary through the shock wave. C_{pa} is 7/2 R for all diatomic and linear molecules and 4R for all polyatomic molecules with three degrees of rotational freedom. The three conservation equations can be written as

$$\frac{V_0^2}{2} + (\mu+1)\frac{p_0}{\rho_0} = \frac{V_1^2}{2} + (\mu+1)\frac{p_1}{\rho_1} \qquad (49)$$

$$\rho_0 V_0 = \rho_1 V_1$$

$$p_0 + \rho_0 V_0^2 = p_1 + \rho_1 V_1^2 .$$

μ = 6 for linear molecules, and μ = 7 for general polyatomic molecules. The Rankine-Hugoniot equations can be obtained immediately as discussed in Chapter III. It should be noted that the velocity of sound should now be calculated by considering only the active degrees of freedom.

The surprising result now emerges that the flow velocities, temperature, pressure, and density ratios across a shock wave are identical for all diatomic and linear molecules; the sonic velocity is different for each gas, however. A similar but numerically different relation holds for all general polyatomic molecules. It should be repeated, however, that this result is valid only when the vibrational energy can be assumed constant across a shock wave. If the relaxation time is very short, no general relations can be derived for the shock wave characteristics immediately behind the shock without a detailed consideration of the shock wave from a gas-kinetic point of view. To a first approximation, the relaxation time must be very much greater than 10^{-9} second if the analysis above is to be valid. Inspection of the relaxation times listed in Table IX, pages 77 and 78, shows that this condition is not satisfied for some polyatomic gases.

The values of the temperature, density, and pressure ratios that exist just behind shock waves in carbon dioxide have been included in Figs. 4 through 6. Thus, for a particular shock velocity, the flow parameters change abruptly to the values indicated by subscript 1. They then change slowly to the equilibrium values, 2.

It is interesting to note that the pressure behind a shock wave in carbon dioxide changes only slightly, while the initial density and temperature ratios may differ by approximately 50 per cent from their equilibrium values. The Rankine-Hugoniot values based on room-temperature specific heat may be considered roughly an average between the actual initial and final values for carbon dioxide. The Rankine-Hugoniot values plotted for nitrogen represent also parameters immediately behind

the shock wave because the vibrational degree of freedom is essentially

not excited at room temperature. No attempt has been made to calculate

the shock wave parameters immediately behind a shock wave in sulfur hexa-

fluoride because relaxation time data are not available. As a rule of

thumb, however, the relaxation time is very short whenever the change in

specific heat is large. Therefore, it may not be safe to assume that the

relaxation time for sulfur hexafluoride is very large compared to 10^{-9}

second.

The regions of flow in the ideal shock tube can be summarized

by referring to the plot of pressure against position shown in Fig. 15.

The constant initial pressure in the expansion chamber extends to the

shock wave. Immediately behind the shock the pressure is p_1, as calcu-

lated above. The pressure gradually rises to its equilibrium value, p_2,

far behind the shock wave. This limit value is maintained until the foot

of the rarefaction wave is reached. The pressure than increases through

the rarefaction wave up to the initial compression chamber value, p_3. A

more complete picture of the various flow regions in a shock tube may be

gained by reference to the x-t diagram of shock tube flow shown on page 74.

3. Approximate Calculation of the Time Dependence of the Flow Parameters Behind a Shock Wave

If the temperature changes that occur in the flow region behind

a shock wave are assumed small, so that the relaxation time, equilibrium

vibrational energy, and total internal energy of the flow behind the

shock wave may be considered constant, Eq 47 can be integrated immediately.

FIG 15
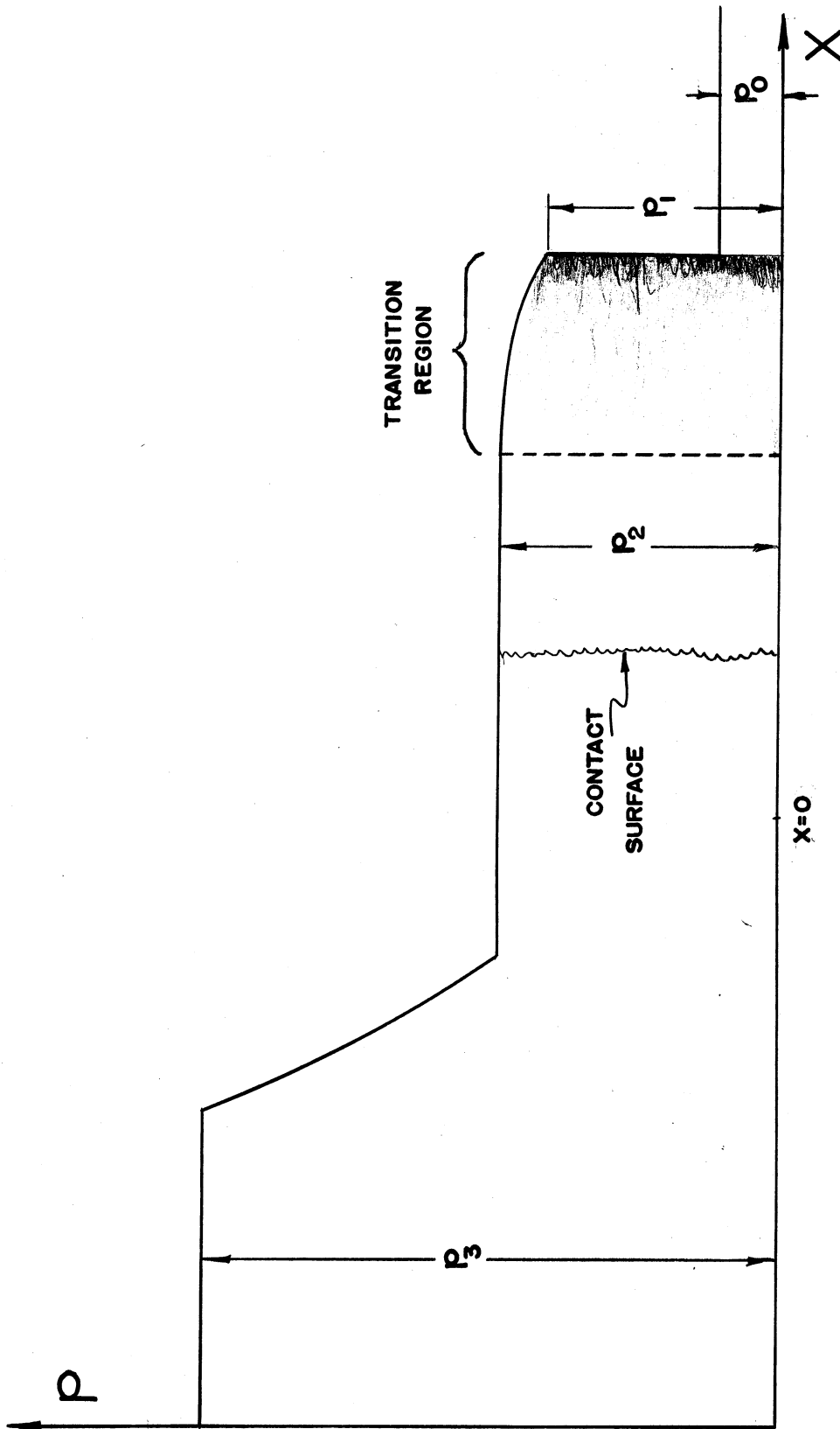
VARIOUS FLOW REGIONS IN A SHOCK TUBE

Thus

$$E_v - E_{v_2}' = \left(E_{v_0}' - E_{v_2}'\right) e^{-\frac{t}{\tau}}$$ (50)

where E_{v_α}' is the vibrational energy in equilibrium with the temperature in region α. The total internal energy of the flow is assumed constant, so that variations in E_v are compensated by variations in the opposite direction in the energy of the translational and rotational degrees of freedom, E_a. The local temperature can be defined in terms of the energy in these latter degrees of freedom. C_{va} is the constant specific heat associated with these degrees of freedom.

$$T = \frac{E_a}{C_{va}}$$

Thus

$$T = \frac{1}{C_{va}} \left(E - E_v\right) .$$

$$T = \frac{1}{C_{va}} \left[E - E_{v_2}' - \left(E_{v_0}' - E_{v_2}'\right) e^{-\frac{t}{\tau}} \right] .$$

Because there is not time for the vibrational energy of the gas to change as it passes through the shock wave

$$T_1 = \frac{E - E_{v_0}'}{C_{va}} .$$

Therefore,

$$T - T_2 = \left(T_1 - T_2\right) e^{-\frac{t}{\tau}} .$$ (51)

Thus, under these assumptions, the temperature behind a shock wave changes exponentially from its initial to its final value.

The flow velocity can be determined as a function of time from the conservation equations for mass and momentum.

$$\frac{RT}{V} + V = \frac{RT_2}{V_2} + V_2 = 2C.$$

2C is not related in a simple way to any of the reference speeds derived from the energy equation for an ideal gas with constant specific heat. The flow velocity is the root of the equation

$$V^2 - 2CV + RT = 0$$

$$V = C + \sqrt{C^2 - RT}.$$

The flow velocity can be made an explicit function at the time by substituting Eq 51 for T.

The density can be found from the conservation of mass equation:

$$\rho = \frac{\rho_2 V_2}{C + \sqrt{C^2 - RT}}.$$

The equation of state may now be used to determine the pressure variation:

$$p = \frac{\rho_2 V_2 T}{T_2 \left(C + \sqrt{C^2 - RT} \right)}.$$

As expected, $u = u_1$, $\rho = \rho_1$, and $p = p_1$ when $t = 0$; and $u = u_2$, $\rho = \rho_2$, and $p = p_2$ when $t = \infty$.

These results for the time dependence of the flow parameters can now be written out as:

$$T = T_2 + (T_1 - T_2)\, e^{-\frac{t}{\tau}}$$

$$V = C + \sqrt{C^2 - R\left[T_2 + (T_1 - T_2)\, e^{-\frac{t}{\tau}}\right]} \qquad (52)$$

$$\rho = \frac{\rho_2 V_2}{C + \sqrt{C^2 - R\left[T_2 - (T_1 - T_2)\, e^{-\frac{t}{\tau}}\right]}} \qquad (53)$$

$$p = \frac{\rho_2 V_2}{T_2}\ \frac{\left[T_2 + (T_1 - T_2)\, e^{-\frac{t}{\tau}}\right]}{C + \sqrt{C^2 - R\left[T_2 - (T_1 - T_2)\, e^{-\frac{t}{\tau}}\right]}} . \qquad (54)$$

Thus, the general statement can be made that when the temperature range is small, the temperature changes exponentially from its initial to its final value. The flow velocity, density, and pressure approach equilibrium at approximately the same rate but not as simple exponentials. Figs. 16a and 16b are graphical representations of the time dependence of the flow variables behind a shock wave in CO_2 whose initial Mach number is 2. It may be seen that velocity, density, and pressure approach their equilibrium values very nearly exponentially. This calculation may therefore be considered as a first-order correction to the simple exponential adjustments predicted by Bethe and Teller. It is not convenient, however, for mathematical reasons, to express the results as a simple exponential plus a correction term.

It should be re-emphasized that the preceding analysis refers to the variation of flow parameters behind a stationary shock wave, and

FIG 16a
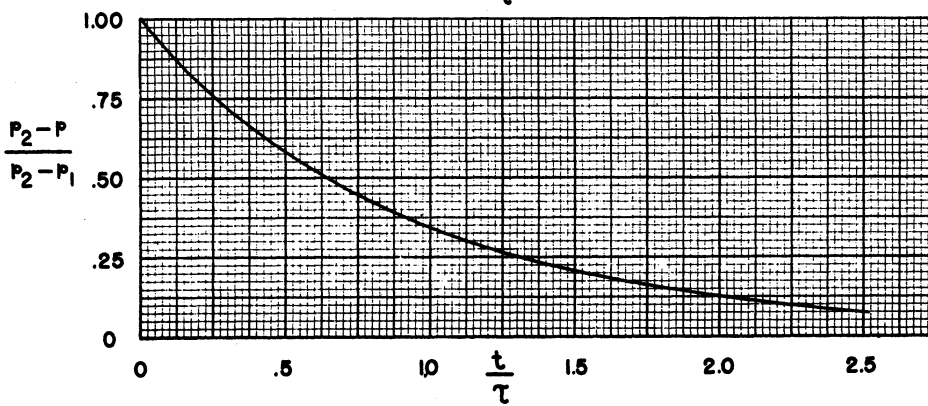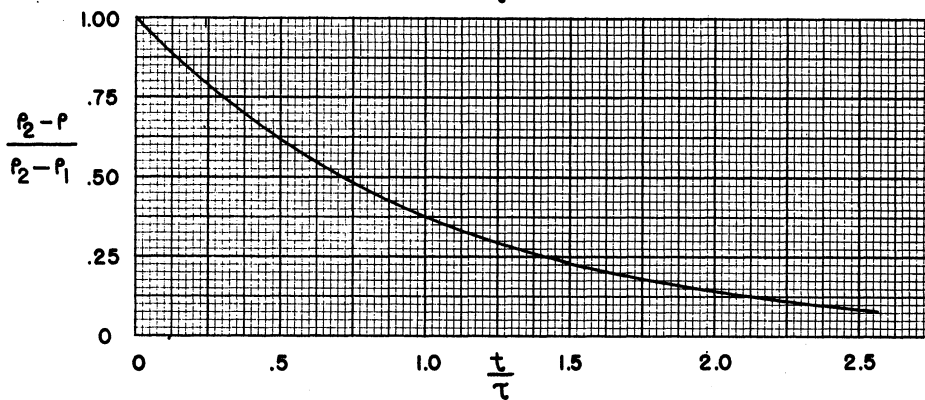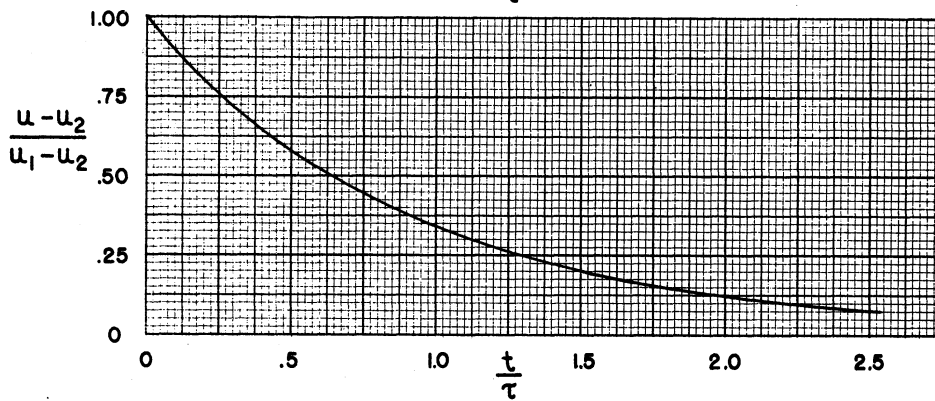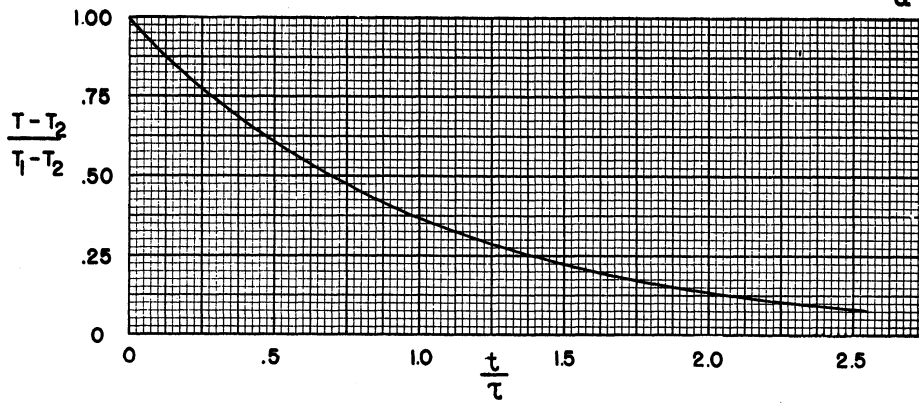
FLOW VARIABLES BEHIND A SHOCK WAVE

FIG 16$_b$
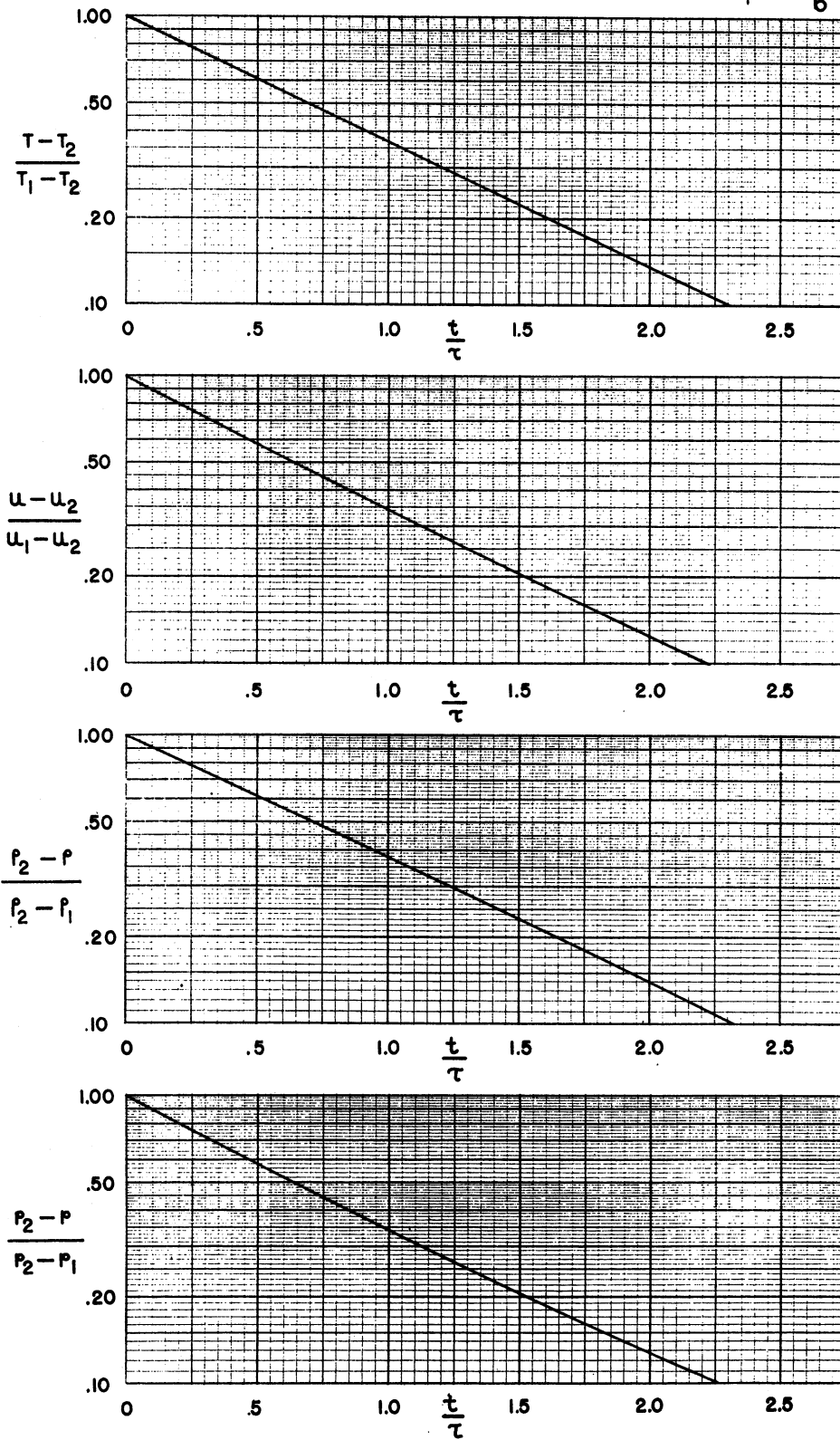
FLOW VARIABLES BEHIND A SHOCK WAVE

the time variable is uniquely related to distance behind the shock wave.
The actual space variation of the flow parameters behind a shock wave
can be determined parametrically by integrating the velocity equation;
that is,

$$X = \int_0^t V(t)\, dt \ .$$

(55)

This equation together with Eqs 51, 52, 53, and 54 determine the space
dependence of the temperature, flow velocity, density, and pressure be-
hind a shock wave.

If curves similar to those in Figs. 16a and 16b were calculated
with distance behind the shock wave as abscissa, they would resemble Figs.
16a and 16b, except that the initial rates of change would be somewhat
reduced because the initial velocity is greater than the equilibrium value.
However, no fundamental change would be produced in the character of the
curves or in the relations between the curves.

The assumptions upon which this approximate calculation rests
can now be reviewed and enumerated:

1. The change in temperature in the flow field behind the
shock wave was assumed small enough so that the relaxations could be
considered constant.

2. The change in temperature behind the shock was assumed
small enough so that E_v', the equilibrium vibrational energy, could be
considered constant. This assumption is more restrictive than the first,
because the vibrational energy varies as $e^{-1/T}$, while the dependence of
the relaxation time is only as $e^{-1/T^{1/3}}$.

3. The variations of the total internal energy caused by
hydrodynamic processes were neglected. That is, the secondary internal

energy variation resulting from work done on the flow by pressure and density changes was neglected. This assumption is more generally valid than the preceding two.

The preceding calculation will be valid only for very weak shocks where the temperature change behind the shock is of the order of 50°C or less.

For stronger shocks the above assumptions are no longer valid. The flow variables may then be calculated from the following equations:

The fundamental relation between vibrational energy, time, and temperature is given by Eq 47.

$$\frac{d E_v}{dt} = \frac{E_v{'} - E_v}{\tau}$$

The dependence of τ on temperature and pressure must now be considered.

$E_v{'}$ may be determined from the Einstein equation,

$$E_v{'} = \frac{\eta h \nu}{e^{\frac{h\nu}{kT}} - 1} .$$

The first law of thermodynamics for an adiabatic process gives a relation between the internal energy of the gas and the work done on the gas by pressure forces:

$$d E_v + d E_a - \frac{p}{\rho^2} d\rho ,$$

where E_v is the energy associated with the vibrational degrees of freedom, and E_a is the kinetic energy of the translational and rotational degrees of freedom.

The local temperature may be defined in terms of the energy of the active degrees of freedom and also by the equation of state

$$T = \frac{E_a}{C_{Va}} = \frac{p}{R\rho} \quad .$$

In addition, the flow variables must also be solutions of the continuity equation and Euler's equation:

$$V \frac{d\rho}{dx} + \rho \frac{dV}{dx} = 0$$

$$\rho V \frac{dV}{dx} + \frac{dp}{dx} = 0 \quad .$$

This system of equations can, in principle, be solved for the time and space dependence of the flow parameters behind a strong shock wave. It should be mentioned that this flow is not isentropic for all nontrivial cases.

4. Position-Time Curves for the Flow in the Real Gases of a Shock Tube

Perhaps the processes occurring in the real gases in a shock tube can be better understood by reference to Fig. 17, which is an x-t plot of the shock tube flow. The path, R, of the head of the rarefaction wave is strictly a straight line, because the rarefaction wave moves into the gas of the compression chamber with the local, constant sound speed in the undisturbed gas. However, the velocities of the shock wave, contact surface, and rarefaction foot will all be influenced by vibrational relaxation in the gas of the expansion chamber. In general, the flow velocity immediately behind a shock wave is less than its equilibrium value. Therefore, during the first instant of flow, the velocity produced by the rarefaction wave must be less than the velocity needed to match the equilibrium value behind the shock wave. As a result, the foot of

FIG 17
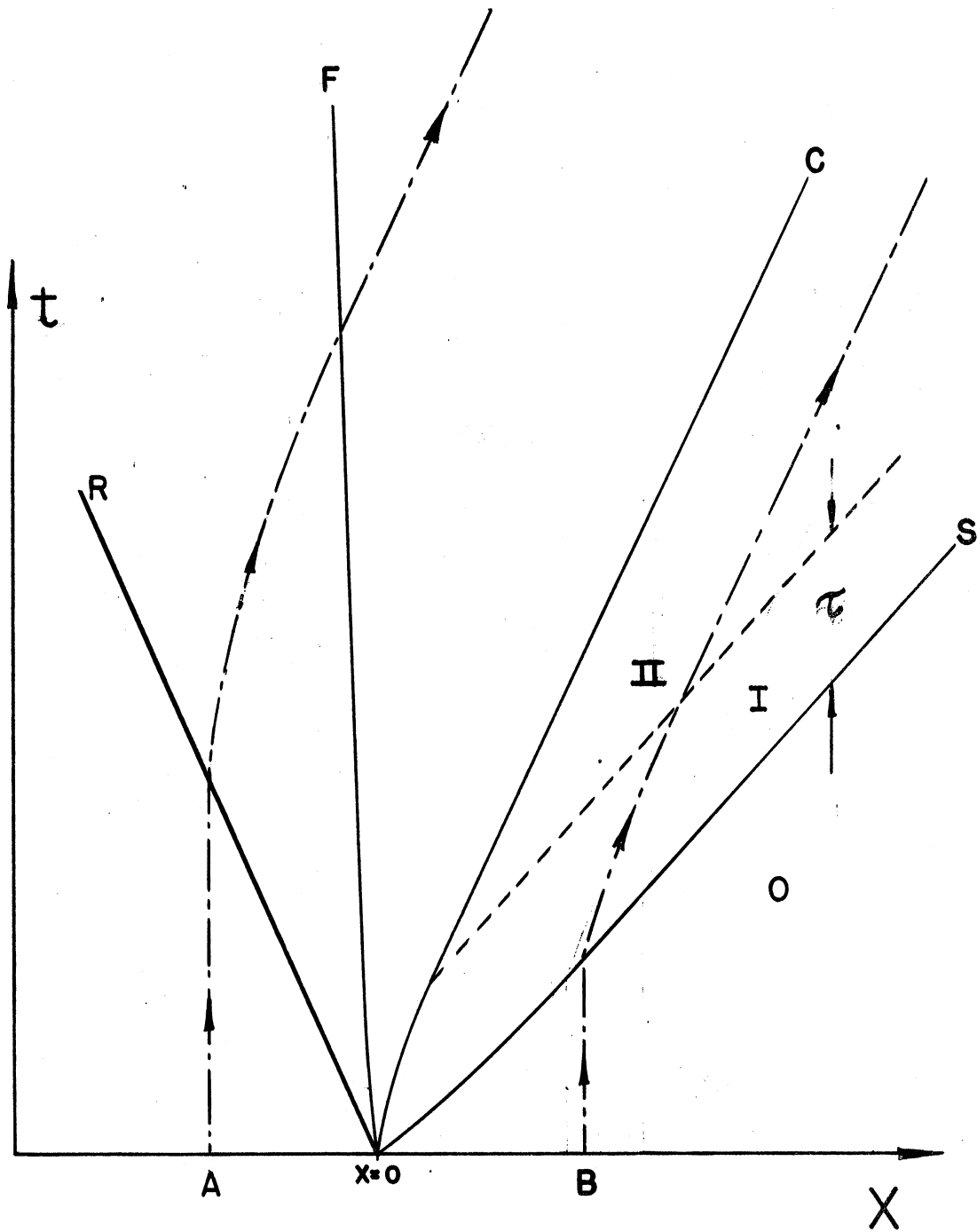
X — T   DIAGRAM   OF   THE

FLOW   IN   A

REAL   SHOCK   TUBE

the rarefaction wave will move more slowly in the positive x direction

during the early stages of the flow. The contact surface likewise has

an initial velocity somewhat lower than its final value. On the other

hand, the initial pressure ratio across the shock wave is larger than

expected because the rarefaction wave is not as complete, initially, as

it is after the flow has reached equilibrium. The shock wave, therefore,

has a high initial velocity. After the flow has existed for a time of

the order of the relaxation time, the velocities of the shock wave, con-

tact surface, and foot of the rarefaction wave become constant at values

which may be determined from shock theory for a gas with temperature-

dependent specific heat. For example, the initial and final values of

shock velocity, flow velocity, and pressure ratio across the diaphragm

are given in Table VIII for U/a_0 = 2.34 in carbon dioxide.

TABLE VIII

INITIAL AND FINAL VALUES OF SHOCK VELOCITY, FLOW VELOCITY,

AND PRESSURE RATIO ACROSS THE RAREFACTION WAVE

FOR U/a_0 = 2.34 IN CARBON DIOXIDE

Shock Velocity (mm/μsec)		Flow Velocity (mm/μsec)		Pressure Ratio Across Rarefaction Wave	
initial	final	initial	final	initial	final
.659	.631	.450	.459	.448	.440

It can also be seen that the gas initially in the expansion

chamber is divided into three regions. There is the uniform initial

state, O, in front of the shock wave; there is the region, I, in which

the flow parameters change from their values immediately behind the shock wave to their equilibrium values; and there is region II, another region of constant state in which the flow parameters may be determined from variable specific heat theory as discussed in Chapter III.

Representative particle paths, A and B, in the compression and expansion chambers are indicated by dot-dash lines. The particle path in the compression chamber is similar to the path derived from ideal shock-tube theory; but the world line for a gas particle in the expansion chamber is no longer made up of two straight segments of a broken line. Now the world line changes slope abruptly at the shock wave and then continues to bend further toward the x-axis throughout region I. In region II the particle path is a straight line parallel to the path of the contact surface.

The pressure distribution corresponding to a particular time is shown in Fig. 15.

5. Effects of Vibrational Relaxation Investigated in the Shock Tube

a. Variable Region Behind the Shock. Since there is a region of variable state behind shock waves, it is important to determine whether or not this region can seriously affect experiments conducted in a shock tube. The variable which determines if the effects of vibrational relaxation may be important is the relaxation time. If the time for the adjustment is very long or very short compared to the duration of uniform flow in a shock tube, vibrational relaxation, as such, can be ignored.

According to Griffith,[25] the relaxation times for most polyatomic gases are of the order of one microsecond or less. Table IX, which is a

---

[25] Griffith, Wayland, "Vibrational Relaxation Times in Gases", Journal of Applied Physics, 21, 1319 (1950).

TABLE IX[25]

RELAXATION TIMES FOR VARIOUS GASES

Gas	Temp. °F	Relaxation Time μ sec	Gas Purity and Foreign Gas Present Investigation
Hydrogen	58	0.021 (rot.)	99.8%, 0.2% H_2O
Nitrogen	60	<0.002 (rot.)	
Nitrous oxide	65	1.12	98-99%, 1-2% N_2
Carbon dioxide	65	6.95	99.956%, 0.044% H_2O
Carbon dioxide (comm.)	65	2.02	n% H_2O
Sulfur dioxide	68	0.37	99.988%, 0.002% H_2O
Ammonia	63	0.12	99.5%, 0.005% H_2O
Methane	60	0.48	99%, 1% C_2H_6, N_2, CO_2
Methyl chloride	72	0.202	99.5%, <0.008% H_2O
Freon 22	70	0.10	97%, <0.005% H_2O
Freon 12	67	0.090	95%, <0.001% H_2O
Ethane	57	0.003	95%, 5% C_2H_4, C_3H_8, C_3H_6
Ethylene	60	0.207	99.5%, 0.5% air
Propylene	70	<0.006	99%
Propane	70	<0.007	99%
Ethylene oxide	86	1.23	99.8%
Butane	70	<0.018	99%
Butadiene	70	<0.013	99.77%, 0.23% C_4H_{10}

TABLE IX (Cont'd.)

Gas	Temp. °F	Relaxation Time μ sec	Literature References

Results reported in the literature:

Gas	Temp. °F	Relaxation Time μ sec	Literature References
Oxygen	70	1000	Reference a
Carbon monoxide	1800	10	b
Chlorine	70	18	c
Nitric oxide	60	· 0.8 (el. excit.)	d
Hydrogen	77	0.018 (rot.)	e
	60	0.02 (rot.)	f
Deuterium	60	0.015 (rot.)	f
Carbon dioxide	70	10.8	f
	70	10.26	g
Nitrous oxide	67	0.92	c
	70	1.44	g
Carbonyl sulfide	70	0.86	g
	70	1.67	c
Carbon disulfide	70	0.70	g
Sulfur dioxide	70	0.181	g
Water vapor	415	0.037	h
Ammonia	70	0.4	i
Ethylene	70	0.238	j
Methane	230	0.84	c

[a] H. O. Kneser and V. O. Knudsen, Ann. der Phys. 21, 682 (1935).

[b] G. G. Sherratt and E. Griffiths, Proc. Roy. Soc. London 147A, 292 (1934).

[c] A. Eucken and S. Aybar, Zeits. f. physik. Chemie B46, 195 (1940); A. Eucken and R. Becker, ibid. 27, 219 (1934).

[d] H. O. Kneser, Ann. d. Physik. 39, 261 (1941); J. Acous. Soc. Am. 5, 122 (1933).

[e] E. S. Stewart, Phys. Rev. 69, 632 (1946).

[f] A. van Itterbeek and R. Vermaelen, Physica 9, 345 (1942).

[g] E. F. Fricke, J. Acous. Soc. Am. 12, 245 (1940).

[h] A. Kantrowitz and P. Huber, J. Chem. Phys. 15, 275 (1947).

[i] O. Steil, Zeits. f. physik. Chemie B31, 343 (1936).

[j] W. T. Richards and J. A. Reid, J. Chem. Phys. 2, 193 (1934); W. T. Richards 4, 561 (1936).

compilation of relaxation times for various gases, is from the article

by Griffith. It can be seen that carbon dioxide has a relaxation time

longer than any other polyatomic gas listed. Therefore, if the length of

the transition region behind shocks produced in a shock tube in carbon

dioxide is found to be small compared to the characteristic dimensions

of an experiment, then relaxation effects as such will be unimportant

for all polyatomic gases insofar as they disturb the uniform flow in

the shock tube.

A first approximation to the thickness, d, of the transition

region can be obtained from the equation

$$d = (U - u)\tau \, ,$$

where U and u are the shock and flow velocities calculated from the Ran-

kine-Hugoniot equation, assuming the specific heat to be constant at its

room-temperature value.

The remainder of this section will be devoted to a calculation

of the length of the transition region behind shock waves produced in a

shock tube. The dependence of τ on temperature and density definitely

must be considered in such a calculation.

The experimental data of Eucken and his co-workers, as compiled

by Kantrowitz[26] for the average number of collisions required to excite

molecular vibration in CO_2 as a function of temperature, can be approx-

imated, except at high temperatures, by

$$\eta = \frac{4.04 \times 10^6}{T - 222}$$

---

[26] Kantrowitz, Arthur, Effects of Heat Capacity Lag in Gas Dynamics, NACA ARR No. 4A22 (1944).

The number of collisions which a molecule undergoes per second is

$$N = \sqrt{2}\, \pi\, \eta\, \bar{V}\, \sigma^2$$

where n is the number of molecules per cubic centimeter, $\bar{V}$ is the average molecular velocity, and σ is the molecular diameter. From these two equations, the relaxation time for CO_2 becomes simply

$$\tau = \frac{\eta}{N} = \frac{2.97 \times 10^{-5}}{\rho\sqrt{T}\,(T-222)} \quad \text{seconds.} \tag{55}$$

Both ρ and T in the gas behind the shock wave can be expressed as functions of the shock strength and atmospheric temperature and density. ρ is

$$\rho = \rho_3 \frac{\rho_0}{\rho_3} \frac{\rho}{\rho_0}.$$

ρ_0/ρ_3 can be found from the p_0/p_3 equation, and ρ/ρ_0 is given by the Rankine-Hugoniot equation. Thus

$$\rho = \rho_3 \frac{\xi(\mu_c+\xi)}{1+\mu_E \xi} \left[1 - \frac{a_{0E}\,(\mu_E-1)}{a_{0C}\,(\mu_c-1)} \frac{(1-\xi)}{\sqrt{(\mu_E+1)\,\xi\,(\mu_E+\xi)}} \right]^{\mu_c+1} \tag{56}$$

The temperature behind the shock wave is

$$T = T_0 \frac{1+\mu_E \xi}{\xi(\mu_E+\xi)} \tag{57}$$

By combining Eqs 26, 27, 55, 56, and 57, the following formidable expression for d is obtained

$$d = \cfrac{2.97 \times 10^{-5}\, a_0 \cfrac{1 + \mu_E \xi}{\sqrt{(\mu_E+1)\,\xi\,(\mu_E+\xi)}}}{\rho_3 \sqrt{T_0}\sqrt{\cfrac{\xi(\mu_E+\xi)}{1+\mu_E\xi}}\left[1 - \cfrac{a_{0E}(\mu_c-1)(1-\xi)}{a_{0c}(\mu_c-1)(\mu_E+1)\xi(\mu_E+\xi)}\right]^{\mu_c+1}\left(T_0\sqrt{\cfrac{1+\mu_E\xi}{\xi(\mu_E+\xi)}} - 222\right)} \quad \cdot (58)$$

This function is plotted in Fig. 18 under the assumption that carbon dioxide is used in the expansion chamber and helium in the compression chamber. It is interesting to note that the thickness of the transition region is almost constant, except for very strong shocks, in spite of the fact that the changes in the velocities, temperature, and density are large. The thickness of approximately 3 mm is in good agreement with the estimate of 0.1 inch made by Griffith.[24]

For an initial shock Mach number of 3 in carbon dioxide, a density variation of approximately 25 per cent of the change across the shock wave is to be expected within a distance of 3.5 mm behind the shock wave. An unsuccessful attempt was made to observe this variation with shadowgraph and schlieren photography. The density gradient was simply too small to give an observable effect. However, a similar investigation has been proposed by Griffith at Princeton University. This attempt may be more successful because a Mach-Zehnder interferometer is available for use with that shock tube.

b. Bow-wave curvature. The effect of vibrational relaxation on the flow through an oblique shock wave has been discussed by Ivey and Cline.[27] In particular, they treat the problem of the attached bow wave.

---

[27] Ivey, H. Reese, and Cline, Charles W., Effect of Heat-Capacity Lag on the Flow Through Oblique Shock Waves, NACA TN 2196 (1950).

LENGTH OF TRANSITION REGION BEHIND
SHOCK WAVES IN CARBON DIOXIDE

FIG 18

$\zeta_f = .0052$
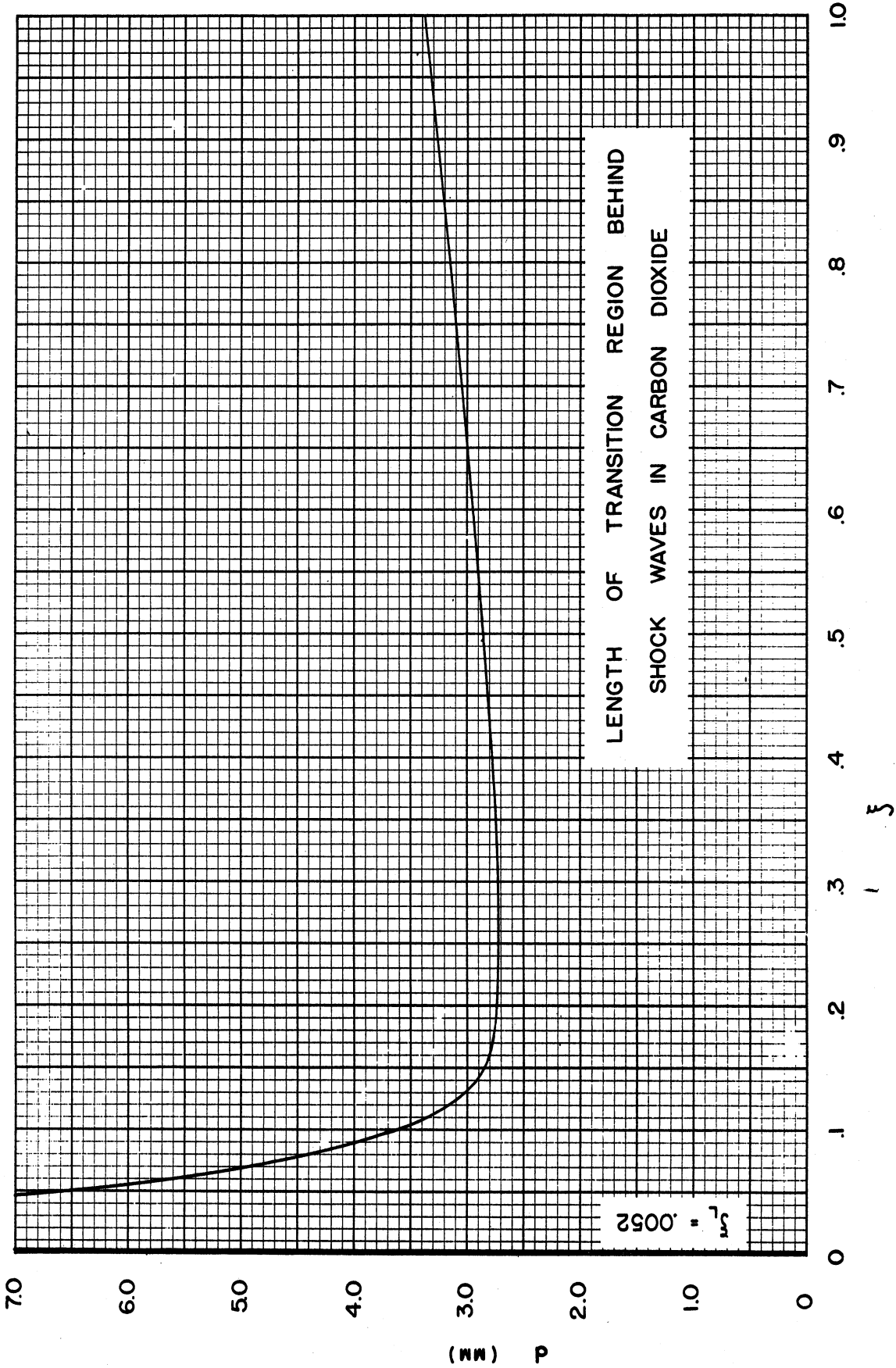
The results of Bethe and Teller are applied to the component of velocity perpendicular to the shock wave. Since an oblique shock wave can be described as a superposition of a normal shock and a uniform flow parallel to the wave, it follows that the flow field behind an oblique shock wave will not be uniform — just as the flow behind a normal shock in a gas with temperature-dependent specific heat is not uniform.

From a frame of reference in which the shock is stationary, the normal component of velocity decreases as the distance from the shock wave increases. This is a direct result of vibrational relaxation. However, the flow component parallel to the shock wave is constant on both sides of the shock. Therefore, the streamlines in the flow behind the shock wave will not be straight. Fig. 19 illustrates this fact.
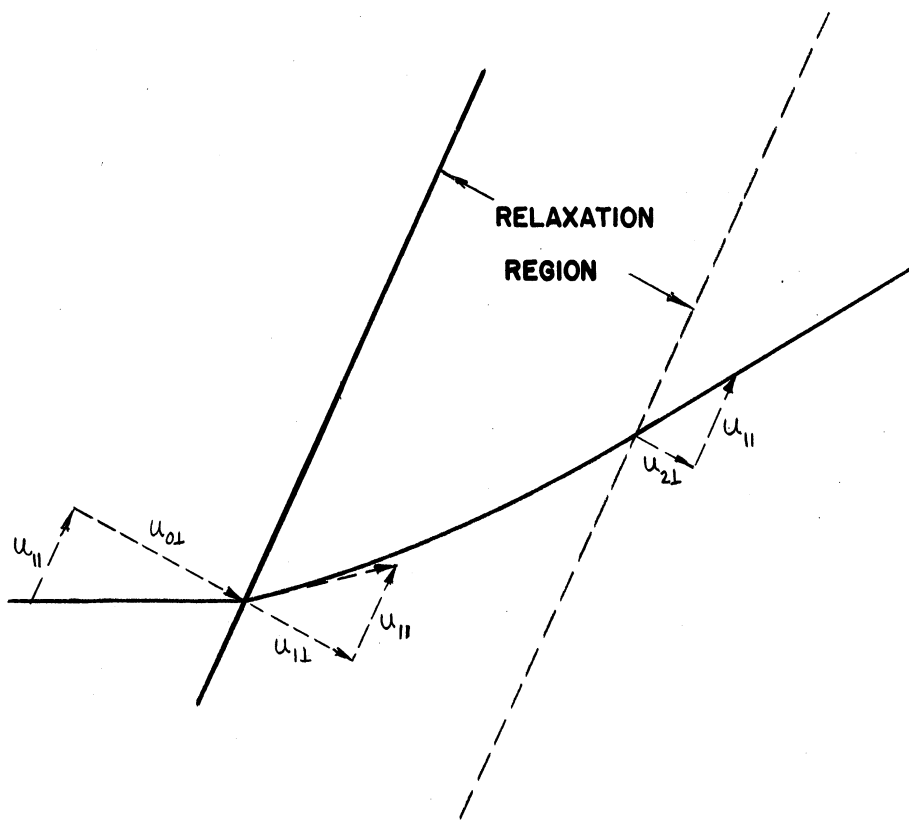
Fig. 19

Streamline Through an Oblique Shock Wave

The shape of the bow wave attached to a wedge in a supersonic
stream can now be discussed. Immediately behind the shock wave, the
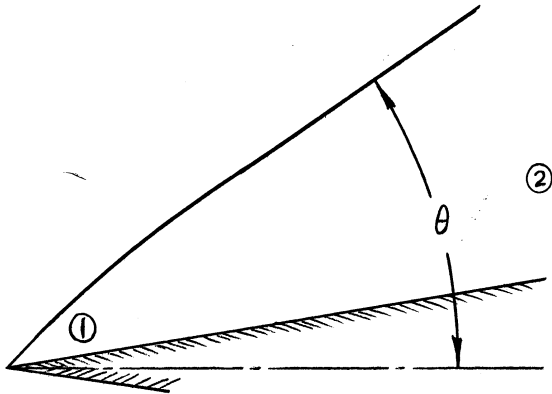
Fig. 20

Effect of Vibrational Relaxation in an
Attached Bow Wave

flow will be as pre-
dicted by ordinary
aerodynamic theory.
However, the values
of γ or μ used in
these equations should
be determined by con-
sidering only the
active degrees of
freedom of the mole-
cule, because insuf-
ficient time will have elapsed for the transfer of energy to the inert

degrees of freedom. Thus the bow-wave angle in region 1 near the tip

of the wedge will be as predicted by the usual oblique shock equations.

However, from region 2, far from the tip of the wedge and the bow wave,

the shock wave and relaxation zone appear only as a thick shock wave.

The flow deflection will be determined from the flow velocity normal to

the shock calculated by assuming the specific heat to be a function of

temperature and from the constant tangential component. Therefore, the

angle, θ, must decrease below the value found at the tip of the wedge

in order to satisfy the boundary condition that the flow near the wedge

be parallel to the surface. Fig. 20 illustrates the type of bow wave

to be expected.

Attempts to observe this curvature have been unsuccessful for

the following two reasons:

1. The simple theory of the bow wave attached to a wedge neglects viscous effects and assumes the wedge to be perfect. However, these assumptions are not valid at the low supersonic Mach numbers obtained in shock tubes. Both the blunt end on a real wedge and the boundary layer which develops along its surfaces cause bow-wave curvature similar to that shown in Fig. 20. This curvature has been found to vary in time. Therefore, it would be very difficult to observe curvature ascribable to relaxation effects because of the similar curvatures, which have not yet been discussed theoretically, caused by viscosity and the imperfect airfoils.

2. Furthermore, the pressure behind a bow wave attached to an airfoil in a low supersonic stream obtained in a shock tube is not more than twice the initial pressure except in extreme conditions. For instance, the pressure behind a shock wave that produces a 10° deflection at a Mach number of 1.5 in air is only 1.7 times the initial pressure. The difference between v_1 and v_2 produced by such weak shocks attached to thin airfoils in air is negligible. Ivey and Cline estimate that curvature of bow waves attached to thin airfoils will not become important in air until the free-stream Mach number reaches 20. The effects would be greater in some polyatomic gases, to be sure, but the differences in specific-heat behavior with temperature are still insufficient to make the curvature appreciable at the Mach numbers attained in a shock tube.

The conclusion that relaxation effects will not noticeably affect bow waves attached to airfoils in a shock tube can be extended to other features of the flow. The temperature increments across shock and expansion waves associated with the transient and steady flow about

thin airfoils are small enough so that the vibrational energy may be assumed constant; therefore, no change in the specific heat of the gas need be considered. However, if shock wave diffraction studies were being conducted in a complex gas, the possibility of specific-heat variations should be carefully considered, especially in the vicinity of strong detached or reflected shock waves and large-angle expansion waves.

c. Reflected shock velocity in carbon dioxide. Relaxation effects should cause the velocity of a shock wave reflected normally from a wall to vary with time. Immediately after reflection the velocity should be that predicted by considering only the active degrees of freedom, if the relaxation time is long. If the relaxation time is short, the initial reflected velocity will be somewhat less than such a calculation would indicate. When the distance between the shock wave and the reflecting surface is much larger than the relaxation zone behind the reflected shock, the shock velocity should be as predicted by considering the specific heat to be a function of temperature.

Before the details of the calculation of the reflected shock velocity for a gas with temperature-dependent specific heat are considered, it might be worthwhile to review the velocity calculation for a gas with constant specific heat. The change in flow speed across a shock wave is given by Eq 27. Thus for a given incident shock strength, the flow velocity behind the wave is

$$u = a_0 \frac{(\mu-1)(1-\xi)}{\sqrt{(\mu+1)\,\xi\,(\mu+\xi)}} \ .$$

However, the boundary condition at the stationary reflecting surface demands that the flow velocity behind the reflected shock must vanish.

As a result, the change in flow speed across the reflected shock is also u. From this condition the reflected shock strength, ξ', can be determined as a function of incident shock strength.

$$u = a_0 \frac{(\mu-1)(1-\xi)}{\sqrt{(\mu+1)\,\xi\,(\mu+\xi)}} = a_1 \frac{(\mu-1)(1-\xi')}{\sqrt{(\mu+1)\,\xi'\,(\mu+\xi')}}$$

$$= a_0 \frac{(\mu-1)(1-\xi)}{\sqrt{(\mu+1)\,\xi\,(\mu+\xi)}} = a_0 \sqrt{\frac{1+\mu\xi'}{\xi'(\mu+\xi)}} \; \frac{(\mu-1)(1-\xi)}{\sqrt{(\mu+1)\,\xi'\,(\mu+\xi')}} \; .$$

From this

$$\xi' = \frac{1+\mu\xi}{\mu+2-\xi} \qquad\qquad (59)$$

ξ' is plotted as a function ξ for several values of μ in Fig. 21. The velocity of the reflected shock wave can then be determined from Eqs 26 and 27. That is, the reflected shock velocity is the shock velocity calculated from Eq 26 minus the incident flow velocity u. Thus

$$U' = a_1 \sqrt{\frac{\mu+\xi'}{(\mu+1)\,\xi'}} - a_0 \frac{(\mu-1)(1-\xi)}{\sqrt{(\mu+1)\,\xi\,(\mu+\xi)}}$$

Substituting Eq 59 and simplifying leads directly to

$$U' = a_0 \frac{2+(\mu-1)\xi}{\sqrt{(\mu+1)\,\xi\,(\mu+\xi)}} \qquad\qquad (60)$$

Unfortunately, when the specific heat is considered as a function of temperature, an analogous explicit expression for the reflected shock velocity cannot be written. Nevertheless, this velocity can be obtained through a step-by-step process similar in principle to that used above. For a given incident shock velocity the flow parameters far behind the shock can be determined from Eqs 33 and 34 as described in

FIG 21
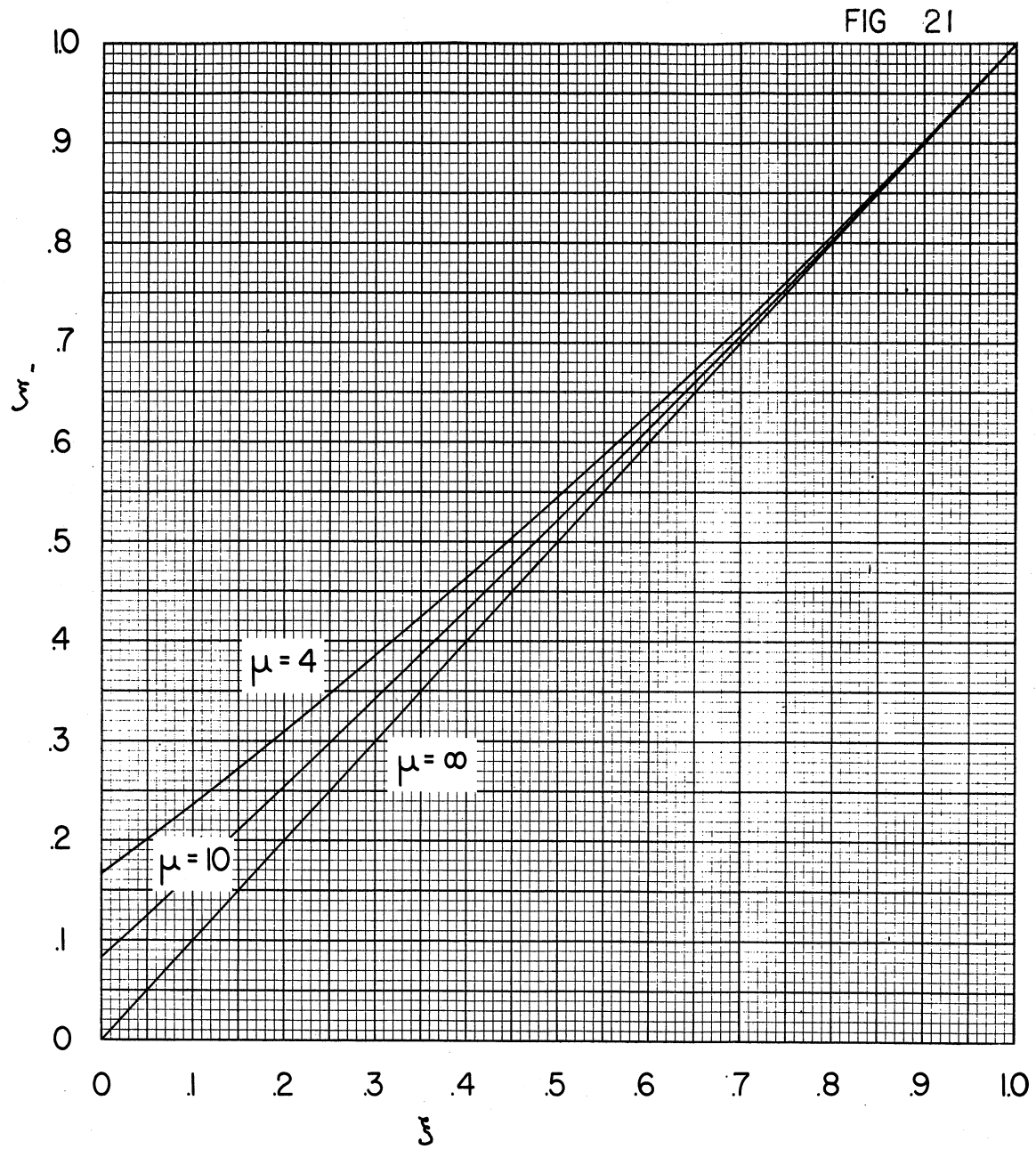
REFLECTED SHOCK STRENGTH

AS A FUNCTION OF

INITIAL SHOCK STRENGTH

Chapter III. These parameters are then considered as initial conditions for the reflected shock wave. Eqs 33 and 34 are used again to determine shock wave parameters under the assumptions that the initial temperature is that of the flow behind the incident shock and the final temperature is less than the temperature behind a reflected shock calculated by constant specific heat theory. Usually several final temperatures are assumed. The boundary condition that the flow velocity at the reflecting surface must vanish may now be applied graphically. From the reflected shock calculations, an initial and final flow velocity are determined. A trial reflected velocity can be obtained by subtracting the primary flow velocity from the initial velocity required by the assumed final temperature. This will be the correct reflected velocity only if it is equal to the final velocity behind the reflected wave calculated from Eq 34. Several attempts may be required before this condition is satisfied. This procedure changes the frame of reference of the reflected shock from a stationary frame of reference to the laboratory frame, and it also imposes the boundary condition that the flow velocity at the reflecting surface must vanish.

Table X, on page 91, shows the initial and the final values of the reflected shock velocity, temperature, and pressure ratio for three shock waves in carbon dioxide.

It is evident that large changes in the shock characteristics occur in the vicinity of the wall during the course of the reflection.

Fig. 22 is an x-t plot of the processes involved in the normal reflection of a shock wave in a gas whose specific heat depends on temperature. The initial reflected velocity is greater than the final value. It is also to be noted that the relaxation zone behind the reflected

FIG 22
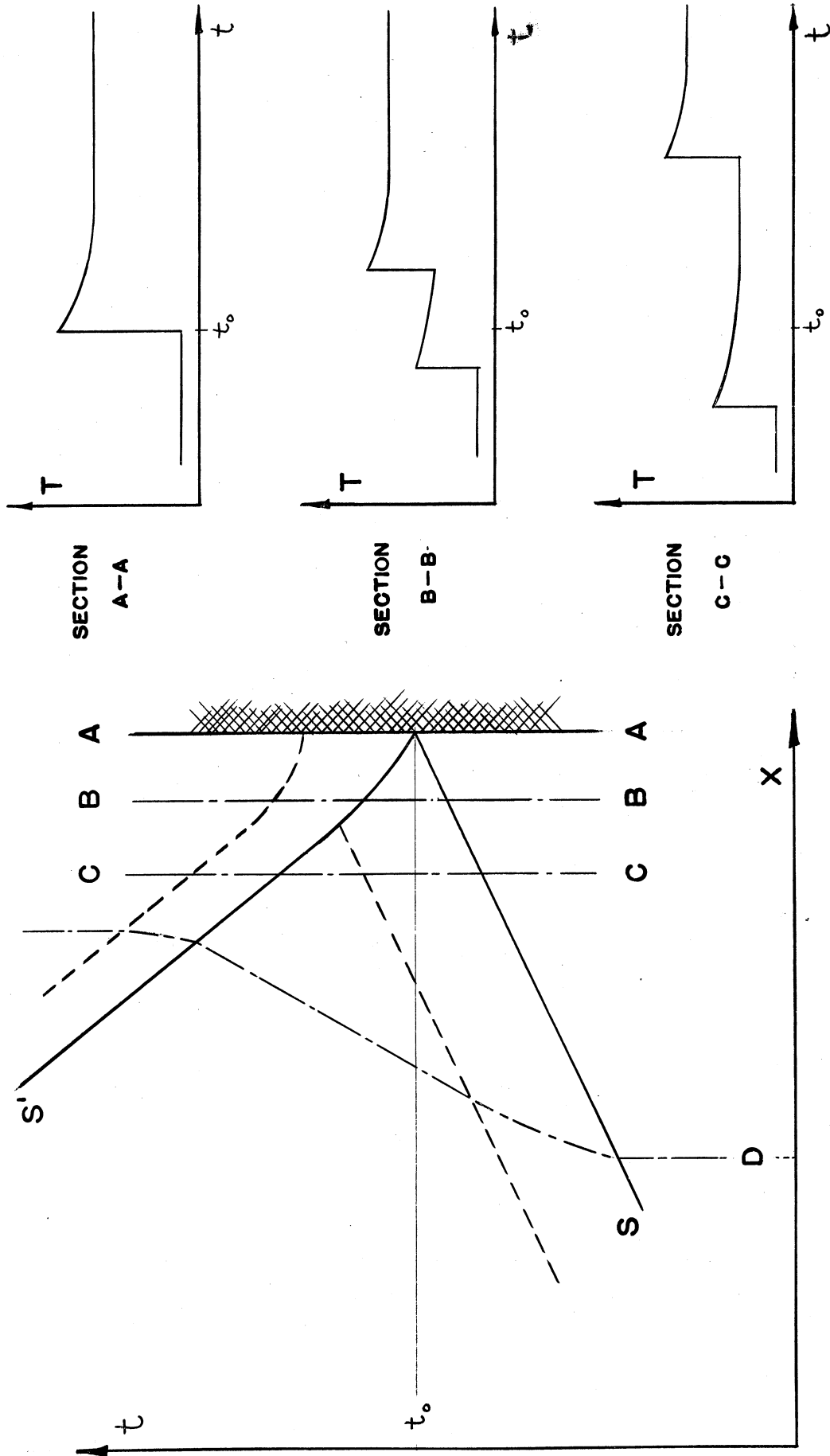
NORMAL   REFLECTION   OF   A   SHOCK   WAVE

TABLE X

INITIAL AND FINAL REFLECTED SHOCK VELOCITIES,

TEMPERATURES, AND PRESSURE RATIOS IN CO_2

Initial Shock Mach Number	ξ Immediately Behind Shock Wave	Initial Reflected Shock Velocity mm/μ sec	Final Reflected Shock Velocity mm/μ sec	Initial Temperature °K	Final Temperature °K	Initial Pressure Ratio	Final Pressure Ratio
4.835	.0398	.475	.262	3104	1771	161.5	242
3.417	.0802	.364	.232	1661	1098	66.7	88.4
2.472	.1550	.301	.219	971	738	26.2	32.1

shock is narrower than behind the incident shock. This result is an immediate consequence of the fact that both the temperature and the density are higher behind the reflected shock wave; the relaxation time is therefore shorter. A representative streamline is also indicated. Fig. 22 also shows temperature-time variation at the Sections AA, BB, and CC of the position-time graph. At the reflecting surface the temperature rises to a high value and then drops to its final value along a path resembling an exponential. On the other hand, at CC, well removed from the wall, the temperature goes through two complete adjustment processes, behind both the incident and reflected shocks. At an intermediate location, BB, the relaxation process behind the incident shock has not been completed before the reflected shock arrives.

A series of experiments was conducted in which the position of the reflected shock wave in carbon dioxide was determined as a function of time for the three shock strengths listed in Table X. Position-time curves of the reflected shock are plotted in Figs. 23, 24, and 25 from data tabulated in Table XI; the calculated initial and final reflected

FIG 23

NORMAL SHOCK REFLECTION

IN

CARBON DIOXIDE

$U/a_o = 4.835$

CALCULATED
FINAL REFLECTED VELOCITY = .262

CALCULATED
INITIAL REFLECTED VELOCITY = .475

TIME (μ SEC)

SHOCK POSITION (MM)

FIG 24

NORMAL SHOCK REFLECTION
IN
CARBON DIOXIDE

$U/a_o = 3.417$

CALCULATED
FINAL REFLECTED VELOCITY = .232

CALCULATED
INITIAL REFLECTED VELOCITY = .364

TIME (μ SEC)

SHOCK POSITION (MM)

FIG 25

NORMAL SHOCK REFLECTION
IN
CARBON DIOXIDE

$U/a_o = 2.472$

CALCULATED
FINAL REFLECTED VELOCITY = .219

CALCULATED
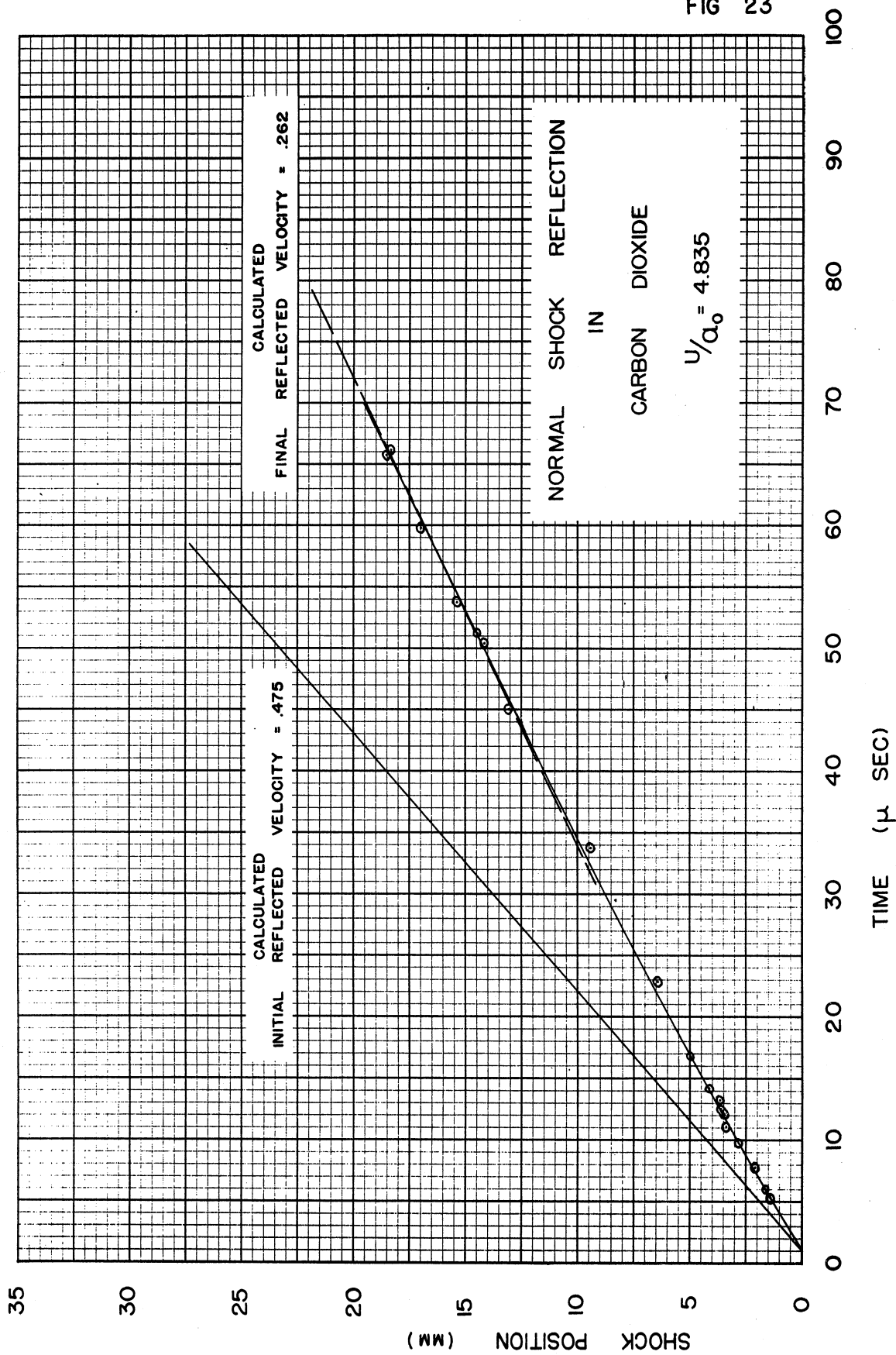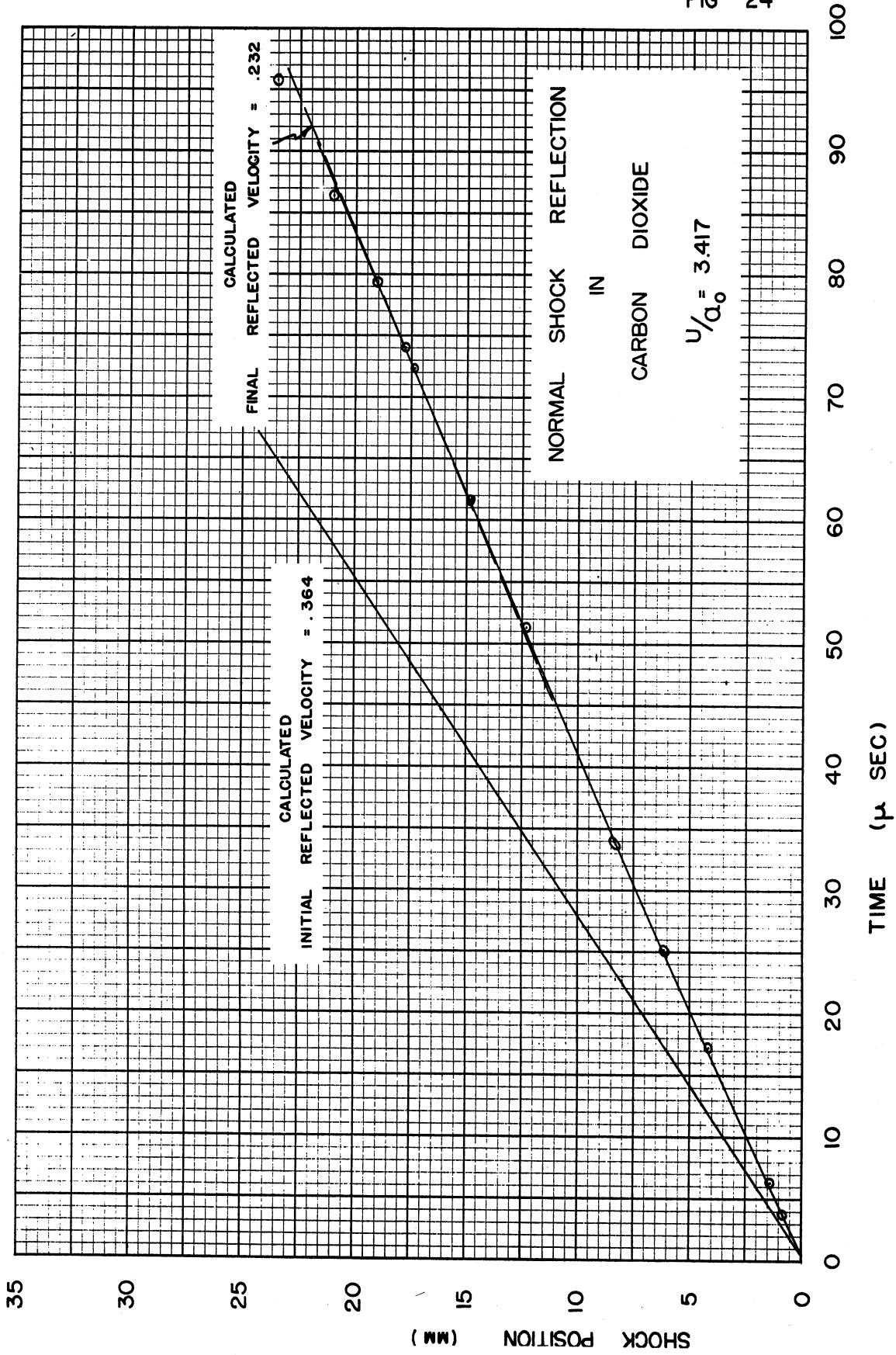INITIAL REFLECTED VELOCITY = .301

SHOCK POSITION (MM)

TIME (μ SEC)

TABLE XI

POSITION-TIME DATA FOR THE NORMAL REFLECTION
OF SHOCK WAVES IN CARBON DIOXIDE

U/a_0 = 4.835		U/a_0 = 3.417		U/a_0 = 2.472	
time	position	time	position	time	position
5.3	1.4	3.8	.8	6.6	1.1
6.0	1.6	6.3	1.4	13.4	2.8
7.7	2.0	17.2	4.2	18.3	4.0
9.8	2.8	25.1	6.2	24.4	5.5
11.1	3.4	33.7	8.3	36.1	8.3
12.1	3.5	33.9	8.4	58.1	13.3
12.4	3.5				
12.5	3.6	51.3	12.3	62.1	14.1
13.2	3.7	61.6	14.8	62.9	14.3
14.1	4.1	72.4	17.3	75.9	17.1
16.8	5.0	74.0	17.8	83.1	18.7
22.8	6.4	79.3	19.0	99.3	22.5
33.6	9.4	86.4	21.0	109.1	25.2
45.0	13.1	95.8	23.5	114.1	26.0
50.4	14.2			139.1	32.0?
51.1	14.5				
53.6	15.4				
59.9	17.0				
65.6	18.5				
66.2	18.1				

velocities are also included in the figures. Fig. 34 is a schlieren photograph of the reflection taken under conditions somewhat different than those of this investigation.

The data for these curves were obtained exclusively from shadowgraph plates. The reflecting obstacle was located so that the primary shock wave could always be seen in the photograph. Accurate determinations of the time since reflection began were obtained from measurements of the location of the incident shock and the measured shock velocity. The curves do not pass through the origin because

measurements of shock position, both of the reflected and the incident

shock, were made to well defined parts of the shadowgraph image; not

necessarily the true shock location. Where necessary, very small cor-

rections to the observed shock positions (maximum of 1 per cent) were

made to compensate for small variations in initial shock velocity.

The fact that the initial reflected velocity seems lower than

predicted is not surprising because this velocity persists only for an

infinitesimal time; and obvious experimental difficulties interfere

with attempts to determine shock velocities earlier than about five

microseconds after the reflection occurs. For instance, for each of the

shock velocities, the first determination is made approximately one

millimeter from the reflecting surface, but this distance is approxi-

mately equal to the thickness of the shadowgraph image of a shock wave.

Examination of Fig. 34 reveals a severe interaction between

the reflected shock wave and boundary layer on the walls and floor of

the tube. This interaction will extend across the tube after approxi-

mately 80 microseconds. Therefore, the reflected shock positions deter-

mined for later times were disregarded in the experimental determination

of the final reflected shock velocity. In Figs. 24 and 25 these late

points fall above the final velocity curve as expected from the nature

of the shock wave - boundary layer interaction.

Because the slope of the position-time curves is not constant,

the velocity of the reflected shock is a function of time. Therefore,

a perturbation of the shock tube flow caused by vibrational relaxation

has been demonstrated. Similar experiments conducted in nitrogen, argon,

and sulfur hexafluoride, described in the appendix to Chapter IV, show

that the reflected shock velocity is constant. One can conclude, therefore, that vibrational relaxation is not important in these gases.

Approximately 40 or 50 microseconds after reflection, the velocity of the reflected shock assumes the value calculated from shock theory derived for a gas with temperature-dependent specific heat. This time of adjustment is what one would expect from the relaxation time of carbon dioxide.

These results will be discussed further in Chapter VI, where the advantages and disadvantages of using specific gases in the expansion chamber of a shock tube will be considered.

APPENDIX TO CHAPTER IV

1. Reflected Shock Velocity in Nitrogen

In order to compare results with carbon dioxide a position-time curve was determined for nitrogen. The results of this experiment are presented in Table XII and Fig. 26. It is apparent that the reflected velocity is constant and in good agreement with that determined from a constant specific heat calculation. In this respect nitrogen behaves differently than carbon dioxide. The apparently contradictory result is easily explained, however, when it is noted that the vibrational relaxation time for commercial nitrogen is estimated[28] to be longer than 5000 microseconds. Therefore, there simply is not time for thermal equilibrium to be established between the various degrees of freedom of nitrogen within the duration of uniform flow in a small shock tube. Thus, the reflection results in nitrogen serve as a verification of the simple constant specific heat theory of normal shock reflection and also demonstrate the validity of Rankine-Hugoniot calculations for shock parameters in nitrogen.

2. Reflected Shock Velocity in Argon

Fig. 27 and Table XII present the results of a similar reflection experiment conducted in argon. This experiment was designed originally to demonstrate exact agreement between constant specific heat theory and experiment. However, the agreement is not quite as good as that found with nitrogen. The reflected velocity is approximately two per cent low.

---

[28] Kantrowitz, Arthur, Heat-Capacity Lag in Turbine-Working Fluids, NACA Restricted Bulletin L4E29 (1944).

FIG 26

NORMAL SHOCK REFLECTION

IN

NITROGEN

$\xi = .0783$

CONSTANT SPECIFIC HEAT VELOCITY = .461

VARIABLE SPECIFIC HEAT VELOCITY = .415

SHOCK POSITION (MM)

TIME (μ SEC)

FIG 27

NORMAL SHOCK REFLECTION

IN

ARGON

$\xi = .0898$

CALCULATED VELOCITY = .534
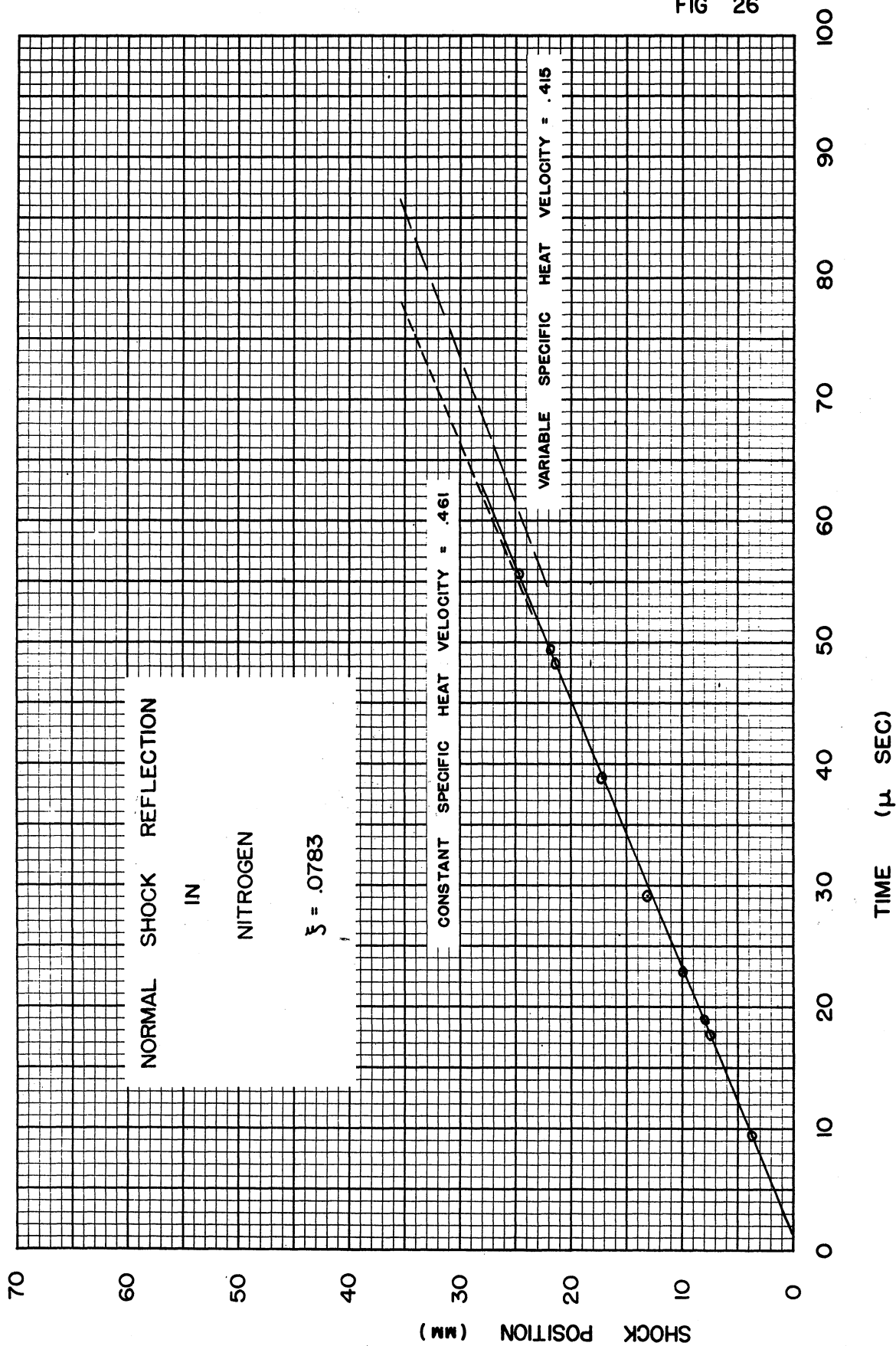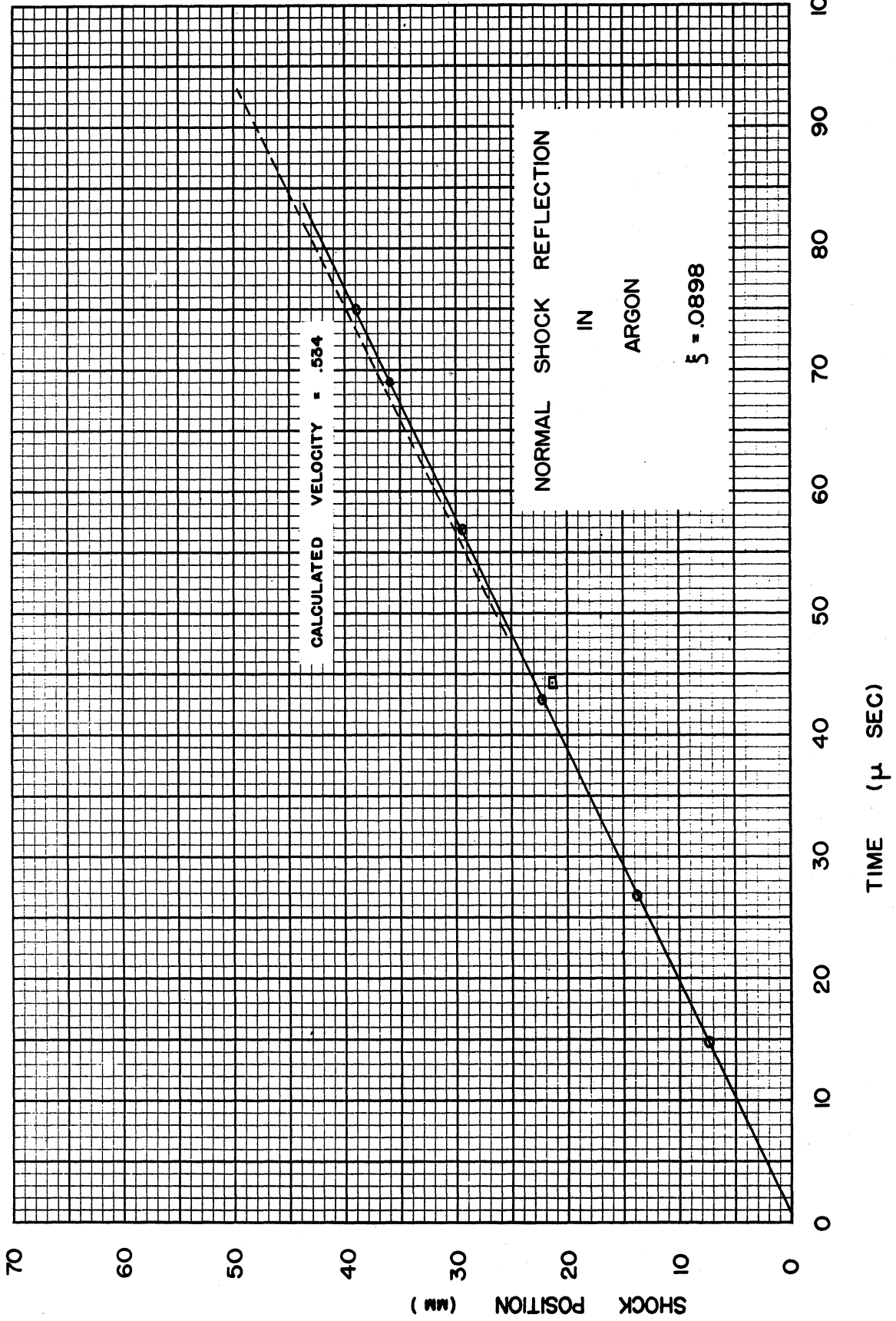
SHOCK POSITION (MM)

TIME (μ SEC)

TABLE XII

POSITION-TIME DATA FOR THE NORMAL REFLECTION OF
SHOCK WAVES IN NITROGEN, ARGON, AND SULFUR HEXAFLUORIDE

Nitrogen ξ = .0783		Argon ξ = .0898		Sulfur Hexafluoride U/a_0 = 3.590	
time	position	time	position	time	position
9.4	3.8	14.8	7.3	18.8	1.2
17.6	7.5	26.8	13.7	27.8	1.9
19.0	8.0	42.8	22.1	29.5	2.1
22.8	9.9	56.9	29.4	56.5	4.2
29.1	13.1	69.0	35.9	81.8	6.1
38.8	17.2	75.0	39.0	108.8	8.4
48.3	21.5			133.2	10.3
49.4	21.9	44.3	21.3	160.9	12.4
55.6	24.7				

The first few pictures obtained using argon indicated a severe
discrepancy in reflected shock velocity between the pictures individually,
and the pictures as a whole and constant specific heat theory. The dis-
crepancies were an order of magnitude larger than anything that had been
found in carbon dioxide or nitrogen. The boxed point at t = 44.2 micro-
seconds is an example.

It was then observed that the entire region behind both the
incident and reflected shocks was luminous. A pink glow could be ob-
served visually. Since the temperature required to excite the ground
state in argon is over 130,000°K, this glow cannot be due to electronic
excitation of this gas. The obvious conclusion is, therefore, that the
glow must result from the excitation of energy levels in the optical re-
gion in some impurity present in the expansion chamber. Unfortunately
the vacuum system, including the tube itself, piping system, and the
vacuum pump, was not designed to produce a vacuum better than 1/7 mm of

mercury or to keep the leak rate below 1/7 to 1/5 mm of mercury per min-
ute. Therefore, a small air contamination will always be present in the
expansion chamber. However, by careful evacuation and flushing of the ex-
pansion chamber with argon, better and better results were obtained. The
results shown in Fig. 27 were obtained by flushing the expansion chamber
three times with argon before firing the tube. It seems a reasonable as-
sumption that if more complete elimination of impurities could be obtained
better agreement with theoretical predictions would result.

The radiation of energy from the flow by any mechanism will have
a similar effect on the flow parameters as the absorption of energy by
vibrational degrees of freedom; that is, kinetic energy will be removed
from the translational and rotational degrees of freedom by both mechan-
isms. The ultimate reservoir for the energy is unimportant. It must be
noted, however, that no relaxation time in the sense used in this chapter
can be associated with the radiation process. The impurity gas will con-
tinue to radiate energy so long as the mechanism for excitation remains.
Therefore, one should expect that the temperature behind the reflected
shock should decrease slowly until some value is reached, independent of
initial shock velocity, where the excitation mechanism could no longer
operate.

The impurity present in by far the largest proportion is atmos-
pheric nitrogen. The lowest excited electronic state is in the ultra-
violet, and a temperature of approximately 100,000°K would be required to
excite it. No mechanism available in the shock tube appears capable of
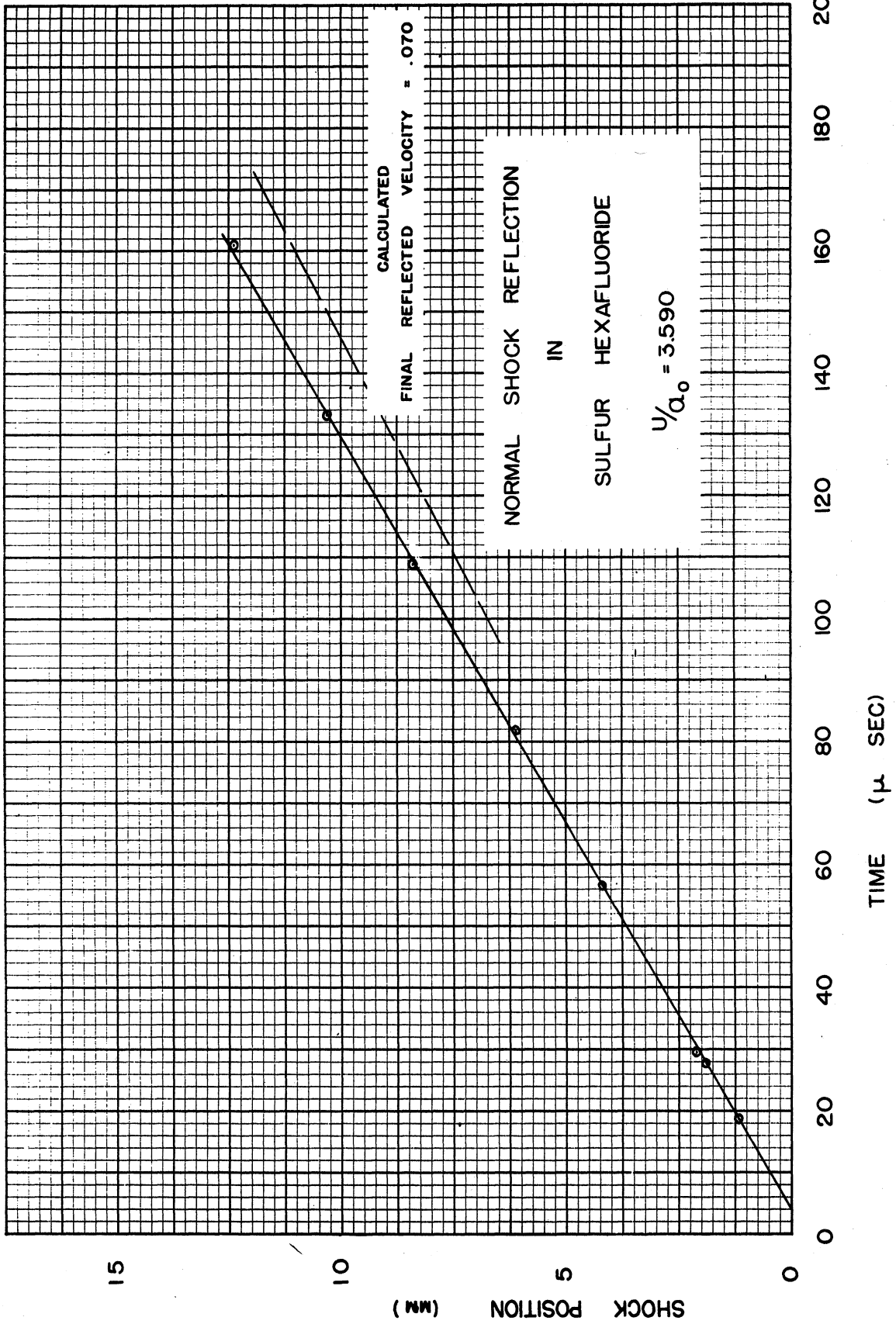exciting this level.

However, oxygen is also present as an impurity to the extent
of approximately 0.1 per cent. The excited electronic levels in oxygen
lie much closer to the ground state than for argon or nitrogen. It is

therefore conceivable that some mechanism, operated by conditions found

in the shock tube, could excite electronic levels of oxygen which would

radiate visible light. The details of this mechanism, if it even exists,

are not understood at the present time. An interesting investigation

for the future might be a further study of this glow. By employing

spectroscopic techniques, it should be possible to identify the radiating

agent and possibly determine the excitation mechanism.

3. Reflected Shock Velocity in Sulfur Hexafluoride

Finally, a similar reflection experiment was conducted in sul-

fur hexafluoride. It is evident from Fig. 28 and Table XII that the

reflected shock velocity is constant, but it is not the value predicted

by a variable specific heat calculation. There are two possible explan-

ations for this result. The initial expansion chamber pressure was only

about 7 mm of mercury. The inevitable air contamination could easily

represent several per cent of this pressure. (The gas supply on hand was

insufficient to allow thorough flushing of the expansion chamber before

each shot.) Since the velocity of sound in air is much higher than that

in sulfur hexafluoride, and since the specific heat function, μ , is

lower for air than for the heavy gas, the reflected shock velocity should

be higher than predicted for pure sulfur hexafluoride. In addition, the

specific heat of this gas as a function of temperature is not as well

known as for carbon dioxide or nitrogen. The only data available are

contained in a short letter to the editor which does not indicate just

how the specific heat was calculated, nor is any experimental verifica-

tion of the calculation presented. If this prediction of the tempera-

ture dependence of the specific heat of sulfur hexafluoride should be in

FIG 28

NORMAL SHOCK REFLECTION
IN
SULFUR HEXAFLUORIDE

$U/a_0 = 3.590$

CALCULATED
FINAL REFLECTED VELOCITY = .070

TIME (μ SEC)

SHOCK POSITION (MM)

error, it might help explain the discrepancy between the calculated and experimentally-determined reflected shock velocity.

At any rate, the fact that the position-time curve is a straight line demonstrates that vibrational relaxation in sulfur hexafluoride is not noticeable in shock tube flow. The relaxation time, therefore, is probably less than one microsecond — a very reasonable value for such a gas.

V. THE DURATION OF UNIFORM FLOW IN A SHOCK TUBE

1. Duration Index

An important consideration in the discussion of the use of various gases in the expansion chamber of a shock tube is the duration of uniform flow, because one of the serious limitations of a shock tube as an instrument for aerodynamic research is the restricted time interval in which experiments can be performed. In this chapter, the influence of the gas parameters on this duration shall be investigated. The surprising result will emerge that the effective duration of uniform flow, as a function of flow Mach number, is practically independent of the gas used in the expansion chamber.

The specific heat will be assumed constant at its room temperature value; and all velocities will be calculated from the Rankine-Hugoniot equations. It has been shown in the preceding chapters that this assumption is not valid in general. However, the effects of variable specific heat are usually not important until the flow Mach number reaches approximately 1.4. The errors introduced by this assumption will be discussed later in this chapter.

Mautz[10] has discussed the general problem of the duration of uniform flow in a shock tube. The essential limitation is the arrival of the contact surface at the test section. The arrival of the reflected shock and of the reflected rarefaction can be postponed indefinitely by increasing the length of the expansion chamber beyond the test section and by increasing the length of the compression chamber. The limiting duration is simply

$$\mathcal{T} = L_w \left(\frac{1}{u} - \frac{1}{U} \right) \qquad (61)$$

where L_w is the distance from the diaphragm to the test section. This is just the difference between the time of arrival of the contact surface and the shock wave. Using the basic shock wave equations, this becomes

$$\mathcal{T} = \frac{L_w}{a_{OE}} \left\{ \frac{\sqrt{(\mu+1)\xi(\mu+\xi)}}{(\mu-1)(1-\xi)} - \sqrt{\frac{(\mu+1)\xi}{\mu+\xi}} \right\} . \qquad (62)$$

Examination of Eq 62 shows that the duration of uniform flow depends strongly on the speed of sound in the expansion chamber. As the speed goes down, the duration goes up. However, this increase is not necessarily significant because the rate at which a stationary flow configuration will be approached will also be reduced.

It is possible to define a dimensionless index depending only on the specific heat function μ and the shock strength ξ which can be used to compare the effective flow durations in various gases. The fundamental assumption is that the rate of development of a stationary flow is directly proportional to the sound speed behind the main shock wave. In other words, it is assumed that, at a given Mach number, the steady-state flow about a given obstacle will be attained in a time α/a_1, where α depends only on the obstacle and the flow Mach number.

The duration index is defined as the duration of uniform flow per unit length of expansion chamber divided by the time for a sound wave to travel a unit distance. Thus

$$D = \frac{\frac{1}{u} - \frac{1}{U}}{\frac{1}{a_1}}$$

or

$$D = \frac{\sqrt{\frac{(\mu+1)\xi(\mu+\xi)}{(\mu-1)(1-\xi)}} - \sqrt{\frac{(\mu+1)\xi}{\mu+\xi}}}{\sqrt{\frac{\xi(\mu+\xi)}{1+\mu\xi}}}$$

Simplifying gives

$$D = \frac{(\mu+1)^{\frac{1}{2}}}{\mu-1} \cdot \frac{(1+\mu\xi)^{\frac{3}{2}}}{(\mu+\xi)(1-\xi)} \tag{63}$$

Note that the duration index is independent of the sound speed.

In most investigations the comparison of effective duration of flow in different gases should be made for constant flow Mach numbers instead of constant shock strengths. Therefore, the Mach number equation

$$M = \frac{(\mu-1)(1-\xi)}{\sqrt{(\mu+1)(1+\mu\xi)}}$$

should be used in conjunction with Eq 63.

Thus, in principle, the relative duration of uniform flow in a shock tube for two different gases can be determined as follows: The values of shock strength corresponding to a particular flow Mach number are first calculated for both gases. The duration indices for these shock strengths are then calculated from Eq 63. The largest D obtained

represents the longest relative duration, and the ratio of effective

durations is given by the ratio of the duration indices.

The duration index has been plotted as a function of Mach num-

ber in Fig. 29, for μ = 4, 6, and ∞ . This figure shows that there is

surprisingly little difference in the relative duration of uniform flow

in various gases.

It is now possible to discuss qualitatively the changes that

will be produced by allowing the specific heat to increase with temper-

ature. It has been shown that at a particular shock velocity the flow

Mach number increases above the constant specific heat value. Further-

more, the duration of uniform flow is decreased because the velocity of

the contact surface is increased, and the speed of sound behind the shock

wave is decreased. These two facts insure that the duration index will

decrease. The variation in Mach number and duration index tend to com-

pensate for each other as the slope of Fig. 29 indicates. In fact, the

changes in Fig. 29, introduced by temperature-dependent specific heat,

are indicated by representative examples for sulfur hexafluoride (the

μ of SF_6 is effectively ∞) and nitrogen. The points marked A, cal-

culated for a particular shock velocity from constant specific heat

equations, become the points A' for the same shock velocity, but calcu-

lated by assuming the specific heat to depend on temperature. It is ap-

parent that, to a first approximation, the relation between duration

index and Mach number is unchanged by considerations of the temperature

dependence of the specific heat.

FIG 29

DURATION INDEX
VERSUS
FLOW MACH NUMBER
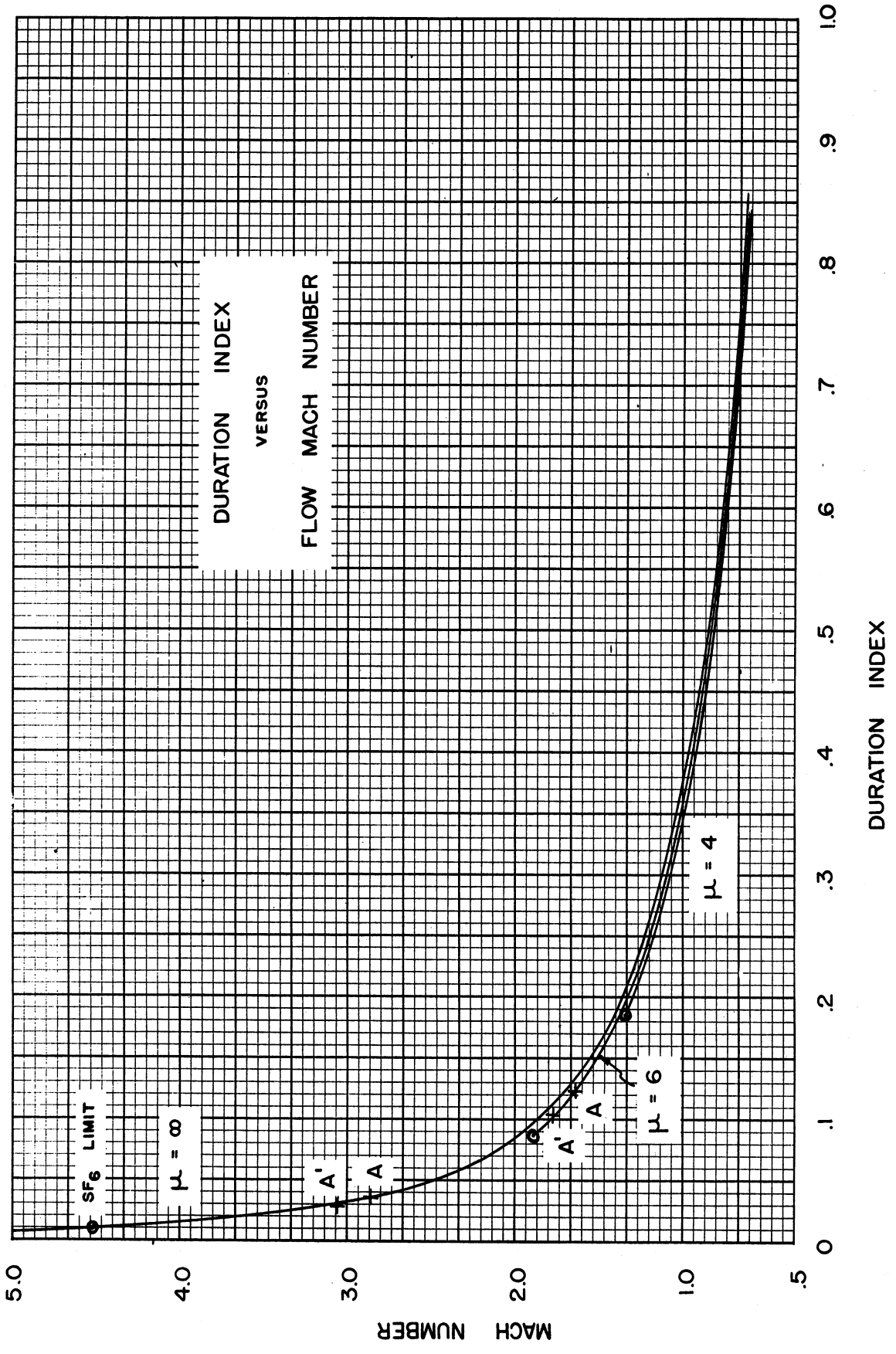
2. The Motion of a Detached Bow Wave as an Indication of the Development of a Steady State

It is known that at high supersonic Mach numbers, a bow wave can be attached to a pointed wedge. If the flow Mach number is decreased, the bow-wave angle (2θ of Fig. 13) is increased. As the Mach number is reduced further, a value is reached at which the bow wave can just be attached to the wedge. Beyond this limit, the wave becomes a detached bow wave and assumes a stable position somewhere in front of the wedge. The distance from the wedge to the bow wave is a function of free-stream Mach number and wedge geometry. If the flow becomes subsonic, the bow wave will recede from the wedge to infinity. In the shock tube, one can determine the distance between the bow wave and the wedge as a function of the time since the flow began at the wedge. This distance increases asymptotically from zero to the steady-state value. Mautz has determined the influence of scale and Mach number on the bow-wave detachment in air for two wedge geometries.

The validity of the assumptions made in deriving the duration index was investigated by comparing the time of arrival of steady state for the detached bow wave in front of a given wedge at a given Mach number for two very different gases.

In particular, the experiment consisted of determining the displacement of the bow wave as a function of time in front of a 1/16-in. plate with a symmetrical 30° wedge at its leading edge. The free-stream Mach number in both gases, nitrogen and sulfur hexafluoride, was 1.30. The results of these experiments are presented in Figs. 30 and 31 and in Table XV. The arrival of steady state was estimated to be the time
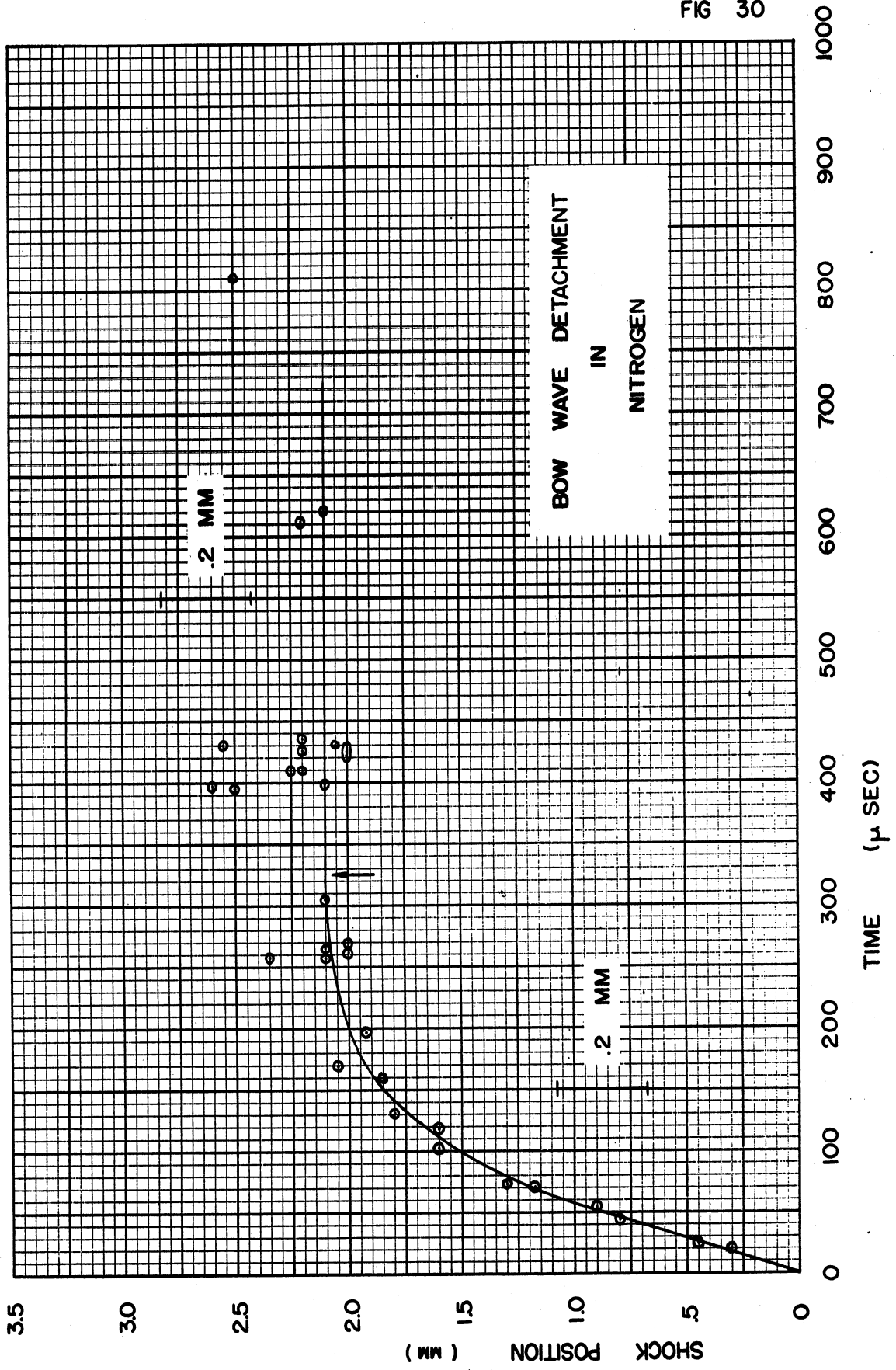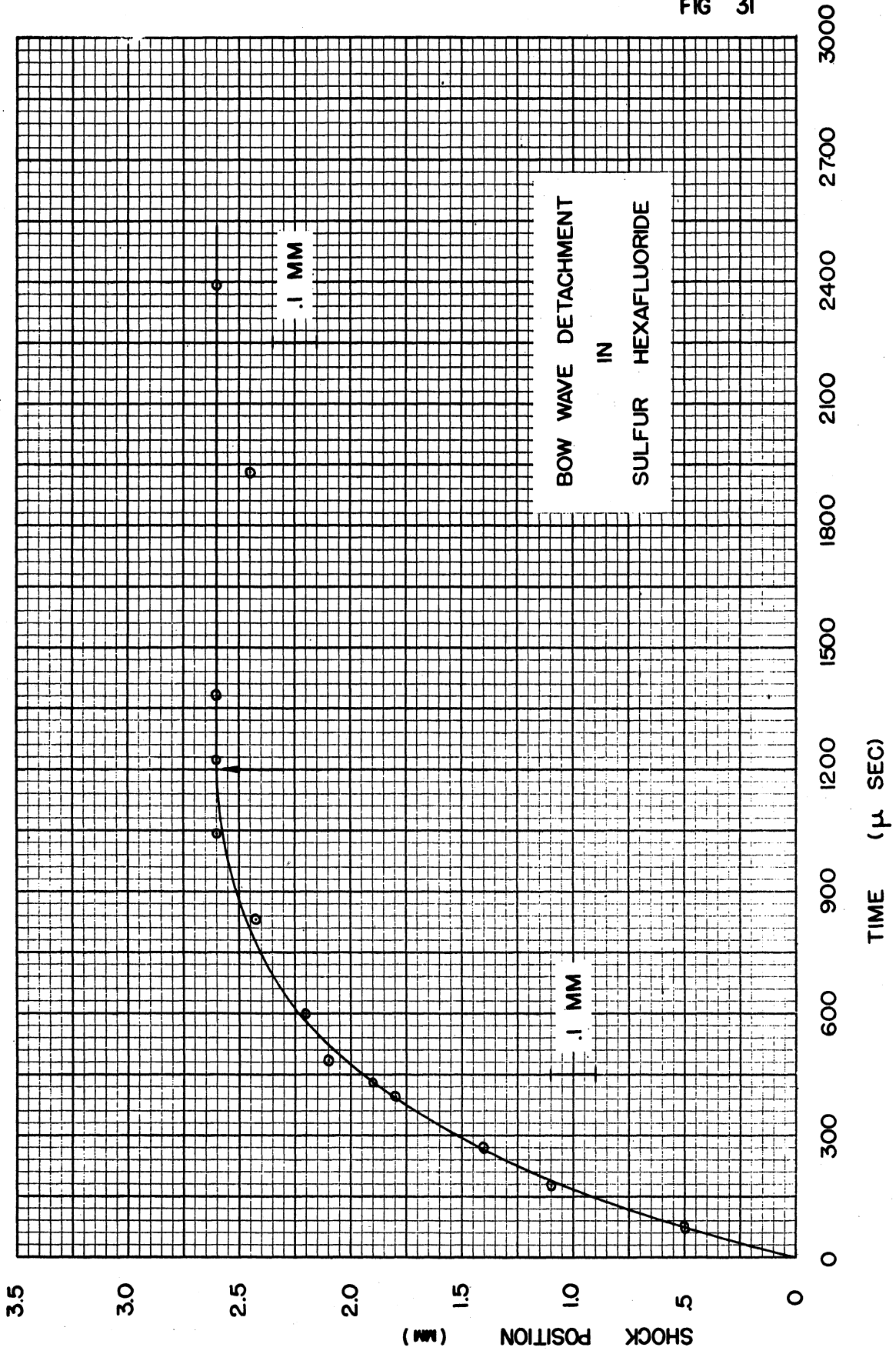
FIG 30

BOW WAVE DETACHMENT
IN
NITROGEN

FIG 31

BOW WAVE DETACHMENT
IN
SULFUR HEXAFLUORIDE

TABLE XIII

DETACHED BOW-WAVE POSITION AS A FUNCTION OF TIME
FOR A 1/16 IN., 30° WEDGE AT MACH NUMBER OF 1.3

Nitrogen		Nitrogen		Sulfur Hexafluoride	
time	position	time	position	time	position
20	.3	395	2.5	73	.5
24	.45	397	2.6	75	.5
44	.8	399	2.1	176	1.1
54	.9	409	2.2	270	1.4
70	1.2	410	2.2_5	394	1.9
72	1.3	421	2.0_5	429	1.8
		425	2.0		
102	1.6			483	2.1
118	1.6	426	2.2	599	2.2
131	1.8	428	2.0	830	2.4
160	1.8_5	430	2.0_5	1043	2.6
170	2.0_5	430	2.5_5	1225	2.6
197	1.9	435	2.2_5	1381	2.6
207	2.0	611	2.2	1932	2.4
251	2.1	621	2.1	2390	2.6
258	2.3_5				
		809	2.5		
262	2.0				
265	2.1				
265	2.1				
269	2.0				

when the bow wave reached a stable position. These estimates are indicated in the figures.

The measurement of bow-wave detachment was made to well defined parts of the shock wave image. It was possible to measure to the white leading edge of the shadowgraph negative of the shock wave in sulfur hexafluoride; however, it was necessary to measure to the white-black interface of shock waves in nitrogen. Therefore, no significance can be ascribed to the difference in steady-state position of the bow wave in the two gases.

The measurements in nitrogen were complicated by a multiplicity of the bow wave presumably caused by boundary-layer interaction and by boundary-layer growth on the wedge itself. Measurement errors of approximately .2 mm may be expected. The three high points in Fig. 29 at approximately 400 microseconds are not the result of poor measurements, however.

Boundary-layer interaction is apparently less important in sulfur hexafluoride because no bow-wave multiplicity can be detected. As a result, the position measurements are probably accurate to .1 mm.

It was then possible to verify the assumption on which the derivation of the duration index rests; namely that the steady state will be reached in a time α/a_1 where α depends only on the particular model and the Mach number. The values of α determined from this experiment for nitrogen and sulfur hexafluoride are given below.

$$t_s = \alpha/a_1$$

for nitrogen:

$$325 = \frac{\alpha_{N_2}}{.5516} \quad ; \quad \alpha_{N_2} = 179$$

for sulfur hexafluoride:

$$1200 = \frac{\alpha_{SF_6}}{.1447} \; ; \; \alpha_{SF_6} = 174$$

Also, the theoretical duration of uniform flow was calculated for both gases by using Eq 63. Next, the ratio of steady-state time to total duration was determined for both gases. Finally, the inverse ratio of the above ratios was compared with the ratio of the duration indices for the two gases. In other words, the ratio of the duration indices was compared with the experimental ratio of relative durations. The actual figures used are tabulated below.

		Nitrogen	Sulfur Hexafluoride
(a)	time of arrival of steady state	325	1200
(b)	theoretical duration of uniform flow	1670	6800
(c)	a/b	.195	.176
(d)	duration index	.209	.224

$$\text{Ratio of relative durations} = \frac{.195}{.176} = 1.11$$

$$\text{Ratio of duration indices} = \frac{.224}{.209} = 1.07$$

These results are surprising in that the values of α for nitrogen and sulfur hexafluoride agree within approximately 3 per cent and the ratio of duration indices is in good agreement with the duration ratio as determined experimentally. In fact, the agreement is better than could be expected from the type of measurements made.

The conclusions that can be safely drawn are that the rate of approach of steady state depends linearly on the sound speed behind

the primary shock wave; and that the relative duration of uniform flow

in the expansion chamber is practically independent of the gas used.

VI. FURTHER DISCUSSION OF GAS PARAMETERS AND
SPECIFIC GASES FOR SHOCK TUBE WORK

The preceding chapters of this paper have discussed some of the problems of using gases other than air in a shock tube. In particular, the influence of variations of specific heat with temperature were considered in detail for the compression and expansion chambers. This final chapter will discuss the additional influence of a large number of other physical and chemical properties, some of which are compiled in Table XVI for representative gases. The results obtained below are not new: they are immediate consequences of the basic shock equations and physical logic. However, the results are necessary and important to anyone interested in using complex gases in a shock tube. First, the influence of specific gas parameters will be considered, then the applicability of particular gases for shock tube research will be discussed, and finally, representative photographs of flows in several gases will be presented.

1. Effects of Gas Parameters

a. Specific Heat Function

(i) The specific heat function, $\mu = (\gamma + 1)/(\gamma - 1)$, plays a fundamental role in shock tube theory. The limiting Mach number that can be obtained in the expansion chamber is

$$M = \frac{(\mu-1)(1-\xi)}{\sqrt{(\mu+1)(1+\mu\xi)}}$$

TABLE XIV

CHEMICAL AND PHYSICAL PROPERTIES OF GASES

Gas	Molecular Weight	γ	μ	Viscosity at room temp. (μ poise)	Index of Refraction	Chemical Activity	Boiling Point °C
N_2	28.02	1.40	6	176	1.0003	inert	- 195.8
Air	28.8	1.40	6	185	1.00024	inert	
H_2O	18.02	1.37	6.41	93	1.00026	inert	100
CO_2	44.01	1.304	7.58	150	1.00045	inert	- 78.5
CCl_4	153.84	1.13	16.4	100	1.00177	inert	76.7
$n-C_5H_{12}$	72.15	1.086	24.3	67	1.0017	inert	36.2
SF_6	146.06	1.096	21.9		1.00078	very inert like N_2	- 63.8
H_2	2.016	1.41	5.88	87	1.00014	inert	- 252.8
He	4.003	1.667	4	194	1.000036	inert	- 268.9
A	39.94	1.667	4	222	1.00028	inert	- 185.7
Cl_2	70.91	1.355	6.63	133	1.00077	active	- 33.7
Br_2	159.83	1.32	7.25	155	1.00113	active	58.78
$TeCl_4$	269.4				1.00260		414
UF_6	352.1			180		attacks metals and glass	56.2

This limit can be raised by increasing the μ of the gas in the expansion chamber, that is, by using a polyatomic gas. However, when this is done, the shock theory derived under the assumption of constant specific heat is no longer valid because the specific heat of complex gases usually depends strongly on the temperature. Fortunately, however, the specific heat variations always produce a further increase in flow Mach number. Thus the use of complex gases in the expansion chamber increases the flow Mach number limit in two ways.

(ii) Another important parameter of the flow in the expansion chamber which depends on μ is the temperature ratio across the shock wave. Simple shock theory predicts a temperature ratio of

$$\frac{T}{T_0} = \frac{1 + \mu \xi}{\xi(\mu + \xi)} \tag{64}$$

As $\mu \to \infty$, $T_1/T_0 \to 1$ for a given shock strength.

Physically this can be interpreted by noting that gases with large μ have more vibrational degrees of freedom excited than gases with μ of 7 or smaller. Therefore, these internal degrees of freedom can absorb a larger relative proportion of the kinetic energy transformed into internal energy at the shock wave. This means that the translational kinetic energy of these gases is not increased nearly as much by a shock wave as in the case of monatomic or diatomic gases.

Furthermore, a comparison of the temperature ratios for different gases should be made at constant flow Mach number, not at constant shock strength. Eq 28 shows that for a given Mach number, as μ increases so does ξ . By differentiating Eq 64 at constant μ one obtains

$$\frac{d\frac{T}{T_0}}{d\xi} = -\frac{\mu + 2\xi + \mu\xi^2}{\xi^2(\mu+\xi)^2}$$

It is evident that increasing ξ decreases T/T_0 for a particular gas.

The fact that the temperature ratio across a shock wave that produces a particular Mach number may be reduced by using a complex rather than a simple gas in the expansion chamber is important for two reasons. The first of these is illustrated by Fig. 11, which shows the shock wave parameters in sulfur hexafluoride. Even though the specific heat of this gas is strongly dependent on temperature, the difference between the Rankine-Hugoniot and variable specific heat parameters for a given Mach number is actually less than the differences in carbon dioxide and nitrogen because the actual temperature rise and the relative increase in specific heat across the shock wave are smaller for sulfur hexafluoride than for the other gases. In other words, the effects of temperature-dependent specific heat will be noticed at a lower flow Mach number in carbon dioxide and nitrogen than in sulfur hexafluoride.

The second reason is that a large part of the work to be done in shock tubes in the future will involve the determination, by means of gauges, of pressures on various parts of obstacles. Most pressure gauges now available have such high temperature coefficients that they cannot be used for this work. The use of complex gases in the expansion chamber may reduce the temperature behind the shock sufficiently to allow crystal gauges to be used in situations where mechanical gauges must otherwise be employed.

(iii) Finally, the initial pressure ratio p_0/p_3 across the diaphragm required to produce a particular shock strength depends on μ .

In Eq 1, the effect of μ_E on a_{OE} can, in general, be neglected with respect to its effects in other parts of the equation. Differentiation of the equation indicates that p_0/p_3 decreases with increasing μ_E at constant ζ and μ_c.

b. Molecular Weight.

The molecular weight of a gas enters the theory of shock waves through the sound speed.

$$a = \sqrt{\frac{\gamma R T}{m}} \ .$$

The role of the molecular weight is much more important than that of γ in this equation, because m can be increased easily by a factor of 5, but γ can be reduced by only about 30 per cent in going from a diatomic to a complex gas.

(i) The velocity of sound at room temperature is important in several places in shock tube theory. Consider first the p_0/p_3 relation discussed in the last section. The decrease in sound speed and increase in μ obtained by using complex gases in the expansion chamber lead to a increased pressure ratio across the diaphragm for a given flow Mach number. For instance, the initial pressure ratio required to produce a Mach number of 1.1, using nitrogen in both chambers, is approximately 0.014; while the ratio required to produce the same Mach number with sulfur hexafluoride in the expansion chamber and nitrogen in the compression chamber is 0.162, an increase of p_0 by more than a factor of 10.

(ii) The effect of the molecular weight and sound speed on the duration of uniform flow in a shock tube was discussed in Chapter V. It was pointed out that the duration was inversely proportional at constant shock strength to the sound speed in the expansion chamber. It

123

follows that the time duration of uniform flow may be increased manyfold, at constant Mach number by using a complex gas. In Chapter V it was shown that this added duration does not mean that flow phenomena will develop to a higher degree, but it does mean that more time is available in which to make measurements of the hydrodynamic variables behind the shock wave. Thus, the resolution or time response required in the measuring instruments can be reduced; or conversely, the details of the flow can be examined in more detail with given instruments if the longer duration and slower flow development are available. It is obvious that this constitutes a great advantage in shock tube research because the resolution of most gauges available today is not satisfactory for shock tube pressure measurements.

c. Index of Refraction.

The optical effect produced by a given density gradient in a flow is directly proportional to the index of refraction and to the absolute pressure of the gas. As Table XVI shows, the indices of refraction of complex gases are much greater than that of air. This fact, coupled with the fact that the expansion chamber pressure is usually increased by using heavy gases, results in photographs of flows in heavy gases that show much more detail and, therefore, provide more information than similar flows in air.

In fact, two new classes of information can be obtained under certain conditions. If a gas is used whose index of refraction is very large (CCl$_4$ for instance), the small disturbances produced by dirt and imperfections on the windows are made visible. More precisely, the wakes produced by these disturbances can be seen. These wakes indicate

particle paths which become streamlines in the steady state; they are visible until wall boundary layer thickens to the point where the imperfections are completely buried in the layer. Thus, for the first time, a method is available for photographing streamlines in a supersonic flow without injecting particles of some type into the stream. Three examples of streamline photographs are shown in Figs. 35, 36, and 37. Furthermore, the index of refraction of almost all heavy gases is sufficient to make Mach lines from small imperfections in models visible. These Mach lines make it possible to determine the flow Mach number in the vicinity of airfoils.

d. Viscosity Coefficient.

In physical investigations of shock wave - boundary layer interactions or boundary layer growth, it would be convenient to be able to vary the Reynolds number at constant Mach number over wide ranges. This can be accomplished to a certain extent by varying the initial pressure in the expansion chamber while keeping the pressure ratio across the diaphragm fixed. However, the Reynolds number of supersonic flows can be changed conveniently only by a factor of approximately 10 in this way. Larger variations can be obtained by varying the viscosity coefficient by changing the gas in the expansion chamber. Table XVI lists the viscosity coefficients for several gases. This method of varying Reynolds number has the definite disadvantage that the specific heat ratio is usually changed also; but it should be considered, at least until the significance of Reynolds number in a compressible supersonic flow is established and the important variables in the various interactions are determined.

e. Chemical Activity.

        Several gases which would be ideal for shock tube work insofar

as their specific heat, molecular weight, and index of refraction are

concerned cannot be used because of their chemical properties. For in-

stance, chlorine, bromine, uranium hexafluoride, and many acid gases

would corrode the metal parts of the tube. Carbon tetrachloride under-

goes some reaction*after several hundred microseconds under the condi-

tions found behind strong shock waves. The chemical activity and stabil-

ity of a particular gas must be investigated before it can be considered

for shock tube work.

f. Boiling Point.

        Many of the heavier organic and inorganic compounds are liquids

at room temperature. This does not necessarily exclude them from consi-

deration because, in many instances, the vapor pressure of the gas at

room temperature is greater than the desired expansion chamber pressure.

The boiling point of CCl_4, for instance, is 76.7°C. Supersonic phenomena

can be investigated with this gas; but at room temperature the vapor pres-

sure is too small to allow transonic or subsonic flows to be obtained in

the ordinary way. In general, it is desirable to use a gas with as low

a boiling point as possible.

g. Solubility.

        The final physical property of gases to be considered is solu-

bility. Some heavy gases are difficult to use in a shock tube because

they dissolve in and contaminate the oil in the vacuum pumps and manometers

_____

*
  The temperature behind the shock is not high enough to cause thermal
  dissociation, and the reaction seems to be concentrated in the boundary
  layer. It may be that carbon tetrachloride reacts with absorbed water
  vapor on the windows of the tube.

126

and the rubber in various vacuum connections. However, special precautions can be taken to flush all chambers and lines completely before evacuating the system. These precautions will minimize this contamination.

2. Choice of Specific Gases for Use in a Shock Tube

a. General Aerodynamic Investigations.

For general aerodynamic investigations the best gas combination is hydrogen in the compression chamber and nitrogen in the expansion chamber. Some of the advantages of nitrogen compared with air have been mentioned in the earlier chapters. These advantages and several others will now be stated and discussed.

1. Since nitrogen and hydrogen do not react, hydrogen can be used in the compression chamber if nitrogen is used in the expansion chamber. Hydrogen cannot be used with air. The advantages of using hydrogen are discussed in Chapter II and illustrated in Fig. 1.

2. The specific heat of nitrogen varies very slowly with temperature; in fact, more slowly than air because oxygen has a lower vibrational frequency than nitrogen.

3. The vibrational relaxation time for commercial nitrogen has been estimated to be longer than 5000 microseconds. This time is so long that specific heat variations in nitrogen do not have time to take place during the interval of interest in the shock tube. Therefore, all shock wave calculations can be made with the relatively simple Rankine-Hugoniot constant specific heat equations.

4. Humidity variations are completely eliminated. The most important effect of humidity on the shock tube flow enters through the

velocity of sound in the shock velocity equation, 26. The velocity of

sound of moist air is

$$a_h = \frac{a_d}{\sqrt{1 - .320 \frac{P_w}{P}}}$$

where a_h is the velocity in humid air, a_d is the velocity in dry air, P

is the barometric pressure and P_w is the partial pressure of water vapor.

This equation can be obtained from the equation $a = \sqrt{\gamma RT/M}$. Daily

humidity variations are sufficient to require correction of measured

shock velocity if accurate shock strength determinations are desired.

5. The effect of water vapor on the relaxation times of air

is very pronounced. For instance, on a humid day the relaxation time

of atmospheric nitrogen may be reduced to approximately 100 microseconds

(Kantrowitz). A similar reduction is made in the relaxation time of

oxygen. Under these conditions small relaxation effects might be notice-

able behind strong shock waves. These effects would change as humidity

changed and they might introduce small errors into experimental results.

In view of these definite advantages of nitrogen, as compared

to air, for use in the shock tube for aeronautical research, it is sug-

gested that nitrogen be used in the expansion chamber of the shock tube

wherever possible.

b. Physical Investigations.

To the physicist, the study of the flow in heavy gases is as

interesting as the flow in air. The range of problems which can be

treated in a shock tube can be increased markedly by using a heavy, poly-

atomic gas in the expansion chamber. It is necessary, however, to

consider the specific heat as a function of temperature for complex gases
in the calculation of shock wave characteristics. In general, relaxation
effects can be ignored because the relaxation times for most polyatomic
gases are less than one microsecond.

Sulfur hexafluoride is perhaps the most suitable complex gas
for general experimentation. It has a low boiling point and can be com-
pared in chemical stability to nitrogen. Its molecular weight and spe-
cific heat function are high. Its index of refraction is almost three
times that of air. This value is not as high as that found in some other
heavy gases; but it is sufficient for most purposes. Finally, compressed
sulfur hexafluoride is available in large cylinders from gas supply houses.

n-Pentane would be ideal for investigations of boundary layers
because of its high index of refraction and low viscosity. Low viscos-
ity provides a high Reynolds number for a given characteristic length.

Investigations of relaxation effects can best be conducted in
carbon dioxide, which has a relaxation time longer than any other common
polyatomic gas.

Streamlines can be photographed in some heavy gases. They have
been seen in carbon tetrachloride and ethyl iodide, and, no doubt, would
be visible in several other gases.

c. Representative Photographs of Flows in Complex Gases.

In this section, several photographs will be presented which
serve to demonstrate what can be done with heavy complex gases in the
shock tube.

Fig. 32 shows a photograph of the detached bow wave in sul-
fur hexafluoride in front of a 1/16-in. plate with a 30° angle at its

leading edge. Some of the details of the starting process whereby steady state is reached can be seen.

Fig. 33 is an example of the subsonic flow in petroleum ether.* The starting vortex, three rarefaction waves, the early stages of a separated turbulent boundary layer, and several interesting shock wave interactions are visible.

A schlieren photograph of the normal reflection of a shock wave in carbon dioxide is shown in Fig. 34. The lambda shock caused by very severe reverse flow in the boundary layer on the floor and walls of the tube is easily seen.

Figs. 35, 36, and 37 are examples of flows in carbon tetrachloride in which particle paths can be seen. The definitely subsonic character of the flow between the detached bow wave and the first corner on the lower surface of the wedge in Fig. 35 is to be compared with the supersonic character of the flow behind the attached bow wave in the same region of Figs. 36 and 37. In both of these photographs, the Mach number in the various regions of the flow can be determined from measurements of Mach angles.

Which particular complex gas should be used for a particular investigation must be determined by considering the special requirements of the investigation and the physical and chemical properties of various gases. It is thought that some of the advantages of the use of complex gases in the investigation of hydrodynamic phenomena in a shock tube have been demonstrated by the several flow photographs shown on the following pages.

---

* Petroleum ether is a mixture of hydrocarbons boiling between 30° and 40°C. This mixture has properties similar to pentane; but it is not suggested for shock tube use because the concentration of the various fractions in the vapor phase will vary in time.
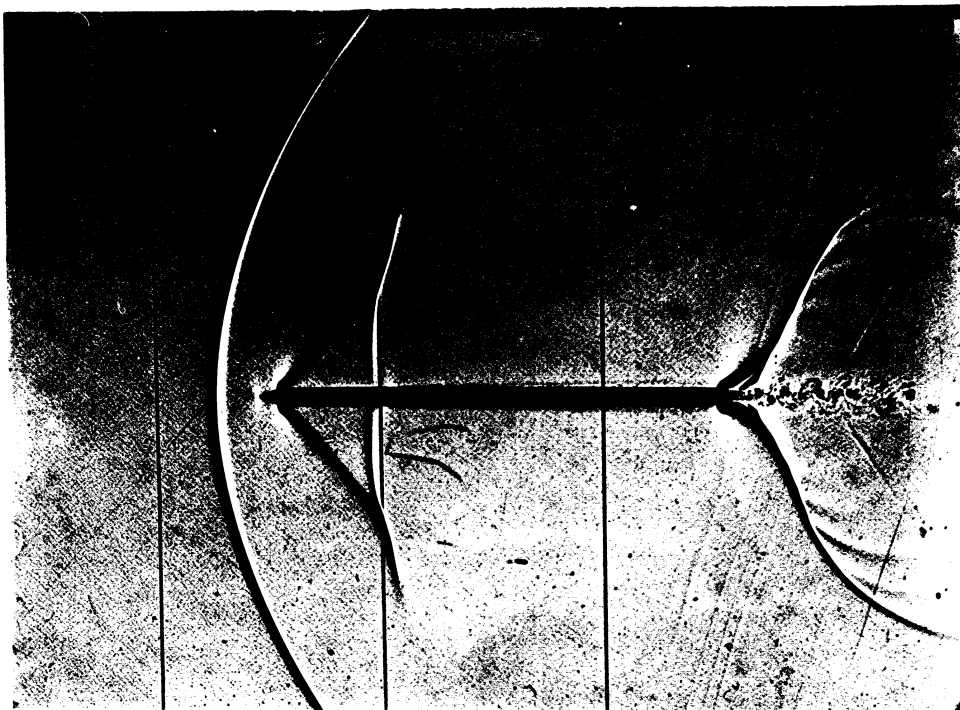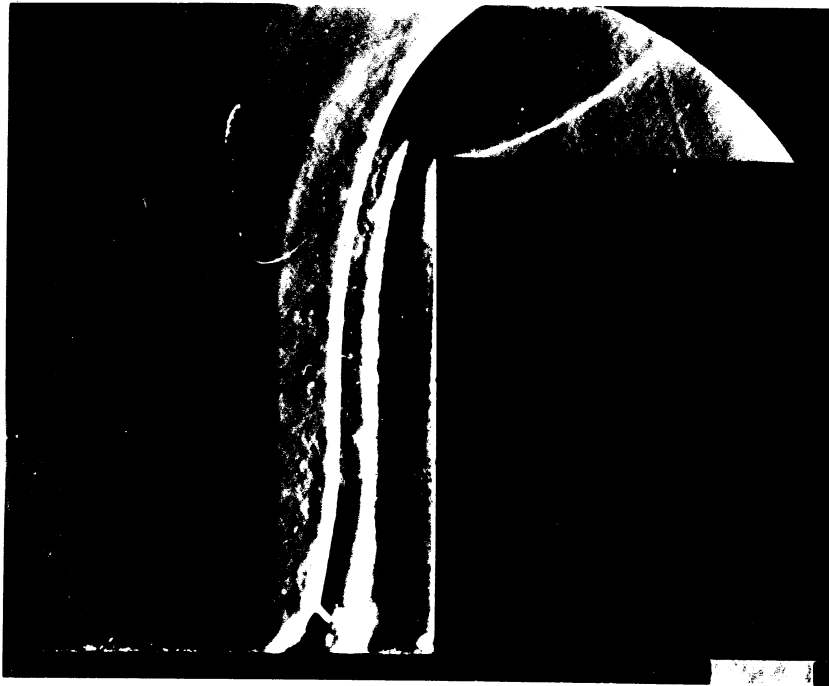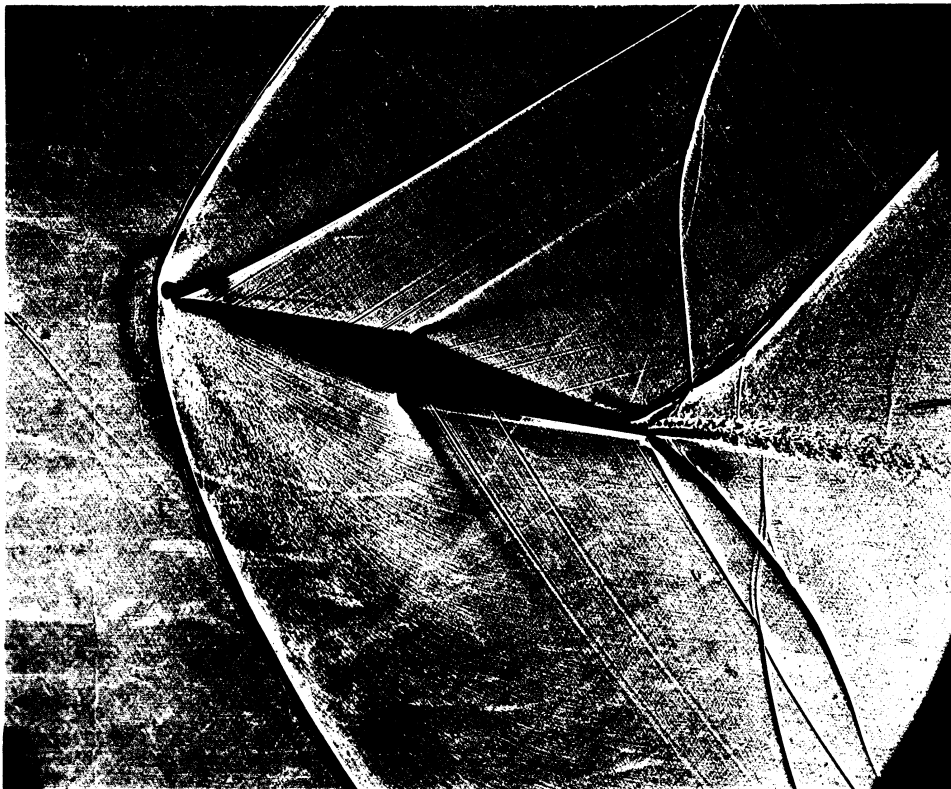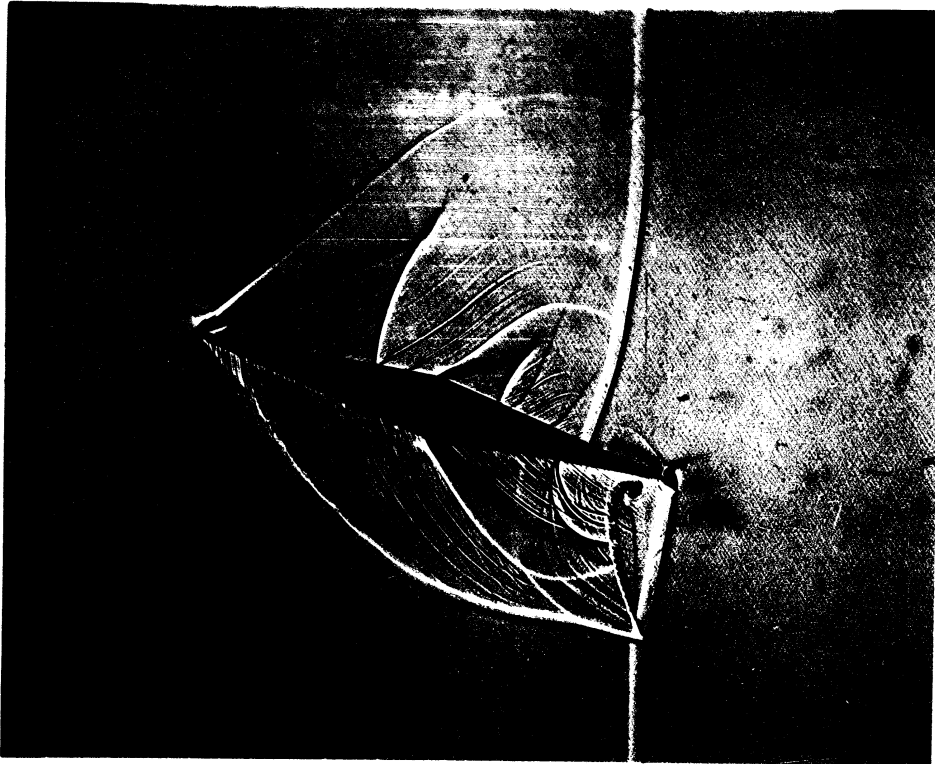
DETACHED BOW WAVE IN SULFUR

HEXAFLUORIDE

FIG 33
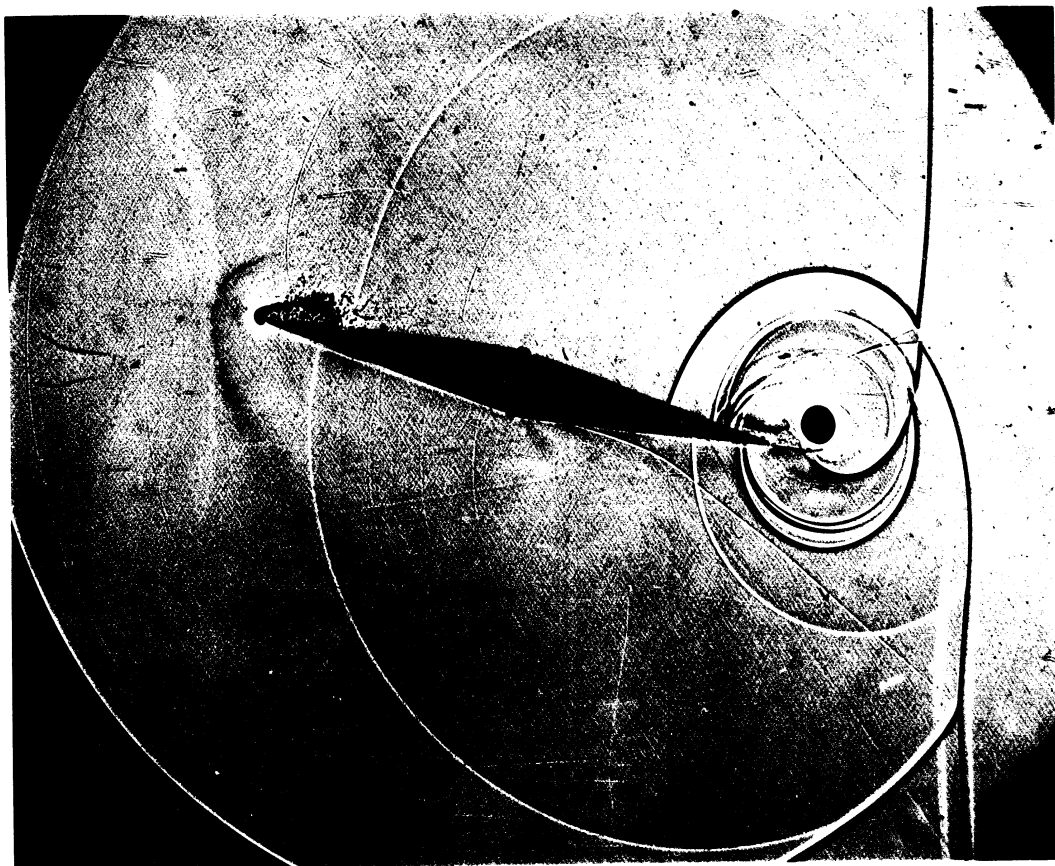
SUBSONIC FLOW IN PETROLEUM ETHER

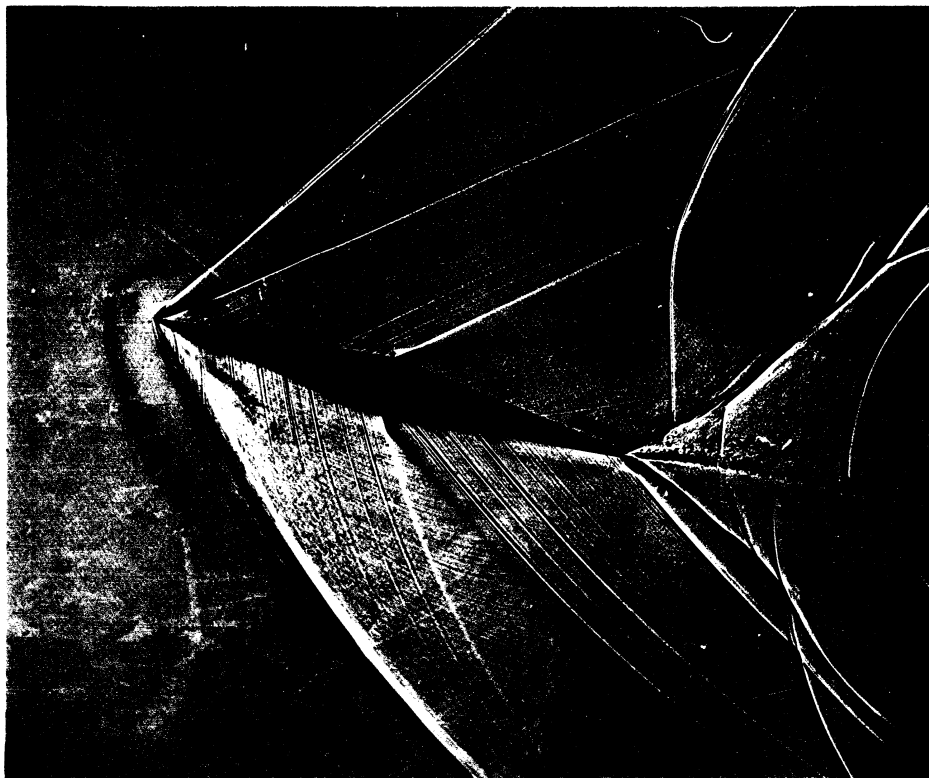NORMAL SHOCK REFLECTION IN

CARBON DIOXIDE

FIG 35

DETACHED BOW WAVE IN CARBON TETRACHLORIDE

IN FRONT OF A WEDGE AT AN

ANGLE OF ATTACK

FIG 36

ATTACHED BOW WAVE IN CARBON TETRACHLORIDE
ON A WEDGE AT AN ANGLE OF ATTACK
EARLY PHOTOGRAPH

FIG 37

ATTACHED BOW WAVE IN CARBON TETRACHLORIDE
ON A WEDGE AT AN ANGLE OF ATTACK
LATE PHOTOGRAPH

VII. CONCLUSIONS

The strongest shock wave that can be produced by a given initial pressure ratio across the diaphragm of a shock tube may be obtained by using hydrogen in the compression chamber. However, oxygen must be removed from the expansion chamber when hydrogen is used in the compression chamber in order to prevent an explosion in the tube, which could be initiated by the high temperature behind the shock wave reflected from the end of the expansion chamber.

Expressions for the flow velocity produced by a rarefaction wave in a gas with temperature-dependent specific heat and in a van der Waals' gas were derived. It was shown that both of these departures from the ideal conditions assumed in the derivation of the Taub equation are negligible for hydrogen. However, they might be important if a polyatomic gas were used in the compression chamber for a special investigation.

Shock wave equations analogous to the Rankine-Hugoniot equations were developed for shock waves in an ideal gas with temperature-dependent specific heat. The flow parameters calculated from these equations showed that the temperature behind a shock wave is lower than calculated from the Rankine-Hugoniot equations. Furthermore, the pressure and density behind the shock, and the flow Mach number in the shock tube, are higher than predicted by the simple theory.

The effect of vibrational relaxation on the flow parameters behind a shock wave was investigated, and an approximate calculation of the time dependence of these parameters was made. It was shown that for

weak shocks the temperature changed exponentially from its initial to its final value, while the other parameters followed a pseudo-exponential law. The velocity of a shock wave in carbon dioxide reflected normally from a wall was found to vary in time. The measured equilibrium velocity agreed with the predictions of theory assuming temperature-dependent specific heat. The variation of reflected shock velocity is the direct result of vibrational relaxation.

The influence of the specific heat ratio of gases on the relative duration of uniform flow in a shock tube was demonstrated by the introduction of a dimensionless parameter, the duration index, which depends only on μ and ξ. At a given Mach number the ratio of the duration indices of two gases is also the ratio of the effective durations of uniform flow in the gases. It was shown that, to a good approximation, for a particular Mach number the duration index is independent of the gas used in the expansion chamber. The fundamental assumption made in the derivation of the duration index is that the rate of development of a steady-state flow configuration is proportional to the sound speed behind the shock wave. This assumption was verified experimentally for the special case of a detached bow wave in nitrogen and sulfur hexafluoride.

Finally, the effects of a large number of chemical and physical properties of gases on the applicability of the gas for shock tube research were discussed. Nitrogen was found to be the most satisfactory gas for use in the expansion chamber for standard aeronautical research, and sulfur hexafluoride the most satisfactory for the investigation of the physical details of hydrodynamic phenomena.

BIBLIOGRAPHY

1. Vieille, Paul, "Sur les Discontinuities produites par le detent brusque de gas compremés", Comptes Rendus, 129, 1228-1230 (1899).

2. Kobes, K., "Die Durchschlagsgeschwindigkeit bei den Luftsauge- und Druckluftbremsen", Zeitschrift des Osterreichischen Ingenieur- und Architekten-Vereines, 62, 558 (1910).

3. Schardin, H., "Bemerkungen zum Druckausgleichvorgang in einer Rohr-leitung", Physikalische Zeitschrift, 33, 60 (1932).

4. Payman, W., and Shepherd, W. F. C., "Explosion Waves and Shock Waves: VI, The Disturbance Produced by Bursting Diaphragms with Compressed Air", Proceedings of the Royal Society, A-186, 293-321 (1946).

5. Reynolds, George T., A Preliminary Study of Plane Shock Waves Formed by Bursting Diaphragms in a Tube, OSRD Report No. 1519, June, 1943.

6. Smith, Lincoln G., Photographic Investigation of the Reflection of Plane Shocks in Air, OSRD Report No. 6271, November, 1945.

7. Bleakney, W., Fletcher, C. H., and Weimer, D. K., "The Density Field in Mach Reflection of Shock Waves", Physical Review, 76, 323 (1949).

8. Bleakney, W., and Taub, A. H., "Interaction of Shock Waves", Reviews of Modern Physics, 21, 584 (1949).

9. Mautz, C. W., Geiger, F. W., and Epstein, H. T., "On the Investigation of Supersonic Flow Patterns by Means of a Shock Tube", Physical Review, 74, 1872 (1948).

10. Mautz, C. W., The Use of the Shock Tube in the Production of Uniform Fields of Transonic and Supersonic Flow, Dissertation, University of Michigan, 1949.

11. Geiger, F. W., On the Shock Tube as a Tool for the Investigation of Flow Phenomena, Dissertation, University of Michigan, 1949.

12. Geiger, F. W., and Mautz, C. W., The Shock Tube as an Instrument for the Investigation of Transonic and Supersonic Flow Patterns, Report on ONR Contract N6-ONR-232, TO IV, Engineering Research Institute, University of Michigan, 1949.

13. Bleakney, Walker, The Diffraction of Shock Waves Around Obstacles and the Transient Loading of Structures, Princeton University, Technical Report II-3, Contract N6-ONR-105, TO II, March 16, 1950.

14. White, D. R., Weimer, D. K., and Bleakney, Walker, The Diffraction of Shock Waves Around Obstacles and the Resulting Transient Loading of Structures, Princeton University, Technical Report II-6, Contract N6-ONR-105, TO II, August 1, 1950.

15. Uhlenbeck, G. (submitting work done by R. E. Duff and R. N. Hollyer, Jr.), Diffraction of Shock Waves Around Various Obstacles, Engineering Research Institute, University of Michigan, Report No. 50-1, Contract N6-ONR-232, TO IV, March 21, 1950.

16. Hollyer, R. N., Jr., and Duff, R. E., The Effect of Wall Boundary Layer on the Diffraction of Shock Waves Around Cylindrical and Rectangular Obstacles, Engineering Research Institute, University of Michigan, Report No. 50-2, Contract N6-ONR-232, TO IV, June 21, 1950.

17. Duff, R. E., and Hollyer, R. N., Jr., The Diffraction of Shock Waves Through Obstacles with Various Openings in Their Front and Back Surfaces, Engineering Research Institute, University of Michigan, Report No. 50-3, Contract N6-ONR-232, TO IV, November 7, 1950.

18. Hollyer, R. N., Jr., and Duff, R. E., Growth of the Turbulent Region at the Leading Edge of Rectangular Obstacles in Shock Wave Diffraction, Engineering Research Institute, University of Michigan, Report No. 51-2, Contract N6-ONR-232, TO IV, January 18, 1951.

19. Richards, W. T., "Supersonic Phenomena", Review of Modern Physics, 11, 36-64 (1939).

20. Bethe, H. E., and Teller, E., Deviations from Thermal Equilibrium in Shock Waves, Aberdeen Proving Grounds, Ballistic Research Laboratory, Report No. X-117.

21. Kassel, Louis S., "Thermodynamic Functions of Nitrous Oxide and Carbon Dioxide", Journal of the American Chemical Society, 56, 1838 (1934).

22. Meyer, Gerald E., and Buell, C. E., "Note on the Specific Heat of Sulfur Hexafluoride", Journal of Chemical Physics, 16, 744 (1948).

23. Notes and Tables for Use in the Analysis of Supersonic Flow, by the Staff of the Ames 1 x 3 ft Supersonic Wind-Tunnel Section, NACA, TN 1428 (1947).

24. Landau, L., and Teller, E., "Zur Theorie der Schalldispersion", Physikalische Zeitschrift der Sowjetunion, 10, 34 (1936).

25. Griffith, Wayland, "Vibrational Relaxation Times in Gases", Journal of Applied Physics, 21, 1319 (1950).

26. Kantrowitz, Arthur, Effects of Heat Capacity Lag in Gas Dynamics, NACA ARR No. 4A22 (1944).

27. Ivey, H. Reese, and Cline, Charles W., Effect of Heat-Capacity Lag on the Flow Through Oblique Shock Waves, NACA TN 2196 (1950).

28. Kantrowitz, Arthur, Heat-Capacity Lag in Turbine-Working Fluids, NACA Restricted Bulletin L4E29 (1944).